



HAL
open science

Reference cross sections for charged-particle monitor reactions

A. Hermanne, A.V. Ignatyuk, R. Capote, B.V. Carlson, J.W. Engle, Mark A. Kellett, T. Kibédi, G. Kim, F.G. Kondev, M. Hussain, et al.

► **To cite this version:**

A. Hermanne, A.V. Ignatyuk, R. Capote, B.V. Carlson, J.W. Engle, et al.. Reference cross sections for charged-particle monitor reactions. Nuclear Data Sheets, 2018, 148, pp.338-382. 10.1016/j.nds.2018.02.009 . cea-04142337

HAL Id: cea-04142337

<https://cea.hal.science/cea-04142337v1>

Submitted on 27 Jun 2023

HAL is a multi-disciplinary open access archive for the deposit and dissemination of scientific research documents, whether they are published or not. The documents may come from teaching and research institutions in France or abroad, or from public or private research centers.

L'archive ouverte pluridisciplinaire **HAL**, est destinée au dépôt et à la diffusion de documents scientifiques de niveau recherche, publiés ou non, émanant des établissements d'enseignement et de recherche français ou étrangers, des laboratoires publics ou privés.

Reference Cross Sections for Charged-particle Monitor Reactions

A. Hermanne,¹ A. V. Ignatyuk,² R. Capote,^{3,*} B. V. Carlson,⁴ J. W. Engle,⁵ M. A. Kellett,⁶
 T. Kibédi,⁷ G. Kim,⁸ F. G. Kondev,⁹ M. Hussain,¹⁰ O. Lebeda,¹¹ A. Luca,¹² Y. Nagai,¹³ H. Naik,¹⁴
 A. L. Nichols,¹⁵ F. M. Nortier,⁵ S. V. Suryanarayana,¹⁴ S. Takács,¹⁶ F. T. Tárkányi,¹⁶ and M. Verpelli³

¹*Cyclotron Department - TONA, Vrije Universiteit Brussel, Brussels, Belgium*

²*Institute of Physics and Power Engineering (IPPE), Obninsk, Russia*

³*NAPC–Nuclear Data Section, International Atomic Energy Agency, Vienna, Austria*

⁴*Instituto Tecnológico de Aeronáutica, Brazil*

⁵*Los Alamos National Laboratory (LANL), USA*

⁶*CEA, LIST, Laboratoire National Henri Becquerel (LNE-LNHB), France*

⁷*Australian National University (ANU), Canberra, Australia*

⁸*Kyungpook National University, Republic of Korea*

⁹*Argonne National Laboratory (ANL), USA*

¹⁰*Government College University, Lahore, Pakistan*

¹¹*Nuclear Physics Institute, Rez, Czech Republic*

¹²*National Institute of Physics and Nuclear Engineering “Horia Hulubei”, Romania*

¹³*Japan Atomic Energy Agency (JAEA), Tokaimura Naka, Ibaraki-ken, Japan*

¹⁴*Bhabha Atomic Research Centre (BARC), Trombay, Mumbai, India*

¹⁵*University of Surrey, Guildford, UK*

¹⁶*Institute for Nuclear Research, Debrecen, Hungary*

(Received 31 July 2017; revised received 9 and 30 October 2017; accepted xx November 2017)

Evaluated cross sections of beam-monitor reactions are expected to become the *de-facto* standard for cross-section measurements that are performed over a very broad energy range in accelerators in order to produce particular radionuclides for industrial and medical applications. The requirements for such data need to be addressed in a timely manner, and therefore an IAEA coordinated research project was launched in December 2012 to establish or improve the nuclear data required to characterise charged-particle monitor reactions. An international team was assembled to recommend more accurate cross-section data over a wide range of targets and projectiles, undertaken in conjunction with a limited number of measurements and more extensive evaluations of the decay data of specific radionuclides. Least-square evaluations of monitor-reaction cross sections including uncertainty quantification have been undertaken for charged-particle beams of protons, deuterons, ³He- and ⁴He-particles. Recommended beam monitor reaction data with their uncertainties are available at the IAEA-NDS medical portal www-nds.iaea.org/medical/monitor_reactions.html.

CONTENTS

| | | | |
|--|---|---|----|
| I. INTRODUCTION | 2 | F. Evaluated Cross Sections and Excitation Functions for Beam Monitor Reactions | 8 |
| A. Mission of IAEA: Importance of Medical and Industrial Applications of Radionuclides | 2 | II. MONITOR REACTIONS FOR PROTON BEAMS | 9 |
| B. Needs for Evaluated Data – Start of Programmes | 3 | A. ²⁷ Al(<i>p,x</i>) ²² Na | 9 |
| C. Significance of Nuclear Data in Monitoring Charged-particle Beams | 4 | B. ²⁷ Al(<i>p,x</i>) ²⁴ Na | 9 |
| D. Decay Data Needs for Charged-particle Monitor Reactions | 4 | C. ^{nat} Ti(<i>p,xn</i>) ⁴⁸ V | 11 |
| E. Recommended Curves and their Uncertainties | 6 | D. ^{nat} Ti(<i>p,x</i>) ⁴⁶ Sc | 12 |
| | | E. ^{nat} Ni(<i>p,x</i>) ⁵⁷ Ni | 13 |
| | | F. ^{nat} Cu(<i>p,xn</i>) ⁶² Zn | 13 |
| | | G. ^{nat} Cu(<i>p,xn</i>) ⁶³ Zn | 14 |
| | | H. ^{nat} Cu(<i>p,xn</i>) ⁶⁵ Zn | 15 |
| | | I. ^{nat} Cu(<i>p,x</i>) ⁵⁶ Co | 15 |
| | | J. ^{nat} Cu(<i>p,x</i>) ⁵⁸ Co | 16 |
| | | K. ^{nat} Mo(<i>p,x</i>) ^{96m+g} Tc | 16 |

* Corresponding author: r.capoteno@iaea.org

| | |
|---|----|
| III. MONITOR REACTIONS FOR DEUTERON BEAMS | 18 |
| A. $^{27}\text{Al}(d,x)^{22}\text{Na}$ | 18 |
| B. $^{27}\text{Al}(d,x)^{24}\text{Na}$ | 19 |
| C. $^{nat}\text{Ti}(d,xn)^{48}\text{V}$ | 19 |
| D. $^{nat}\text{Ti}(d,x)^{46}\text{Sc}$ | 20 |
| E. $^{nat}\text{Cu}(d,xn)^{62}\text{Zn}$ | 21 |
| F. $^{nat}\text{Cu}(d,xn)^{63}\text{Zn}$ | 21 |
| G. $^{nat}\text{Cu}(d,xn)^{65}\text{Zn}$ | 22 |
| H. $^{nat}\text{Fe}(d,x)^{56}\text{Co}$ | 23 |
| I. $^{nat}\text{Ni}(d,x)^{61}\text{Cu}$ | 23 |
| J. $^{nat}\text{Ni}(d,x)^{56}\text{Co}$ | 24 |
| K. $^{nat}\text{Ni}(d,x)^{58}\text{Co}$ | 25 |
| IV. MONITOR REACTIONS FOR ^3He BEAMS | 25 |
| A. $^{27}\text{Al}(^3\text{He},x)^{22}\text{Na}$ | 25 |
| B. $^{27}\text{Al}(^3\text{He},x)^{24}\text{Na}$ | 26 |
| C. $^{nat}\text{Ti}(^3\text{He},x)^{48}\text{V}$ | 27 |
| D. $^{nat}\text{Cu}(^3\text{He},x)^{66}\text{Ga}$ | 27 |
| E. $^{nat}\text{Cu}(^3\text{He},x)^{63}\text{Zn}$ | 28 |
| F. $^{nat}\text{Cu}(^3\text{He},x)^{65}\text{Zn}$ | 28 |
| V. MONITOR REACTIONS FOR ^4He BEAMS | 29 |
| A. $^{27}\text{Al}(\alpha,x)^{22}\text{Na}$ | 29 |
| B. $^{27}\text{Al}(\alpha,x)^{24}\text{Na}$ | 30 |
| C. $^{nat}\text{Ti}(\alpha,x)^{51}\text{Cr}$ | 30 |
| D. $^{nat}\text{Cu}(\alpha,x)^{66}\text{Ga}$ | 31 |
| E. $^{nat}\text{Cu}(\alpha,x)^{67}\text{Ga}$ | 32 |
| F. $^{nat}\text{Cu}(\alpha,x)^{65}\text{Zn}$ | 32 |
| VI. SUMMARY AND CONCLUSIONS | 33 |
| Acknowledgements | 33 |
| References | 34 |

I. INTRODUCTION

A. Mission of IAEA: Importance of Medical and Industrial Applications of Radionuclides

Within Article II, Objectives, of the IAEA Statute: “*The (International Atomic Energy) Agency shall seek to accelerate and enlarge the contribution of atomic energy to peace, health and prosperity throughout the world*”.

The IAEA document on “Medium Term Strategy 2012–2017” stated clearly: *The Agency will seek to support the safe and effective use of radiation medicine for the diagnosis and treatment of patients. . . In the area of utilisation of research reactors and accelerators for radioisotope production and radiation technology, the Agency will support Member States in building capacity for sustainable production and related quality assurance systems, and ensure accessibility to products and techniques that have a unique added value . . .*

Hence, development and optimisation of radionuclide production both for industrial and medical applications are of considerable and indisputable interest to the IAEA. Cyclotrons and other particle accelerators, available in recent years in an increasing number of countries, often with support of the IAEA, are being used for the production of radioisotopes for both diagnostic and therapeutic purposes. The physical basis of their production is described through interaction of charged particles, such as protons, deuterons and alphas, with matter. These processes have to be well understood in order to produce radioisotopes to high-purity in an efficient and safe manner.

Deficiencies, however, still exist in:

- knowledge of optimal production routes,
- minimisation of contaminants/impurities,
- decay data: half-lives, energies and emission probabilities for α , β , γ and X-rays.

Optimisation involves a selection of the projectile energy range that will maximise the yield of the product and minimise that of the radioactive impurities. Whereas the non-isotopic impurities produced can be mostly removed by chemical separations, the level of isotopic impurities can be suppressed, or at least decreased significantly, only by using enriched isotopes as target materials and/or by a careful selection of the particle energy range effective in the target. Besides commercial or in-house medical radionuclide production, reactions with low- energy charged particles are of primary importance for several industrial and scientific applications. Some examples are (see also Ref. [1]):

- ion-beam analysis techniques use many specific reactions to identify material properties, surface analysis in industrial applications, thin layer and on-line activation analysis,

- dose rate estimations around nuclear installations,
- production of radionuclide sources for industry, research and agriculture (calibration sources, tracers, high intensity sources for irradiations),
- understanding of nucleo-synthesis and reaction rates in nuclear astrophysics and cosmochemistry.

A common characteristic of all above-mentioned applications is the need for accurate and reliable cross-section data consistent over a wide energy range.

B. Needs for Evaluated Data – Start of Programmes

During the second half of the 20th century, many laboratories reported a large body of experimental cross-section data relevant to radionuclide production, and the Nuclear Reaction Data Centres (NRDC) network compiled most of these data into EXFOR [2]. Although in the 1980s the production methods were well established for about a dozen commercially available medical radionuclides, no evaluated or recommended nuclear datasets were available. The need for standardisation was pointed out at two pioneering IAEA meetings:

- Consultants’ Meeting on Nuclear Data for Medical Radioisotope Production, IAEA Headquarters, Vienna, April 1981 [3],
- Consultants’ Meeting on Data Requirements for Medical Radioisotope Production, Institute of Physical and Chemical Research (RIKEN), Tokyo, April 1987 [4].

Based on the recommendations made at these meetings, the first modest attempt was made by the IAEA to collect the available information on monitor reactions [5]. Further discussions occurred at a larger Advisory Group Meeting on Intermediate Energy Data for Applications held in October 1990 in Vienna [6]; as a consequence a Working Group on Nuclear Data for Medical Applications was set-up. However, no systematic effort had been devoted to the standardisation of available cross-section data.

Such a task would be too ambitious for any single national laboratory, implying a need for well-focused international effort. Under these circumstances, the IAEA decided to undertake and organise a Co-ordinated Research Project (CRP) entitled “Development of Reference Charged Particle Cross-section Database for Medical Radioisotope Production”. The project was initiated in 1995. Focus was placed on the radionuclides most commonly used for diagnostic purposes and on the related beam monitor reactions in order to meet data needs at that time. That project represented the first major international effort dedicated to the standardisation of cross-section data for radionuclide production through light charged-particle nuclear reactions and for monitoring the characteristics

of the particle beams used in these productions (protons, deuterons, ³He and α -particles). This CRP involved eleven experts from nine institutes and national radionuclide production centres. The participants met at three Research Co-ordination Meetings held in Vienna, Austria in 1995 [7], Faure (Cape Town), South Africa in 1997 [8], and Brussels, Belgium in 1998 [9]. Although the major emphasis in the CRP was on the energy region up to 30 MeV, higher energy data up to 60–80 MeV were also considered.

The methodology to obtain recommended data involved:

- compilation of published experimental production cross-section data for the radioisotopes most commonly used in diagnostic nuclear medicine (SPECT procedures and β^+ emitters) and for the most important monitor reactions (data cut-off 1999),
- evaluation and selection of the datasets,
- fitting by different theoretical nuclear reaction codes and statistical methods. Choice of best fit,
- development of calculation tools for predicting unknown data.

In addition to the cross sections, yields of the radionuclides calculated from the recommended data were provided for users. However, the evaluation methodology for charged particle data was not yet well developed, and some teach-in effort was initially necessary. The CRP produced a much needed database and an **IAEA-TECDOC-1211** handbook was published in 2001 [1]. An on-line version was made available at the medical portal www-nds.iaea.org/medical/monitor_reactions.html. This database was partly updated by inclusion of new experimental data, corrections of factual errors and a systematic spline fit in 2007 [10–12]. Although the recommended cross sections were believed to be accurate enough to meet the demands of all current applications, further development of the evaluation methodology and more experiments were needed for determination of the uncertainties and their correlations. Also the growing number of emerging radionuclides, especially for β^+ imaging [13] and therapeutic applications (see CRP on “Nuclear Data for Production of Therapeutic Radionuclides” [14]) necessitated a widening of the scope of the existing database.

The IAEA Nuclear Data Section has sponsored various meetings to discuss possible nuclear data requirements for medical applications up to 2025–2030. Specific recommendations from three meetings [15–17] were brought together in June 2011 to formulate the scope, work programme and deliverables of a CRP designed to focus on further improvements to specific charged-particle monitor reactions and nuclear data for medical radionuclides.

This paper has been prepared to serve as the final documentation of an International Atomic Energy Agency (IAEA) Coordinated Research Project that began in 1992 and terminated in 2016 with the following objectives:

- update and broaden the cross-section database given in IAEA-TECDOC-1211 [1],
- undertake a full survey of new literature data and earlier experiments,
- perform dedicated experiments,
- correct (if needed) published datasets for up to date monitor cross sections or nuclear decay characteristics,
- evaluate (if necessary re-evaluate IAEA-TECDOC-1211) and select datasets,
- fit with Padé statistical approach,
- produce new recommended data with uncertainties (for monitor reactions).

The results of this CRP have been made available to users in two forms:

- three parallel reports without tabulated recommended values in referenced scientific journals dealing respectively with monitors (lead author A. Hermanne, this report), diagnostic radionuclides (lead author F. Tárkányi, about 100 reactions) and therapeutic radionuclides (lead author J.W. Engle, about 40 reactions),
- all numerical recommended values and yields placed in the on-line medical database of the IAEA (prepared by S. Takács).

C. Significance of Nuclear Data in Monitoring Charged-particle Beams

Experimental determinations of cross sections and excitation functions of charged particle reactions for radionuclide production rely mostly on an activation process (bombardment of a target with a particle beam) followed by γ -spectroscopic identification and quantification of the induced activity. Calculation of particle energy-dependent cross sections is then performed from the activation formula,

$$A(E) = \lambda N(E) = n\sigma(E)\Phi(1 - \exp(-\lambda t)), \quad (1)$$

where $A(E)$ – is the measured activity of the radionuclide produced at a given energy E and corrected to end of bombardment (EOB) (Bq), λ – is the decay constant of the produced radionuclide (s^{-1}), $N(E)$ – is the number of nuclei produced in the target after irradiation, n – is the surface density of target nuclei (cm^{-2}), $\sigma(E)$ – is the cross section for the production of the radionuclide at a given energy E (cm^2), Φ – is the flux of incident beam particles (s^{-1}), and t – the irradiation time (s).

A reliable and accurate knowledge of the energy and intensity of the bombarding particles is required. Faraday cup measurements of beam current (collecting the

charge passing through the sample, mostly 10–100 nA) are sometimes not possible or not accurate enough because of leakage currents, secondary electrons, non-total stoppage, and straggling. Direct energy measurement requires complicated techniques that are often unavailable at the research facility (analysing magnets, time of flight techniques). The use of monitor reactions is a simple, convenient and inexpensive means of determining the energy and intensity of the bombarding beam. Selected materials are activated in the beam under study by well-known nuclear reactions, and the calculated cross sections obtained are compared with recommended values (best activation curves over a wider energy range). Physically admissible corrections to beam energy and intensity are applied to the initially estimated beam characteristics until good agreement is obtained between the measured and recommended excitation functions [18, 19].

The monitoring of beam parameters is also essential in numerous other applications such as charged particle activation analysis, thin layer activation, estimation of neutron yield and residual activity of accelerator components, calculation of activity for radiation safety and simulation of radiation damage. When using monitor reactions to characterise charged particle beams, reliable and accurate cross-section data are required as the excitation functions have to be known at the “standard” level. Therefore, the decision was made to include in this CRP the first attempt to produce uncertainties for the recommended data of the monitor reactions. The most important and commonly employed nuclear reactions for monitoring light ion charged particle beams (p , d , ^3He , α) are considered and some promising new reactions on previously used targets were included.

D. Decay Data Needs for Charged-particle Monitor Reactions

The transformation of count rates obtained directly from γ -ray spectroscopy to the activity produced at a reference time relies on a sound knowledge of the emission probabilities (intensities) of appropriate γ -ray lines and on the half-life of the radionuclide in order to correct for decay during the irradiation, cooling and measurement times. However, the values used by the authors of experimental studies are not always the most up to date, and can vary due to the fact that the sources of the decay data may well have different values. We recommend decay data retrieved from the ENSDF database [20] by one of the two most popular retrieval codes - LiveChart of Nuclides (developed by the IAEA Nuclear Data Section) [21] or NuDat (version 2.6; developed by US National Nuclear Data Center, Brookhaven National Laboratory) [22]. Available radionuclide decay-data evaluations should also be considered from the database of the Decay Data Evaluation Project (DDEP) which is maintained at the Laboratoire National Henri Becquerel [23].

Recommended decay data do change as a consequence

TABLE I. Decay data of radionuclides formed from proton, d , ^3He , and α monitor reactions as present in IAEA-TECDOC-1211 [1], the monitor update undertaken in 2007 [10], ENSDF [20], and the Coordinated Research Project (CRP) evaluations^a.

| Radionuclide | TECDOC-1211 | update 2007 | ENSDF ^b | Coordinated Research Project |
|-------------------|----------------------------------|-------------|--------------------|--|
| | T _{1/2} of radionuclide | | | |
| ²² Na | 2.60 y | 2.602 y | 2.6018 (22) y | |
| ²⁴ Na | 14.96 h | 14.659 h | 14.997 (12) h | |
| ⁴⁶ Sc | - | - | 83.79 (4) d | |
| ⁴⁸ V | 15.98 d | 15.975 d | 15.9735 (25) d | |
| ⁵¹ Cr | 27.70 d | 27.704 d | 27.7010 (11) d | |
| ⁵⁶ Co | 77.70 d | 77.7 d | 77.236 (26) d | |
| ⁵⁸ Co | - | - | 70.86 (6) d | |
| ⁵⁷ Ni | 1.50 d | 1.503 d | 35.60 (6) h | |
| ⁶¹ Cu | 3.40 h | 3.333 h | 3.339 (8) h | 3.366 (33) h (Eval. by M.-M. Bé) |
| ⁶² Zn | 9.26 h | 9.26 h | 9.193 (15) h | |
| ⁶³ Zn | 38.1 min | 38.1 min | 38.47 (5) min | 38.33 (10) min (Eval. by A.L. Nichols) |
| ⁶⁵ Zn | 244.10 d | 244.1 d | 243.93 (9) d | |
| ⁶⁶ Ga | 9.49 h | 9.49 h | 9.49 (3) h | 9.305 (8) h (Eval. by F.G. Kondev) |
| ⁶⁷ Ga | 3.26 d | - | 3.2617 (5) d | |
| ^{96g} Tc | - | - | 4.28 (7) d | |
| Radionuclide | E _γ (keV) | | | |
| ²² Na | 1274.5 | 1274.53 | 1274.537 (7) | |
| ²⁴ Na | 1368.6 | 1368.598 | 1368.626 (5) | |
| ⁴⁶ Sc | - | - | 889.277 (3) | |
| | - | - | 1120.545 (4) | |
| ⁴⁸ V | 983.5 | 983.501 | 983.525 (4) | |
| | 1312.0 | 1312.046 | 1312.106 (8) | |
| ⁵¹ Cr | 320.1 | 320.084 | 320.0824 (4) | |
| ⁵⁶ Co | 846.8 | 846.812 | 846.770 (2) | |
| | 1238.3 | 1238.317 | 1238.288 (3) | |
| ⁵⁸ Co | - | - | 810.7593 (20) | |
| ⁵⁷ Ni | - | 127.226 | 127.164 (3) | |
| | 1377.6 | 1377.62 | 1377.63 (3) | |
| ⁶¹ Cu | 283.0 | 282.956 | 282.956 (10) | 282.956 (2) (Eval. by M.-M. Bé) |
| | 656.0 | 656.008 | 656.008 (10) | 656.008 (4) (Eval. by M.-M. Bé) |
| ⁶² Zn | - | 548.38 | 507.60 (10) | |
| | 596.7 | 596.70 | 596.56 (13) | |
| ⁶³ Zn | 669.8 | 669.76 | 669.62 (5) | 669.93 (4) (Eval. by A.L. Nichols) |
| | 962.2 | 962.17 | 962.06 (4) | 962.01 (3) (Eval. by A.L. Nichols) |
| ⁶⁵ Zn | 1115.5 | 1115.518 | 1115.539 (2) | |
| ⁶⁶ Ga | - | - | 833.5324 (21) | 833.5324 (21) (Eval. by F.G. Kondev) |
| | 1039.3 | 1039.35 | 1039.220 (3) | 1039.220 (3) (Eval. by F.G. Kondev) |
| ⁶⁷ Ga | 184.6 | 184.578 | 184.576 (10) | |
| | - | 300.218 | 300.217 (10) | |
| ^{96g} Tc | - | - | 778.22 (4) | |
| | - | - | 812.54 (4) | |
| | - | - | 849.86 (4) | |
| Radionuclide | I _γ (%) ^c | | | |
| ²² Na | 99.94 | 99.94 | 99.940 (14) | |
| ²⁴ Na | 100.0 | 100 | 99.9936 (15) | |
| ⁴⁶ Sc | - | - | 99.9840 (10) | |
| | - | - | 99.9870 (10) | |
| ⁴⁸ V | 99.99 | 99.99 | 99.98 (4) | |
| | 97.49 | 97.49 | 98.2 (3) | |
| ⁵¹ Cr | 9.83 | 9.83 | 9.910 (10) | |
| ⁵⁶ Co | 99.9 | 99.9 | 99.9399 (23) | |
| | 67.0 | 67.0 | 66.46 (12) | |
| ⁵⁸ Co | - | - | 99.450 (10) | |
| ⁵⁷ Ni | - | 12.9 | 16.7 (5) | |
| | 77.9 | 77.9 | 81.7 (24) | |
| ⁶¹ Cu | 12.5 | 12.2 | 12.2 (22) | 12.0 (17) (Eval. by M.-M. Bé) |
| | 10.66 | 10.8 | 10.8 (20) | 10.4 (15) (Eval. by M.-M. Bé) |
| ⁶² Zn | - | 15.2 | 14.8 (14) | |
| | 25.7 | 25.7 | 26.0 (20) | |
| ⁶³ Zn | 8.4 | 8.4 | 8.2 (3) | 8.19 (32) (Eval. by A.L. Nichols) |
| | 6.6 | 6.6 | 6.5 (4) | 6.50 (16) (Eval. by A.L. Nichols) |
| ⁶⁵ Zn | 50.75 | 50.75 | 50.04 (10) | |
| ⁶⁶ Ga | - | - | 5.9 (3) | 5.9 (3) (Eval. by F.G. Kondev) |
| | 37.9 | 37.9 | 37.0 (20) | 37.0 (20) (Eval. by F.G. Kondev) |
| ⁶⁷ Ga | 20.4 | 20.4 | 21.410 (10) | |
| | - | 16.6 | 16.64 (12) | |
| ^{96g} Tc | - | - | 99.760 (10) | |
| | - | - | 82 (3) | |
| | - | - | 98 (4) | |

^a Tables II, III, IV, and V exactly provide the decay data recommended for monitoring.^b ENSDF nuclear structure and decay data can be easily extracted, understood and studied in an attractive user-friendly manner by means of LiveChart of Nuclides [21] and NuDat [22].^c γ -ray intensities I_γ defined in energy order per each product radionuclide as presented in the listing of the E_γ data above.

of improved measurements and re-evaluations, and appropriate references to the adopted data are often missing in published cross-section articles. Hence, substantial efforts were made during the course of this CRP to check and, if necessary, correct the published cross-section values in order to rectify the impact of outdated or erroneous decay data, as well as stimulate re-evaluations and updates of the decay data for selected radionuclides with respect to specific problems noted in the past (*e.g.*, disagreements between cross sections calculated for different γ -lines, or disagreements for radionuclides obtained from the same target in the same experiment). This situation can be best illustrated by the evolution of the reference decay data for the monitor reactions presented in Table I. New evaluations were undertaken within the project for three activation products used in specific monitor reactions (^{61}Cu , ^{63}Zn , and ^{66}Ga), and were presented at the Second Research Coordination Meeting by Kellett, Nichols, and Kondev [24]. Full reports for the first two evaluations have been published in Ref. [25]. Results for these and other decay-data evaluations for both diagnostic and therapeutic radionuclides studied in this CRP will be published as a separate report elsewhere (lead author A.L. Nichols).

Both LiveChart [21] and NuDat [22] provide identical data, since they are both retrieval codes for data taken from the same ENSDF database [20]. However, differences outside quoted evaluated uncertainties exist between ENSDF [20] and DDEP [23] values (*e.g.*, for ^{24}Na and ^{57}Ni half-lives, probably due to their differing evaluation dates and/or methodologies). The recommended half-lives, and γ -ray energies and emission probabilities adopted in the cross-section calculations are listed in Tables II, III, IV, and V for particular reactions with proton, deuteron, ^3He and α beams, respectively (these decay data are taken from Ref. [22] which is effectively the ENSDF database). An uncertainty contribution from the decay data of 3-5% was considered as appropriate by the compilers in their assignment of the total experimental cross-section uncertainty (see Sec. I.F). Correlations between different experiments due to the use of the same decay data were neglected.

E. Recommended Curves and their Uncertainties

A purely statistical fit over the selected data points can be performed when the status of the experimental dataset is appropriate (*i.e.*, a reasonable number of independent measurements has been performed and collected with reliable estimations of their uncertainties and without inexplicable discrepancies). Often such fits use analytical functions, the most prominent being polynomials or the ratio of two polynomials. An analytical approximation based on the ratio of two polynomials was proposed by Padé over one hundred and twenty years ago [26], and has become one of the most important interpolation techniques of statistical mathematics [27, 28]. The Padé fitting method is briefly described in the following paragraphs for complete-

ness. The method of fitting applied in the present project was comprehensively described in the original reference by Vinogradov *et al.* [29] and some important questions concerning applications are presented in Refs. [30, 31]. A brief summary of the application of the method to beam-monitor reactions was given in Ref. [1].

A Padé-II approximant for a function $F(x)$ is a rational function $p_L(x)$ given as a ratio of two polynomials, which is described by altogether L parameters exactly matching the function $F(x)$ in L points. Note that L is an order of the polynomial presentation of the Padé approximant [27, 28]).

The Padé approximant, as a rational function, can be expressed by a set of polynomial coefficients or equivalently by a set of the coefficients of the polar expansion. The polar expansion makes use of analytical properties of rational functions in the complex plane. To this end one uses complex variables $z = x + iy$ and replaces $p_L(x)$ by $p_L(z)$ that can be expanded as

$$p_L(z_j) = c + \sum_l \frac{a_l}{z_j - \eta_l} + \sum_k \frac{\alpha_k(z_j - \epsilon_k) + \beta_k}{(z_j - \epsilon_k)^2 + \gamma_k^2}. \quad (2)$$

This equation is also called the resonance expansion, in which ϵ_k (η_l) and γ_k are the energy and the total half-width of the k -th (l -th) resonance respectively, while α_k (a_l) and β_k are the partial widths and interference parameters. The first sum corresponds to real poles, while the second sum relates to complex poles. A prominent disturbing feature of the numerically generated rational approximants is the appearance of real poles (zero denominators) inside the approximation interval which are physically meaningless and make the approximant unusable. These poles are accompanied closely by real zeros of the numerator, constituting noise doublets that prevent wide use of Padé approximants in data fitting. The noise doublets are not only neutralised but become useful, corresponding to the terms with $z \approx \eta_l$ inside the interval of approximation with relatively small coefficients a_l in the first sum of Eq. (2). These terms are cancelled in the present method and eliminated from the sum to generate satisfactory results. Normally, the noise doublets appear with increasing L at the final stages of the approximation and indicate, together with statistical criteria, that the generation of analytical information is very close to termination. The situation may differ if some points in the experimental input data deviate significantly from the general trend. Under such circumstances, the noise doublets appear at relatively low L near such points that are erroneous, inferior and/or outliers, describing them as local singularities rather than smooth components. When the singularities are eliminated, the resulting regularised curve ignores the particularly adverse points, and in this manner points with such aberrations are identified automatically.

From the point of view of statistical mathematics, the method of discrete optimisation is equivalent to the least-squares technique, and therefore the experimental dataset must be statistically consistent. When there are several

sets of experimental data and discrepancies between different sets are significantly larger than their declared uncertainties, statistical processing of the data is only possible after data selection by an expert. Padé codes construct the approximating rational function and calculate the coefficients of the pole expansion for each resonance in Eq. (2). Thus, we have an analytical expression that can be easily calculated at any energy point.

The Padé approximation is also very convenient for calculations of the data uncertainties and corresponding covariance matrices. Every individual fitting procedure is always based on a minimisation of the χ^2 functional,

$$\chi^2 = \frac{1}{N-L} \sum_{j=1}^N \frac{(p_L(z_j) - F_j)^2}{\sigma_j^2}, \quad (3)$$

where F_j are the available experimental data and σ_j are their uncertainties. Such minimisation is carried out iteratively by means of the discrete optimisation approach. The minimal deviation for a given L is computed by assessing and selecting L points from the available N points, and then determining the corresponding approximants from Eq. (3). Once this process has been completed, L is changed and the iteration is repeated until an overall minimum is found from all discrete possibilities available. The least-squares fitting is based on consideration of Eq. (3), and corresponds to uncorrelated data. Fitted data are independent of each other, and their uncertainties are used to weight each data point. Correlations are taken into account by extending the procedure to the generalised least-squares technique in which the weight is expressed by the inverse of a covariance matrix of the data. One of the advantages of the discrete optimisation technique compared with the continuous least-squares method (LSM) is the possibility of adopting manifold functionals. Theoretical estimates show that the mean quadratic deviation of the approximant found by discrete optimisation from the continuous LSM solution is about a factor of $(N/L)^{1/2}$ less than the average corridor of uncertainty of the analysed data. Thus, the approximant is statistically equivalent to the LSM solution.

Effective codes for practical applications of the Padé approximation have been developed by the Obninsk group [29]. The simplest versions of the codes permit analyses of up to 500 experimental points in terms of a number of parameters $L \leq 40$ and with a ratio limit for analysed functions of up to $\max(F_j)/\min(F_j) \leq 10^6$.

When assessing the uncertainties of a dataset and defining the possible uncertainty of each point, the known connections between the uncertainties of all points also need to be considered. A set of uncertainty data in this form is usually referred to as the covariance matrix of uncertainties. Such a covariance matrix in full diagonal form represents a dataset in which each point possesses independent uncertainty. Covariances of nuclear data can in principle be obtained by analysis of the experimental data if there are enough adequate measurements to define all reactions of interest in their respective energy ranges. These analy-

ses can be reinforced with additional information provided by physics laws and/or theoretical physics models. Such information is very important for the near-threshold regions where experimental data can be extremely contradictory in many cases. When considering a limited amount of experimental data, we are induced to combine the available data with information derived from an analytical model. Thus, the final cross-section covariances are calculated from the updated covariances for the model parameters. This procedure accounts consistently for the experimental uncertainties and the uncertainties of the model parameters to ensure that the final cross-section uncertainties are at least as good as the smaller of the two. Note that cross correlations between different experimental datasets which arise due to common systematic uncertainties are neglected in this work.

As in the case of evaluations based on experimental data only, the main problem of the combined approach remains an estimation of the correlations between the experimental data. The evaluator is normally faced with two significant difficulties when constructing a covariance matrix. The first problem relates to a disagreement between the uncertainty distribution based on the uncertainty estimates declared by authors and the reasonable statistical laws for uncertainties. Attempts to improve the distribution by rejection of some outlying data introduce badly controlled uncertainties in the final results and thwart a proper estimation of the systematic uncertainties, which are crucial for a complete uncertainty evaluation of all the available data. The second difficulty of covariance construction is connected with the essential differences in the matrices obtained with various approximating functions even if the resulting descriptions are practically indistinguishable. As a rule, the local uncertainties corresponding to the diagonal matrix elements increase for a large number of approximating parameters, but the off-diagonal elements responsible for correlations decrease. As a result, the uncertainty of any integral function averaged over a broad energy spectrum depends on the local uncertainties in a rather complex way, and is very sensitive to evaluations of long-range systematic uncertainties.

Analyses of the uncertainties for the present project have been carried out on the basis of the unrecognized uncertainty-estimation method [30]. Along with a consistent consideration of the statistical uncertainties of the experimental data, the method allows the determination of some systematic uncertainties that are usually underestimated by their authors and also the establishment of some implicit correlations of the data. This approach has been successfully used to evaluate the standard neutron cross sections [32], and is applied routinely to construct the uncertainties and corresponding covariance matrices for the Russian neutron data library BROND-3 [33].

The method of the unrecognized uncertainty estimation is based on the *a priori* assumption of equal reliability of all available experimental data, which of course excludes proven erroneous results. However, the systematic and statistical uncertainties of each experimental study are

determined in accordance with the observed distribution of the data. An initial description of the data is required at the beginning, and any deviations can be considered as selective values of the uncertainties. The averaged deviation of the experimental data from the approximating function is regarded as the systematic uncertainty, while the variances of deviations around the averaged values are identified as the statistical uncertainties for each experimental study. An optimal description of all data is achieved by the traditional iteration procedure of minimising the mean squares deviations with the statistical and systematic uncertainties obtained. Rational functions of an optimal order are used for the corresponding approximants, and the problem of small uncertainties (Peelle paradox) is taken into consideration within the minimisation process and construction of the resulting covariance matrices for the approximating function. More details of the method can be found in Ref. [30].

Only total uncertainties are determined in the majority of the experimental studies, and reasonable reconstructions of the corresponding systematic uncertainties are judged to be impossible to achieve in many of these cases. The method described above provides estimates of the systematic uncertainties on the basis of general statistical criteria which are valid for a reasonable number of studies. However, for a small number of the experimental measurements, underestimation of the systematic uncertainties is highly probable. Such underestimations will also occur in those cases whereby the same, very similar or other components of the same experimental equipment are used in a range of different studies, since any corresponding correlations have been neglected.

Analysing the complete set of available data, we have come to the conclusion that realistic total uncertainties cannot be defined as less than 4% for each of the reactions considered. Therefore, an additional systematic uncertainty of 4% has been included as part of each systematic uncertainty derived from statistical analyses of all the recommended cross sections.

F. Evaluated Cross Sections and Excitation Functions for Beam Monitor Reactions

Evaluated excitation functions for monitor reactions with beams of protons, deuterons, ^3He - and α -particles are presented in the following four sections. Along with the reactions discussed in Ref. [1] and updates in 2007 [10], several new and interesting reactions were identified at an IAEA meeting held in 2011 [16]. A total of 34 monitor reactions were defined (11 for protons, 11 for deuterons, 6 for ^3He , and 6 for α -particles), and the methodology for generation of the final evaluated excitation functions was identical. Compilers were designated for all of the monitor reactions, with the first responsibility to gather all existing information on the measured cross sections obtained from experiments in which quasi-mono-energetic particles interact with thin targets. Possible sources were

the data already used in IAEA-TECDOC-2011 and the 2007 update, data from earlier publications overlooked previously, new studies published after the 2007 update, and results of dedicated experiments performed as part of the agreed work programme of this CRP. All data were checked and if necessary and possible corrected for outdated nuclear decay data, erroneous natural abundances of isotopes in elements, or systematic errors (*e.g.*, particle flux) made obvious when comparing a dataset to the bulk of available data. However, a large majority of the data were used without any correction. Uncertainties for all cross-section data were also provided as either the values stated by the original authors, or when unavailable or not credible, the compilers had to assign uncertainties based on their experience with the experimental techniques. After critical analyses of all gathered data, a selection had to be made that was based on the rejection of data from either disputable experiments, or observed inconsistencies with the bulk of the data (mostly because of energy shift or erroneous estimation of the beam intensity). Normalisation of datasets for systematic errors are explicitly indicated in the text. Only in a minority of cases were part of the data in an individual set rejected, and they were more specifically deviating data points obtained at the low-energy end of a long stack irradiated at a high incident energy, or manifest outliers. The selected cross-section data and their uncertainties (original or adapted by the compiler) were transferred to Obninsk for Padé fitting by means of the techniques described in the previous section. Sometimes quoted uncertainties were increased (especially for data points near the threshold) to obtain better statistical consistency, or some discrepant parts of the datasets were deleted. Results of the Padé fit and the uncertainties were transferred to the IAEA in both graphical and listed forms, and are discussed separately for each monitor reaction in Secs. II to V.

A short tabulated reminder of the decay data is given at the beginning of each section (taken from Ref. [22]) as deemed suitable for the identification and quantification of the radionuclide in the irradiated monitor foils. All references of the studies that have given experimental cross sections in the relevant energy domain are listed, while also indicating which sets were not included in the 2007 update [10], followed by an overview of the de-selected datasets with reasons for their rejection. The characteristics of the Padé fit on the remaining datasets are discussed together with the energy-dependent behaviour of the total uncertainties given as percentages (uncertainty derived from statistical analysis combined with an additional 4% systematic uncertainty).

Finally, a short analysis is given of the nuclear reaction channels contributing to the overall excitation function. The notation for the formation reactions is $^AZ(\text{particle}, xn)^{A'}Z'$ if only neutrons are ejected in the reaction, or $^AZ(\text{particle}, x)^{A'}Z'$ when a combination of charged particles and neutrons (possibly as a cluster) are present in the outgoing channel. Each section also contains two figures: one figure that includes all identified

and relevant literature datasets with uncertainty bars as defined by the compilers, and the other figure with only the selected sets and their assessed uncertainties retained for the Padé fit (data points rejected during the fit are removed) and the resulting overall fit that includes uncertainty bands. For several reactions the energy range of the fit (best representation of experimental results) exceeds that of the useful range for monitoring, both at low and high energy end.

II. MONITOR REACTIONS FOR PROTON BEAMS

TABLE II. Reactions for monitoring proton beams and recommended decay data of the activation products ($T_{1/2}$ is the product half-life, and E_γ is the γ -ray energy in keV of the transition with intensity I_γ in %).

| Reaction | $T_{1/2}$ | E_γ (keV) | I_γ (%) | Useful range (MeV) |
|---|---------------------|------------------|----------------|--------------------|
| $^{27}\text{Al}(p,x)^{22}\text{Na}$ | 2.602 y | 1274.537 | 99.940 | 25–1000 |
| $^{27}\text{Al}(p,x)^{24}\text{Na}$ | 14.997 h | 1368.626 | 99.9936 | 30–100 |
| $^{nat}\text{Ti}(p,x)^{48}\text{V}$ | 15.9735 d | 983.525 | 99.98 | 5–100 |
| | | 1312.106 | 98.2 | |
| $^{nat}\text{Ti}(p,x)^{46}\text{Sc}$ | 83.79 d | 889.277 | 99.9840 | 20–80 |
| | | 1120.545 | 99.9870 | |
| $^{nat}\text{Ni}(p,x)^{57}\text{Ni}$ | 35.60 h | 127.164 | 16.7 | 15–100 |
| | | 1377.63 | 81.7 | |
| $^{nat}\text{Cu}(p,xn)^{62}\text{Zn}$ | 9.193 h | 507.60 | 14.8 | 15–100 |
| | | 596.56 | 26.0 | |
| $^{nat}\text{Cu}(p,xn)^{63}\text{Zn}$ | 38.47 min | 669.62 | 8.2 | 5–100 |
| | | 962.06 | 6.5 | |
| $^{nat}\text{Cu}(p,xn)^{65}\text{Zn}$ | 243.93 d | 1115.539 | 50.04 | 5–100 |
| $^{nat}\text{Cu}(p,x)^{56}\text{Co}$ | 77.236 d | 846.770 | 99.9399 | 50–100 |
| | | 1238.288 | 66.46 | |
| $^{nat}\text{Cu}(p,x)^{58}\text{Co}$ | 70.86 d | 810.759 | 99.450 | 30–1000 |
| $^{nat}\text{Mo}(p,x)^{96m+g}\text{Tc}$ | 4.28 d ^a | 778.22 | 99.760 | |
| | | 812.54 | 82.0 | 10–45 |
| | | 849.86 | 98.0 | |

^a Cumulative formation of ^{96g}Tc ($T_{1/2} = 4.28$ d) is measured after the γ -decay of the short-lived ^{96m}Tc ($T_{1/2} = 51.5$ min).

A. $^{27}\text{Al}(p,x)^{22}\text{Na}$

The formation of long-lived ^{22}Na ($T_{1/2} = 2.602$ y), easily assessed through an intense γ -ray line at 1274.537 keV (99.940% intensity), is the most widely used monitoring reaction for protons in the 25–1000 MeV energy range. A grand total of thirty-five publications with experimental cross-section data in the considered energy range were identified in the literature [34–68], and are represented with uncertainties in Fig. 1(a). One data point at 1600 MeV from Lüpke *et al.* (1993) [69] is not represented in Fig. 1(a).

Of those 35 references, the new sources of data added after the previous update of the IAEA monitor reactions website in 2007 [10] were as follows: Buthezezi *et al.* (2006) [36], Cline and Nieschmidt (1971) [37], Dittrich *et al.* (1990) [39], Khandaker *et al.* (2011) [42], Lefort and Tarrago (1963) [44], Marquez and Perlman (1951) [45], Marquez (1952) [46], Michel *et al.* (1995) [48], Morgan *et al.* (2003) [50], Schiekel *et al.* (1996) [51], Taddeucci *et al.* (1997) [54], Titarenko *et al.* (2003) [55], and Titarenko

et al. (2011) [65]. The energy range of the existing proton beam monitors evaluated in 2007 was limited to 100 MeV [10], whereas eight studies with data points above this energy limit appear in the current analysis.

The results of 12 studies were rejected and not considered for further analysis, and the reasons for their removal are given in parentheses: Aleksandrov *et al.* (1988) (data systematically too low) [57], Brun *et al.* (1962) (no numerical values available in reference, high and scattered data) [58], Gauvin *et al.* (1962) (data systematically shifted to higher energy) [59], Grütter (1982) (data systematically too low) [60], Hintz and Ramsey (1952) (data too high) [61], Korteling and Caretto (1970) (data too low) [62], Miyano (1973) (no numerical data available in reference) [63], Pulfer (1979) (data systematically low and scattered) [64], Titarenko *et al.* (2011) (unexplained wide spread of data) [65], Vukolov and Chukreev (1988) (values too high) [66], Walton *et al.* (1976) (data systematically too low) [67], and Williams and Fulmer (1967) (no numerical data available in reference) [68].

The datasets of the remaining 23 papers were used as input for a least-squares Padé fit [34–56]. A Padé function with 26 parameters was fitted to 265 selected data points with $\chi^2 = 1.47$, and covered energies up to 1000 MeV as shown in Fig. 1(b). Uncertainties include a 4% systematic uncertainty, and range from 25% near the reaction threshold to decrease below 4.5% between 44 and 800 MeV, and reach 5.2% at the highest energy. The rather sharp maximum of 43.65 mb at 43.7 MeV arises from a combination of two reactions with clustered emissions: $^{27}\text{Al}(p,\alpha d)^{22}\text{Na}$ (threshold 21.044 MeV) and $^{27}\text{Al}(p,\alpha pn)^{22}\text{Na}$ (threshold 23.325 MeV). The long disputed local bump between 80 and 150 MeV was shown by model calculations (TALYS code) to originate from contributions of the $^{27}\text{Al}(p,3p3n)^{22}\text{Na}$ and $^{27}\text{Al}(p,2p2nd)^{22}\text{Na}$ reactions with 52.7 and 50.4 MeV thresholds, respectively. Those reactions also feature a long high-energy tail of 3.5–6 mb above 100 MeV.

B. $^{27}\text{Al}(p,x)^{24}\text{Na}$

The formation of ^{24}Na ($T_{1/2} = 14.997$ h) with an easily assessed intense γ -ray line at 1368.626 keV (99.9936% intensity) can be used in parallel with ^{22}Na to monitor protons in the 40–1000 MeV range. However, ^{24}Na is likely produced from secondary neutrons in Al-foil stacks, especially above 200 MeV. We suspect this causes the deviation in measured data from the expected physical behaviour of the excitation function, and actively discourages the use of $^{27}\text{Al}(p,x)^{24}\text{Na}$ as a monitor reaction above 200 MeV. To be consistent with the original choices made in the 2007 update [10], all datasets up to 200 MeV were included in the compilation, and the fit and recommendations were limited to below such an energy.

Thirty-eight publications with experimental data up to 1000 MeV were identified in the literature, including 13 references that had data points only above 200 MeV. The

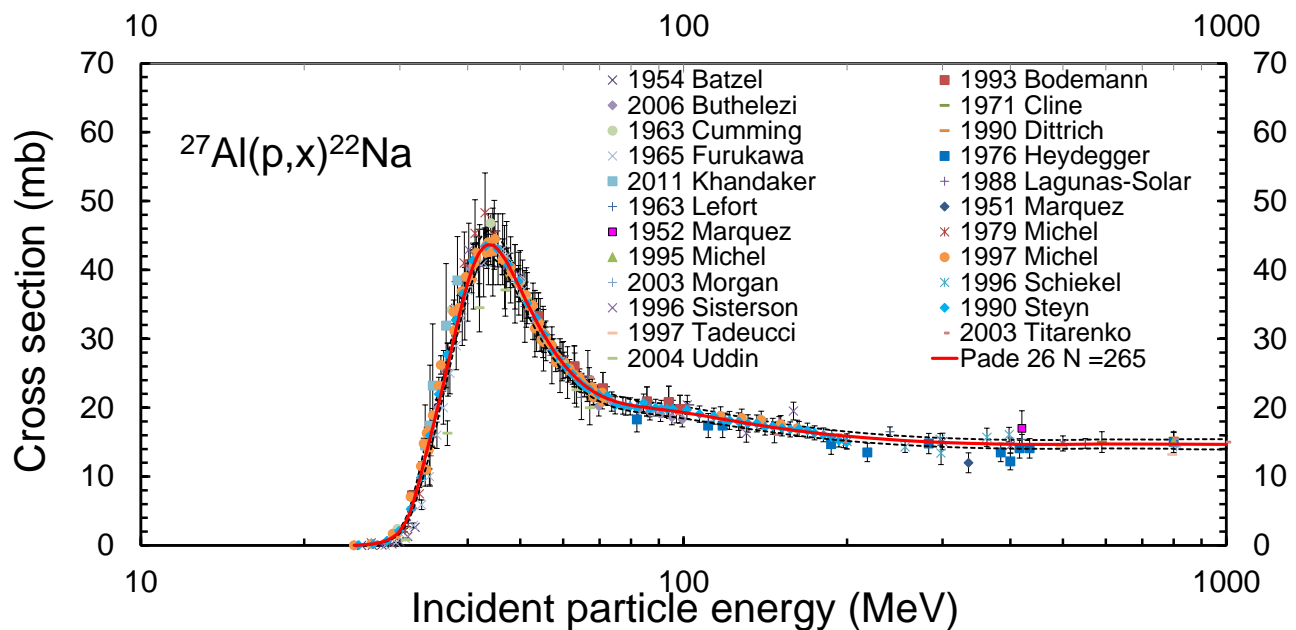
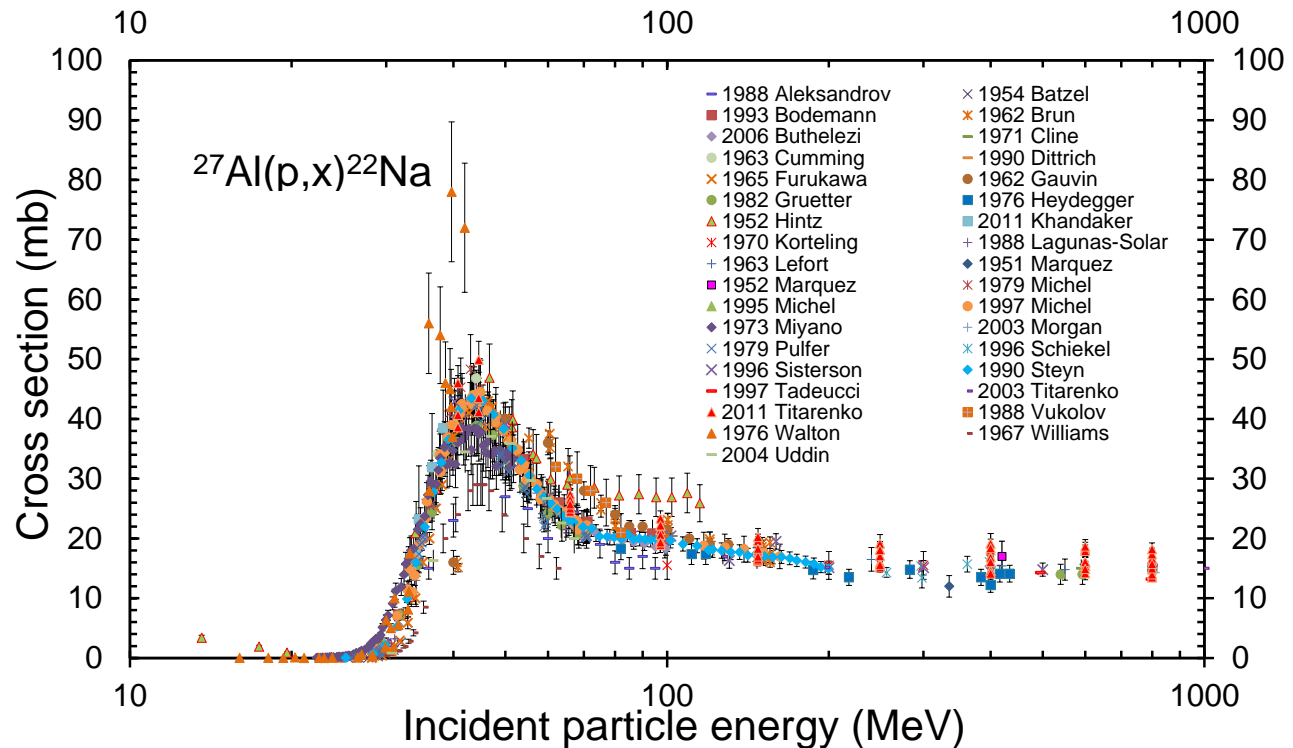


FIG. 1. (Color online) Evaluated Padé fit and experimental data from Refs. [34–68] for the $^{27}\text{Al}(p,x)^{22}\text{Na}$ monitor reaction.

remaining 25 sets from Refs. [35, 38, 42, 43, 49, 55, 56, 58–61, 63–65, 68, 70–79] are represented with uncertainties in Fig. 2(a).

Of those 25 references, the new sources of data added after the previous update of the IAEA monitor reactions website in 2007 [10] were as follows: Bodemann *et al.* (1995) [35], Khandaker *et al.* (2011) [42], Nair *et al.* (1993) [77], Titarenko *et al.* (2003) [55], and Titarenko

et al. (2006) [75].

The results of 13 studies were rejected and not considered for further analysis, and the reasons for their removal are indicated in parentheses: Bodemann *et al.* (1995) (data too high and scattered) [35], Brun *et al.* (1962) (no numerical values available in reference, data high and scattered) [58], Gauvin *et al.* (1962) (data shifted systematically to higher energy) [59], Gilbert (1956) (only one data

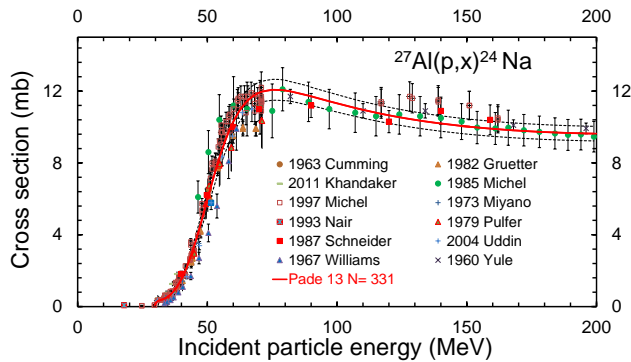
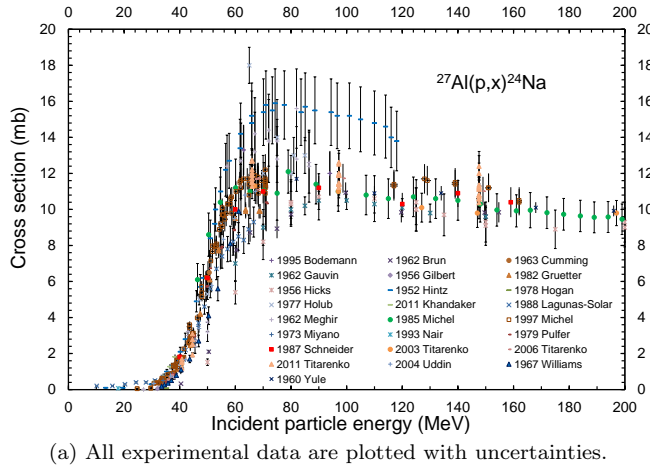


FIG. 2. (Color online) Evaluated Padé fit and experimental data from Refs. [35, 38, 42, 43, 49, 55, 56, 58–61, 63–65, 68, 70–79] for the $^{27}\text{Al}(p,x)^{24}\text{Na}$ monitor reaction.

point, too low) [70], Hicks *et al.* (1956) (scale shifted to higher energy) [71], Hintz and Ramsey (1952) (data too high, internal targets) [61], Hogan and Gadioli (1978) (systematically low and shifted to higher energy) [72], Holub *et al.* (1977) (values too high, strange shape near maximum) [73], Lagunas-Solar *et al.* (1988) (strange shape of the excitation curve) [43], Meghir (1963) (too high, strange shape) [74], Titarenko *et al.* (2003) [55] and Titarenko *et al.* (2006) (suspected contamination with secondary neutrons) [75], and Titarenko *et al.* (2011) (unexplained wide spread, suspected contamination with secondary neutrons) [65].

The datasets of the remaining 12 papers were used for further evaluation [38, 42, 49, 56, 60, 63, 64, 68, 76–79].

A Padé function with 13 parameters was fitted to 331 selected data points up to 200 MeV with $\chi^2 = 1.47$. The fit is compared with selected experimental data in Fig. 2(b). Uncertainties include a 4% systematic uncertainty, and decrease from 100% near the reaction threshold to below 6% above 60 MeV, before reaching 4.2% at the highest energy of 200 MeV. Cluster emission is not important in this case, and the main contribution arises from the $^{27}\text{Al}(p,3pn)$ reaction with a threshold at 32.601 MeV.

C. $^{nat}\text{Ti}(p,xn)^{48}\text{V}$

The $^{nat}\text{Ti}(p,xn)^{48}\text{V}$ reaction on readily available and corrosion resistant titanium is probably the most used monitor route for protons in the low and middle beam energy region (5–30 MeV), although the high energy tail of the excitation curve can also be of importance. The activation product ^{48}V ($T_{1/2} = 15.9735$ d) decays with the emission of two intense γ -ray lines at 983.525 keV (99.98% intensity) and 1312.106 keV (98.2% intensity). Thirty-one publications containing experimental cross-section data with incident particle energies up to 100 MeV were identified in the literature [11, 35, 49, 67, 80–106], and are shown with uncertainties in Fig. 3(a). The two unpublished datasets of Ref. [95] obtained with 17 and 25 MeV incident energy are represented separately as (a) and (b). Ten new references (eleven datasets) added after the previous update of the IAEA monitor reaction website in 2007 [10] are listed in alphabetical order: Bennett *et al.* (2012) [89], Garrido (2011) [92], Garrido *et al.* (2016) [93], Hermanne *et al.* (2011) [94], Hermanne *et al.* (2013a) [95], Khandaker *et al.* (2009) [85], Lebeda (2016a) [97], Takács *et al.* (2011) [101], Takács *et al.* (2013) [102], and Tárkányi *et al.* (2012) [103].

The results of 10 studies were rejected and not considered for further analysis, and the reasons for their removal

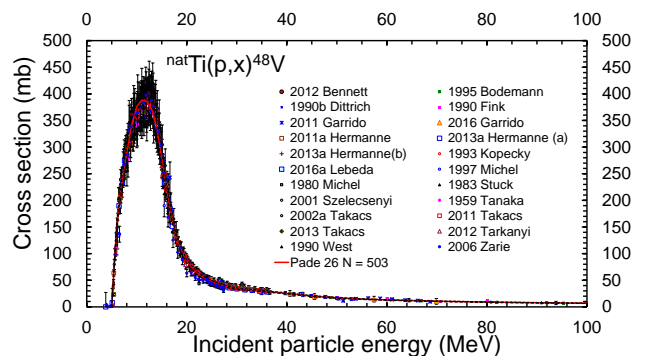
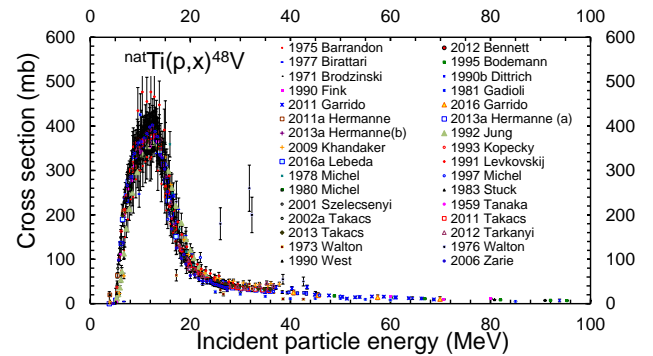


FIG. 3. (Color online) Evaluated Padé fit and experimental data from Refs. [11, 35, 49, 67, 80–106] for the $^{nat}\text{Ti}(p,xn)^{48}\text{V}$ monitor reaction. Ref. [95] contains two datasets indicated as (a) and (b).

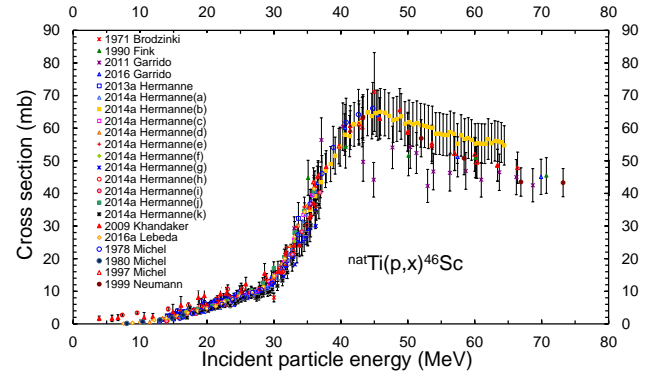
are indicated in parentheses: Barrandon *et al.* (1975) (systematically lower than other studies) [80], Birattari *et al.* (1977) (large shift in energy scale) [81], Brodzinski *et al.* (1971) (experiment with high energy protons, very high uncertainty) [82] Gadioli *et al.* (1981) (no numerical data in the publication) [83], Jung (1992) (shifted to higher energy) [84], Khandaker *et al.* (2009) (shifted to higher energy) [85], Levkovskij (1991) (values too high, even after correction for monitor reaction) [86], Michel *et al.* (1978)(values too high at lower energy) [106], Walton *et al.* (1973) (data systematically too low, unreliable beam current determination) [88], and Walton *et al.* (1976) (data systematically too low, unreliable beam current determination) [67].

The 22 datasets from the remaining 21 papers were used for the least-square fit [11, 35, 49, 87, 89–105]. A Padé function with 26 parameters was fitted to 503 selected data points with $\chi^2=1.15$ up to 100 MeV, as shown in Fig. 3(b). A number of outlying data points from Refs. [49, 92, 94, 103] were rejected from the fitting process, and are deleted from Fig. 3(b). Uncertainties include a 4% systematic uncertainty, and range between 50% near the reaction threshold to a minimum of 4.2% in the 14 to 35 MeV range before increasing to 6.5% at the highest energy. The unique abrupt maximum near 11 MeV ($\sigma_{max}=288$ mb) arises essentially from the $^{48}\text{Ti}(p,n)^{48}\text{V}$ reaction (threshold 4.898 MeV) on the most naturally abundant stable Ti isotope. Owing to the presence of simultaneously generated ^{48}Sc ($T_{1/2}=43.67$ h) from the $^{48}\text{Ti}(p,p2n)$ reaction that emits a γ -ray line at 983.526 keV, measurements for monitoring purposes have to be postponed by at least 14 d to allow the removal of the contaminating signal by decay.

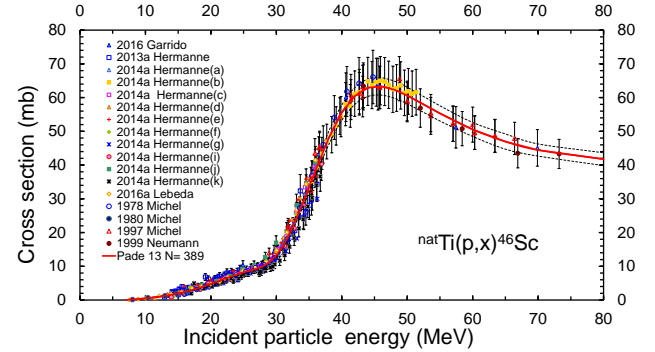
D. $^{nat}\text{Ti}(p,x)^{46}\text{Sc}$

As the availability of a second monitoring reaction on the same target material allows a check of internal consistency within the measurements, the $^{nat}\text{Ti}(p,x)^{46}\text{Sc}$ reaction was included to complement the previously discussed $^{nat}\text{Ti}(p,x)^{48}\text{V}$ reaction. An additional advantage is that the excitation function reaches a maximum at higher energy, and therefore increases the reliability of monitoring in the 20–60 MeV region. The long-lived ^{46}Sc ($T_{1/2}=83.79$ d) decays with the emission of two intense γ -ray lines at 889.277 keV (99.984% intensity) and 1120.545 keV (99.987% intensity). Twelve publications with experimental cross-section data at incident particle energies up to 80 MeV were identified in the literature [49, 82, 85, 91–93, 95, 97, 98, 106–108], and are shown with corresponding uncertainties in Fig. 4(a). Table 3 of Ref. [107] contained eleven sets of unpublished results for this reaction, as also obtained in the other listed experiments.

The reaction was not considered earlier in the IAEA monitor reaction website [10], and therefore all references are new. Five datasets were rejected from further analysis,



(a) All experimental data are plotted with uncertainties.



(b) Selected data compared with evaluated Padé fit based on 13 parameters (solid) and including uncertainty bands (dashed) to give a $\chi^2=1.083$ up to 80 MeV.

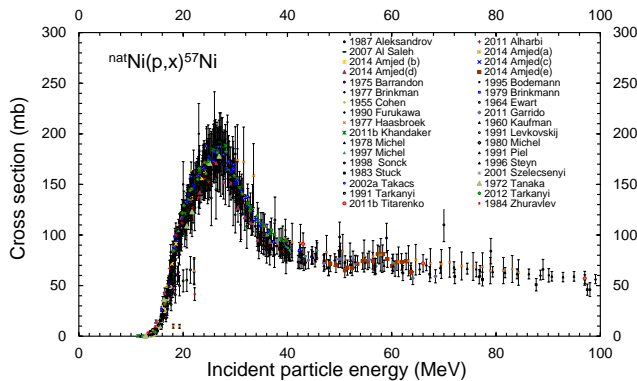
FIG. 4. (Color online) Evaluated Padé fit and experimental data from Refs. [49, 82, 85, 91–93, 95, 97, 98, 106–108] for the $^{nat}\text{Ti}(p,x)^{46}\text{Sc}$ monitor reaction. Ref. [107] contains 11 sets of data labelled 2014a Hermanne(a) to 2014a Hermanne(k).

and the reasons for their removal are indicated in parentheses: Brodzinski *et al.* (1971) (experiment with high energy protons, very high uncertainty) [82], Fink *et al.* (1990) (discrepant data) [91], Garrido (2011) (scattered values, superseded by [93]) [92], Hermanne *et al.* (2014a)(h) (values too high) [107], and Khandaker *et al.* (2009) (values too high) [85]. Additionally, all data points of Hermanne *et al.* (2014a)(b) above 50 MeV were rejected as being too high.

The remaining 17 datasets were used for further evaluation, as taken from Refs. [49, 93, 95, 97, 98, 106–108]. A Padé function with 13 parameters was fitted to 389 selected data points with $\chi^2=1.083$ up to 80 MeV, as shown in Fig. 4(b). Uncertainties include a 4% systematic uncertainty, and range from 50% near the reaction threshold to a minimum of 4.2% from 14 to 35 MeV incident particle energy, before increasing to 6.5% at the highest energy. The slowly rising excitation function with a rather modestly pronounced maximum around 35 MeV arises from a combination of reactions on stable $^{47,48,49}\text{Ti}$ isotopes in which two protons in combination with neutrons are emitted. The low-energy part of this behaviour is dominated by the $^{49}\text{Ti}(p,\alpha)^{46}\text{Sc}$ reaction with a threshold of 1.978 MeV.

E. ${}^{nat}\text{Ni}(p,x){}^{57}\text{Ni}$

The ${}^{nat}\text{Ni}(p,x){}^{57}\text{Ni}$ reaction is a valid alternative monitor reaction over the 20–50 MeV energy range. Activation product ${}^{57}\text{Ni}$ ($T_{1/2} = 35.60$ h) decays with the emission of two easily measured γ -ray lines at significantly different energies: 127.164 keV (16.7% intensity) and 1377.63 keV (81.7% intensity). Adoption of this reaction as a monitor requires an extensive and well-defined detector efficiency calibration undertaken with confidence, along with checks on the up to date acceptability of the γ -ray intensities to be used (see section I.D). Thirty publications with experimental cross-section data at incident particle energies up to 100 MeV were identified in the literature [11, 35, 49, 80, 86, 92, 98–100, 103, 106, 109–127], and are shown with uncertainties in Fig. 5(a). Reference [112] contains five datasets represented separately as 2014 Amjed(a) to (e). Seven new references added after the previous update of the IAEA monitor reaction website in 2007 [10] are listed in alphabetical order: Alharbi *et al.* (2011) [110], Al-Saleh *et al.* (2007) [111], Amjed *et al.* (2014) [112], Garrido (2011) [92], Khandaker *et al.* (2011b) [120], Tárkányi *et al.* (2012) [103], and Titarenko *et al.* (2011b)



(a) All experimental data are plotted with uncertainties.

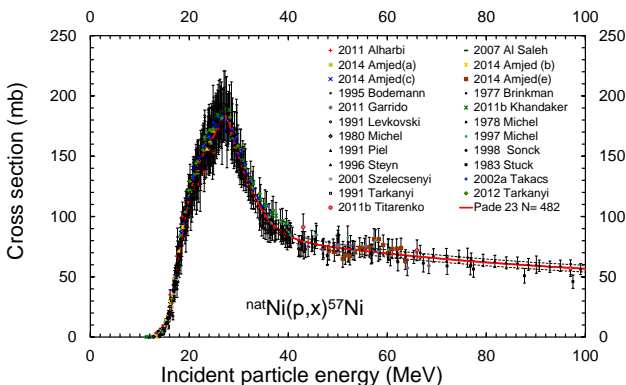
(b) Selected data compared with evaluated Padé fit based on 23 parameters (solid) and including uncertainty bands (dashed) to give a $\chi^2=1.24$ up to 100 MeV.

FIG. 5. (Color online) Evaluated Padé fit and experimental data from Refs. [11, 35, 49, 80, 86, 92, 98–100, 103, 106, 109–127] for the ${}^{nat}\text{Ni}(p,x){}^{57}\text{Ni}$ monitor reaction. Ref. [112] contains 5 sets of data labelled 2013 Amjed(a) to (e).

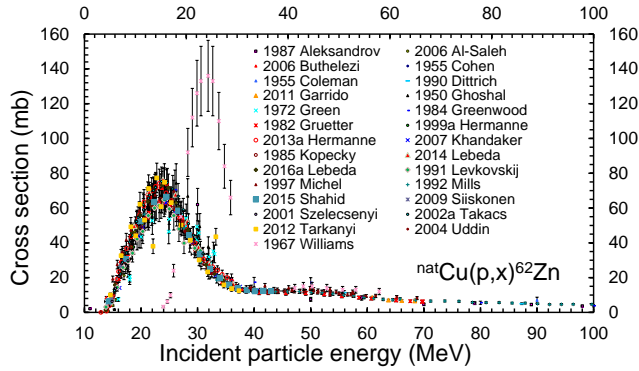
[126].

Ten references were removed from further analysis, and the reasons for their rejection are indicated in parentheses: Aleksandrov *et al.* (1987) (fluctuating values, systematically discrepant) [109], Barrandon *et al.* (1975) (values too low), [80], Brinkmann *et al.* (1979) (cross sections below threshold) [113], Cohen *et al.* (1955) (only one data point, too high) [115], Ewart and Blann (1964) (major energy shift) [116], Furukawa *et al.* (1990) (fluctuating data, original data unavailable) [117], Haasbroek *et al.* (1977) (large energy shift) [118], Kaufman (1960) (values too low) [119], Tanaka *et al.* (1972) (small energy shift) [124], and Zhuravlev *et al.* (1984) (discrepant; neutron-spectrum measurement) [127]. Additionally, the dataset of 2014 Amjed(d) [112] was also discarded.

The remaining 23 datasets were considered in the fitting process, as taken from Refs. [11, 35, 49, 86, 92, 98–100, 103, 106, 110–112, 114, 120–123, 125, 126]. A Padé function with 23 parameters was fitted to 482 selected data points with $\chi^2=1.24$ up to 100 MeV, as shown in Fig. 5(b). Uncertainties include a 4% systematic uncertainty, and range from nearly 100% near the reaction threshold to a minimum of 4.2% over 25 to 40 MeV before increasing to 5% at higher energies. The sharp peak in the excitation function around 27 MeV arises from a combination of the ${}^{58}\text{Ni}(p,pn){}^{57}\text{Ni}$ and ${}^{58}\text{Ni}(p,d){}^{57}\text{Ni}$ reactions with thresholds of 12.43 and 10.16 MeV, respectively.

F. ${}^{nat}\text{Cu}(p,xn){}^{62}\text{Zn}$

The ${}^{nat}\text{Cu}(p,xn){}^{62}\text{Zn}$ monitor reaction is often used in the 15–40 MeV energy range. Activation product ${}^{62}\text{Zn}$ ($T_{1/2} = 9.193$ h) decays with emission of two γ -ray lines at rather similar energies: 507.60 keV (14.8% intensity) and 596.56 keV (26.0% intensity). An advantage of using reactions on Cu for monitoring purposes is that this material is often used as the backing for electroplated targets, and hence insertion of additional monitoring foils is not required. Twenty-seven publications with experimental cross-section data at incident particle energies up to 100 MeV were identified in the literature [11, 36, 39, 49, 56, 60, 68, 86, 92, 95, 97, 100, 103, 109, 115, 128–139] and are shown with uncertainties in Fig. 6(a). Nine new references added after the previous update of the IAEA monitor reaction website in 2007 [10] are listed in alphabetical order: Buthelezi *et al.* (2006) [36], Garrido (2011) [92], Hermanne *et al.* (2013) [95], Khandaker *et al.* (2011) [42], Lebeda (2014) [136], Lebeda (2016) [97], Shahid *et al.* (2015) [138], Siiskonnen *et al.* (2009) [139], and Tárkányi *et al.* (2012) [103]. Seven references were removed from further analysis, and the reasons for their rejection are indicated in parentheses: Aleksandrov *et al.* (1987) (measurement at 20 MeV intervals and large uncertainties) [109], Ghoshal (1950) (values too high, and small energy shift) [130], Green and Lebowitz (1972) (values too low, large scatter energy shift) [131], Greenwood and Smither (1984) (data for ${}^{63}\text{Cu}(p,n)$ above threshold of ${}^{65}\text{Cu}(p,4n)$, good nor-



(a) All experimental data are plotted with uncertainties.

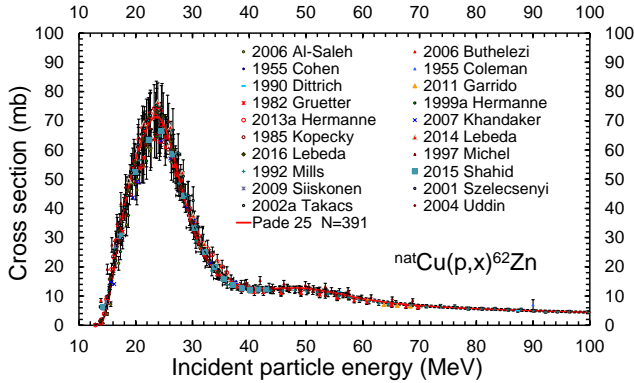
(b) Selected data compared with evaluated Padé fit based on 25 parameters (solid) and including uncertainty bands (dashed) to give a $\chi^2=1.91$ up to 100 MeV.

FIG. 6. (Color online) Evaluated Padé fit and experimental data from Refs. [11, 36, 39, 49, 56, 60, 68, 86, 92, 95, 97, 100, 103, 109, 115, 128–139] for the $^{nat}\text{Cu}(p,xn)^{62}\text{Zn}$ monitor reaction.

malisation not possible) [132], Levkovskij (1991) (data for $^{63}\text{Cu}(p,n)$ above threshold of $^{65}\text{Cu}(p,4n)$, good normalisation not possible) [86], Tárkányi *et al.* (2012) (scattered and outlying data) [103], and Williams and Fulmer (1967) (values too high) [68].

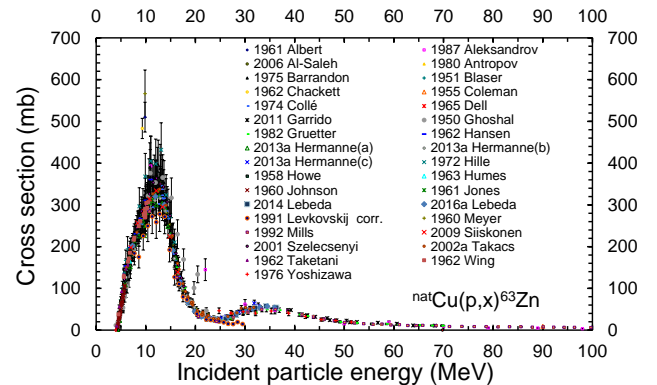
The remaining 20 datasets were considered in the fitting process, as taken from Refs [11, 36, 39, 49, 56, 60, 92, 95, 97, 100, 115, 128, 129, 133–139]. A Padé function with 25 parameters was fitted to 391 selected data points with $\chi^2=1.91$ up to 100 MeV, as shown in Fig. 6(b). Uncertainties include a 4% systematic uncertainty, and range from nearly 80% near the reaction threshold to a minimum of 5.2% over an incident particle energy range of 25 to 40 MeV before increasing to 7.2% at higher energies. The sharp peak in the excitation function around 24 MeV is due to the $^{63}\text{Cu}(p,2n)^{62}\text{Zn}$ reaction, while the smaller second maximum is attributed to the $^{65}\text{Cu}(p,4n)$ reaction.

G. $^{nat}\text{Cu}(p,xn)^{63}\text{Zn}$

The $^{nat}\text{Cu}(p,xn)^{63}\text{Zn}$ monitor reaction has proven more difficult to use, and hence is not as popular as other reactions. Primarily, the short half-life of the product ^{63}Zn ($T_{1/2}=38.47$ min.) makes measurements of the monitor

foils mandatory in the first hours after the end of bombardment, posing both dismantling and detector overload problems. Activity determinations are undertaken by measurement of two γ -ray lines of rather similar energies: 669.62 keV (8.2% intensity) and 962.06 keV (6.5% intensity). Thirty-one publications with experimental cross-section data at incident particle energies up to 100 MeV were identified in the literature [11, 60, 80, 86, 92, 95, 97, 100, 109, 128–130, 136, 137, 139–155], and are shown with uncertainties in Fig. 7(a). Reference [95] gives rise to three datasets represented separately. Five new references added after the previous update of the IAEA monitor reaction website in 2007 [10] are listed in alphabetical order: Garrido (2011) [92], Hermanne *et al.* (2013a) [95], Lebeda (2014) [136], Lebeda (2016) [97], and Siiskonen *et al.* (2009) [139].

Eleven references were removed from further analysis, and the reasons for their rejection are given in parentheses: Albert and Hansen (1961) (only one data point) [140], Aleksandrov *et al.* (1987) (measurement at 20 MeV intervals, and large uncertainties) [109], Blaser *et al.* (1951) (large energy shift) [142], Chackett *et al.* (1962) (only one data point) [143], Ghoshal (1950) (large energy shift) [130], Hille *et al.* (1972) (values too high)



(a) All experimental data are plotted with uncertainties.

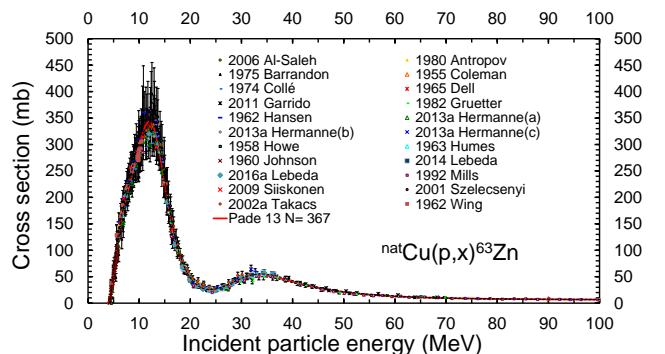
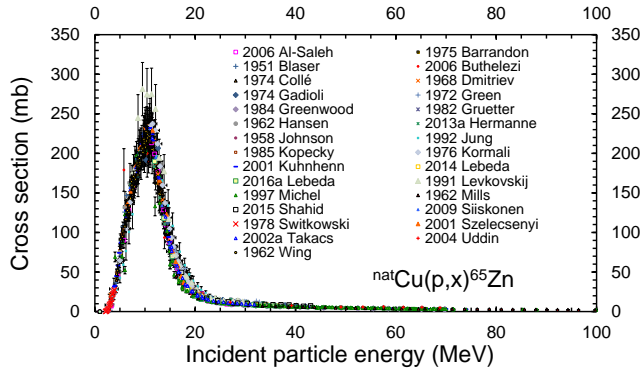
(b) Selected data compared with evaluated Padé fit based on 13 parameters (solid) and including uncertainty bands (dashed) to give a $\chi^2=1.035$ up to 100 MeV.

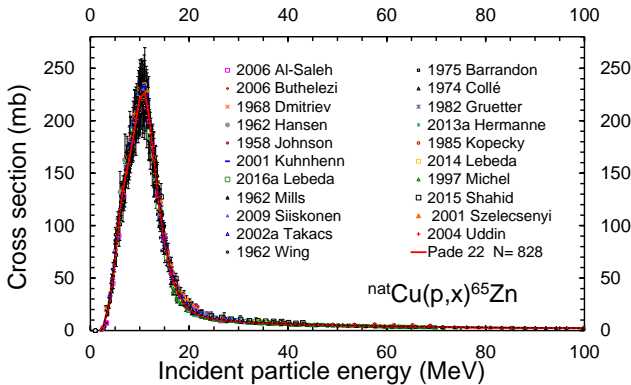
FIG. 7. (Color online) Evaluated Padé fit and experimental data from Refs. [11, 60, 80, 86, 92, 95, 97, 100, 109, 128–130, 136, 137, 139–155] for the $^{nat}\text{Cu}(p,xn)^{63}\text{Zn}$ monitor reaction. Ref. [95] contains 3 datasets represented separately as (a), (b) and (c).

[147], Jones *et al.* (1961) (only one data point) [151], Levkovskij (1991) (only data for the $^{63}\text{Cu}(p,n)$ reaction) [86], Meyer and Hintz (1960) (only one data point) [152], Taketani and Alford (1962) (large uncertainty in energy) [153], and Yoshizawa *et al.* (1976) (energy shift and large uncertainties)[155].

The remaining 22 datasets were considered in the fitting process, as taken from Refs. [11, 60, 80, 92, 95, 97, 100, 128, 129, 136, 137, 139, 141, 144–146, 148–150, 154]. A Padé function with 13 parameters was fitted to 367 selected data points with $\chi^2=1.035$ up to 100 MeV, as shown in Fig. 7(b). Uncertainties include a 4% systematic uncertainty, and range from nearly 10% near the reaction threshold to a minimum of 4.7% at incident particle energies up to 21 MeV, before increasing to 6.5% at the higher energies. The sharp peak in the excitation function around 12 MeV arises from the $^{63}\text{Cu}(p,2n)^{63}\text{Zn}$ reaction, while the smaller second maximum originates from the $^{65}\text{Cu}(p,4n)$ reaction.



(a) All experimental data are plotted with uncertainties.



(b) Selected data compared with evaluated Padé fit based on 22 parameters (solid) and including uncertainty bands (dashed) to give a $\chi^2=1.12$ up to 100 MeV.

FIG. 8. (Color online) Evaluated Padé fit and experimental data from Refs. [11, 36, 49, 56, 60, 80, 84, 86, 95, 97, 100, 128, 131, 132, 135–139, 142, 144, 146, 154, 157, 158, 160–162, 164] for the $^{nat}\text{Cu}(p,xn)^{65}\text{Zn}$ monitor reaction.

H. $^{nat}\text{Cu}(p,xn)^{65}\text{Zn}$

The $^{nat}\text{Cu}(p,xn)^{65}\text{Zn}$ monitor reaction results in long-lived activation product ^{65}Zn ($T_{1/2}=243.93$ d) that decays

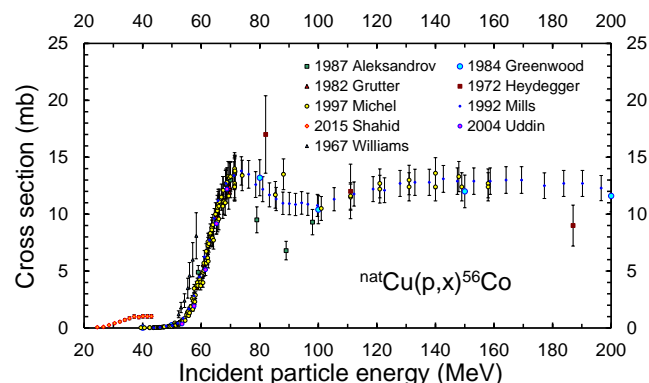
with the characteristic emission of a strong γ -ray line at 1115.539 keV (50.04% intensity), and permits lengthy activity measurements for months after the EOB. Forty-two publications with experimental cross-section data at incident particle energies up to 50 MeV were identified in the literature [11, 36, 49, 56, 60, 80, 84, 86, 90, 95, 97, 100, 128, 131, 132, 135–146, 148–152, 154, 156–164]. Several of these studies contain only one or two data points in the energy region of interest which did not assist greatly in judging the correctness of the energy scale. Therefore, they are not included in Fig. 8(a) because of the availability of other datasets that were more complete (Refs. [90, 140, 141, 143, 145, 148–152, 156, 159, 163] were not considered further). All of the data assessed beyond this initial stage are shown with their uncertainties in Fig. 8(a).

Six new references added since the previous update of the IAEA monitor reaction website in 2007 [10] are listed in alphabetical order: Buthelezi *et al.* (2006) [36], Hermanne *et al.* (2013a) [95], Lebeda (2014) [136], Lebeda (2016) [97], Shahid *et al.* (2015) [138], and Siiskonen *et al.* (2009) [139]. Along with the severely limited datasets noted earlier, eight other references were rejected and not considered for further analysis, and the reason for their removal are indicated in parentheses: Blaser *et al.* (1951) (cross sections energy shifted) [142], Gadioli *et al.* (1974) (cross sections energy shifted) [158], Green and Lebowitz (1972) (values too high) [131], Greenwood and Smither (1984) (values too high) [132], Jung (1992) (data points seem too high) [84], Kormali *et al.* (1976) (cross sections energy shifted) [161], Levkovskij (1991) (cross sections too high) [86], and Switkowski *et al.* (1978) (only neutron emission measurements, and cross-section data too low) [164].

The remaining 21 datasets were considered in the fitting process, as taken from Refs [11, 36, 49, 56, 60, 80, 95, 97, 100, 128, 135–139, 144, 146, 154, 157, 160, 162]. The data of Michel *et al.* (1997) [49] and Buthelezi *et al.* (2006) [36] below 16 MeV and the data point at 10 MeV of Mills *et al.* (1992) [137] were not included in the fitting. A Padé function with 22 parameters was fitted to 828 selected data points with $\chi^2=1.12$ up to 100 MeV, as shown in Fig. 8(b). Uncertainties include a 4% systematic uncertainty, and range from 6% near the reaction threshold to between 4.1% and 4.6% from 8 MeV upwards. Only the $^{65}\text{Cu}(p,n)^{65}\text{Zn}$ reaction contributes, and gives rise to the sharp peak in the excitation function around 11 MeV with $\sigma=226$ mb (threshold at 2.167 MeV).

I. $^{nat}\text{Cu}(p,x)^{56}\text{Co}$

The $^{nat}\text{Cu}(p,x)^{56}\text{Co}$ reaction is of interest to monitor higher-energy proton beams of 45 to 200 MeV by Cu foils, complementing beam monitoring by means of Zn radioisotopes below 50 MeV. Long-lived activation product ^{56}Co ($T_{1/2}=77.236$ d) decays by the emission of several strong γ -ray lines at 846.770 keV (99.9399% intensity) and 1238.288 keV (66.46% intensity), which permits



(a) All experimental data are plotted with uncertainties.

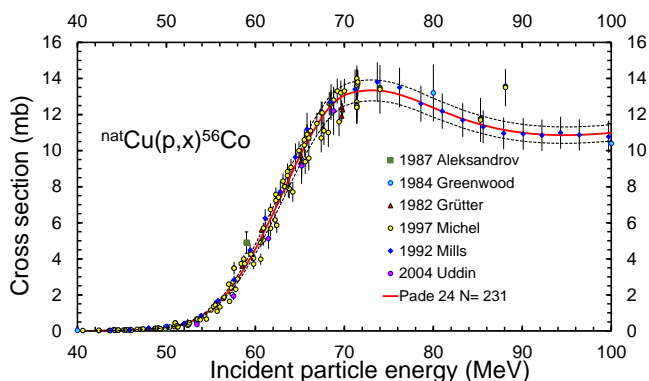
(b) Selected data compared with evaluated Padé fit based on 24 parameters (solid) and including uncertainty bands (dashed) to give a $\chi^2=1.50$ up to 100 MeV.

FIG. 9. (Color online) Evaluated Padé fit and experimental data from Refs. [49, 56, 60, 68, 109, 132, 137, 138, 159] for the $^{nat}\text{Cu}(p,x)^{56}\text{Co}$ monitor reaction.

lengthy activity measurements months after the EOB. Nine publications with experimental cross-section data at incident particle energies up to 200 MeV were identified [49, 56, 60, 68, 109, 132, 137, 138, 159], and are shown with uncertainties in Fig. 9(a). Six data points published in Ref. [35] are included in the extensive list of Ref. [49]. Data from Shahid *et al.* (2015) (all data points are below the threshold, and clearly discrepant) [138], Heydegger *et al.* (1972) (extensively scattered) [159], and Williams *et al.* (1967) (somewhat shifted to lower energy) [68] were not considered for further analysis. The data points of Aleksandrov *et al.* (1987) above 70 MeV [109] are too low, and were deleted during the course of the fitting process.

The remaining datasets as taken from Refs. [49, 56, 60, 109, 132, 137] were considered in the fitting process. A Padé function with 24 parameters was fitted to 231 selected data points with $\chi^2=1.50$ up to 100 MeV, as shown in Fig. 9(b). Uncertainties include a 4% systematic uncertainty, and decrease from nearly 25% at the reaction threshold to below 7% above 50 MeV, and below 5% from 65 MeV upwards. Formation of ^{56}Co by proton-induced reactions is possible by means of the strongly clustered emission $^{63}\text{Cu}(p,\alpha d2n)$ reaction with a threshold at 34.497 MeV.

J. $^{nat}\text{Cu}(p,x)^{58}\text{Co}$

The $^{nat}\text{Cu}(p,x)^{58}\text{Co}$ reaction was added to the list of monitors for proton beams because of the specific shape of the excitation function, with the cross sections extending above 20 mb up to 1000 MeV and showing two maxima at approximately 40 and 100 MeV. Long-lived activation product ^{58}Co ($T_{1/2}=70.86$ d) decays with a characteristically strong γ -ray line at 810.759 keV (99.450% intensity), which permits lengthy activity measurements months after the EOB.

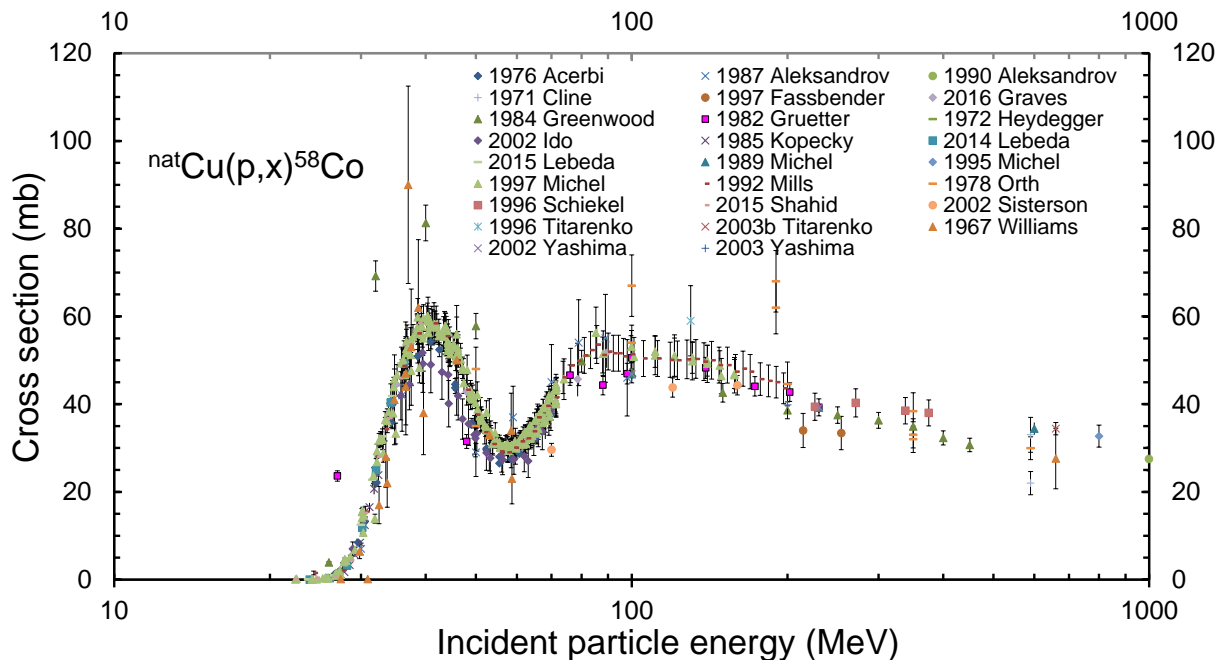
Twenty-six publications with experimental cross-section data at incident particle energies up to 1000 MeV were identified in the literature [37, 48, 49, 51, 60, 68, 109, 132, 135–138, 159, 165–177], and are shown with uncertainties in Fig. 10(a). The equivalent data of Brinkman *et al.* (1977) are clearly discrepant with a maximum cross section of 216.6 mb for an enriched ^{63}Cu target [113], and therefore have not been included in this figure.

Ten references were removed from further analysis, and the reasons for rejection are indicated in parentheses: Cline and Nieschmidt (1971) (two different values at the same energy, large scatter of data) [37], Fassbender *et al.* (1997) (values too low) [167], Greenwood and Smither (1984) (values too high) [132], Grütter (1982) (shift in energy) [60], Heydegger *et al.* (1972) (values too low) [159], Orth *et al.* (1978) (different cross-section values at same energy) [172], Sisterson (2002) (values too low) [173], Titarenko *et al.* (1996) (value too high) [174], Williams and Fulmer (1967) (values too high) [68], and Yashima *et al.* (2002) (thick Cu targets) [176].

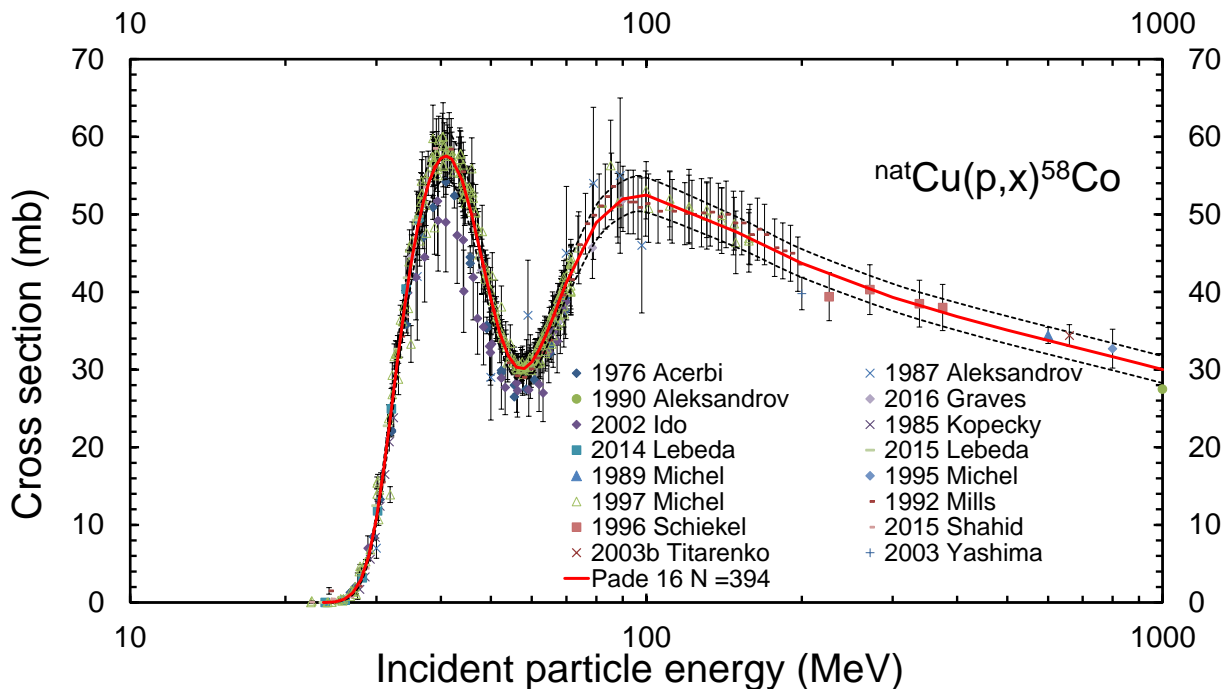
The remaining sixteen datasets were considered in the fitting process [48, 49, 51, 109, 135–138, 165, 166, 168–171, 175, 177]. A Padé function with 16 parameters was fitted to 394 selected data points with $\chi^2=1.74$ up to 1000 MeV, as shown in Fig. 10(b). Uncertainties include a 4% systematic uncertainty, and range from nearly 70% at the reaction threshold to between 4.2% and 6% over all higher beam energies up to 1000 MeV. The first maximum in the excitation function arises from strongly clustered emission reactions on ^{63}Cu ($^{63}\text{Cu}(p,\alpha d)$ with a threshold of 14.228 MeV and $^{63}\text{Cu}(p,\alpha pn)$ with a threshold of 16.488 MeV), while above 35 MeV the clustered emission of the ^{65}Cu ($^{65}\text{Cu}(p,\alpha d2n)$ reaction with a threshold of 32.325 MeV or reactions with individual nucleon emissions contribute to the weaker second maximum with the long tail (such as $^{63}\text{Cu}(p,3p3n)$ with a threshold of 45.237 MeV).

K. $^{nat}\text{Mo}(p,x)^{96m+g}\text{Tc}$

Although the $^{nat}\text{Mo}(p,x)^{96m+g}\text{Tc}$ reaction is not widely used to monitor proton beams, an appropriate evaluation is important to normalise the erroneous maximum cross section used by Levkovskij [86], and so act as an accurate mean of adjusting all of his results for more than 300 measured reactions. The need to correct systematically



(a) All experimental data are plotted with uncertainties.

(b) Selected data compared with evaluated Padé fit based on 16 parameters (solid) and including uncertainty bands (dashed) to give a $\chi^2=1.74$ up to 1000 MeV.FIG. 10. (Color online) Evaluated Padé fit and experimental data from Refs. [37, 48, 49, 51, 60, 68, 109, 132, 135–138, 159, 165–177] for the $^{nat}\text{Cu}(p,x)^{58}\text{Co}$ monitor reaction.

all of the high cross sections listed in Ref. [86] was first documented by Takács *et al.* (2002b) [178] who proposed a reduction of 20% based on their new measurement of this monitor reaction. Among other authors who have discussed this adjustment factor, Qaim *et al.* (2014) [179] have more recently proposed a value of 0.82 ± 0.05 based on a comparison of the results of many proton-induced re-

actions in Ref. [86] with their evaluated cross sections, but not on direct measurements of the monitor cross section. Under these circumstances, compilation of recent publications for $^{nat}\text{Mo}(p,x)^{96m+g}\text{Tc}$ complemented by dedicated experiments, and final fitting of the selected datasets is included in the present study with the aim of obtaining a recommended value for the cross section at 30 MeV,

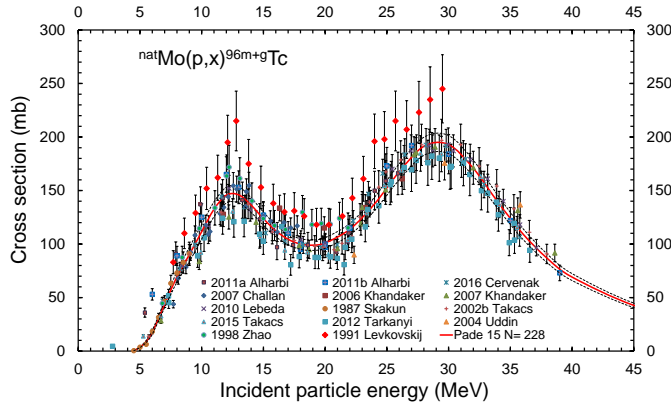


FIG. 11. (Color online) Evaluated Padé fit based on 15 parameters (solid) and including uncertainty bands (dashed) to give a $\chi^2=1.34$ up to 45 MeV. Experimental data are taken from Refs. [56, 103, 110, 134, 178, 180–187] for the $^{nat}\text{Mo}(p,x)^{96m+g}\text{Tc}$ monitor reaction. The original data of Ref. [86] are shown separately.

published as being 250 ± 10 mb by Levkovskij (1991) [86].

The cumulative formation of ground state ^{96g}Tc ($T_{1/2}=4.28$ d) measured after the γ -decay of the short-lived metastable state ^{96m}Tc ($T_{1/2}=51.5$ min.) was determined from the three intense γ -ray lines at 778.22 keV (99.760% intensity), 812.54 keV (82% intensity) and 849.86 keV (98% intensity). Thirteen publications for the $^{nat}\text{Mo}(p,x)^{96m+g}\text{Tc}$ reaction with experimental cross-section data on ^{nat}Mo were selected from the literature [56, 103, 110, 134, 178, 180–187], and are shown with uncertainties in Fig. 11. All were considered for the fitting process. Only one dataset by Bonardi *et al.* (2002) [188] is not shown after been rejected because the data are systematically too high. The original dataset of [86] is also shown in Fig. 11 for visual comparison purposes only.

A Padé function with 15 parameters was fitted to 228 selected data points with $\chi^2=1.34$ up to 45 MeV, as shown in Fig. 11. Uncertainties include a 4% systematic uncertainty, and range from nearly 70% at the reaction threshold to between 4.2% and 6% over energies up to 45 MeV. A value of 192.9 ± 8.4 mb is recommended at 30 MeV, resulting in a ratio of 0.77 ± 0.07 with respect to the Levkovskij (1991) value [86].

III. MONITOR REACTIONS FOR DEUTERON BEAMS

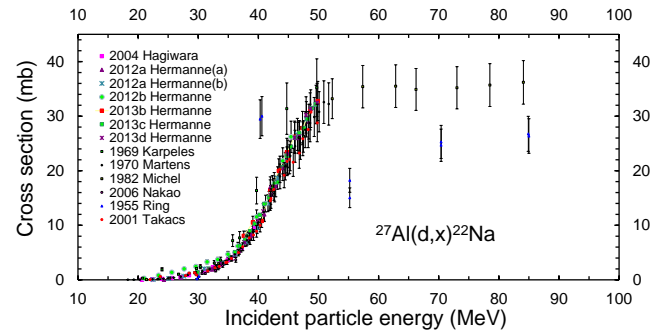
A. $^{27}\text{Al}(d,x)^{22}\text{Na}$

The formation of long-lived ^{22}Na ($T_{1/2}=2.602$ y) can be easily quantified by means of the intense γ -ray line at 1274.537 keV (99.940% intensity), making this reaction the most widely used monitor for deuterons over the energy range from 35 to 100 MeV. Twelve publications with

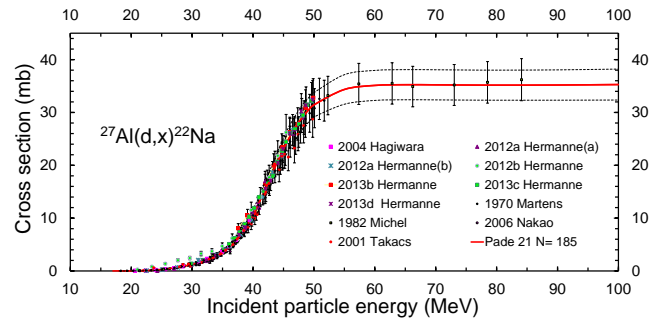
TABLE III. Reactions for monitoring deuteron beams and recommended decay data of the activation products ($T_{1/2}$ is the product half-life, and E_γ is the γ -ray energy in keV of the transition with intensity I_γ in %).

| Reaction | $T_{1/2}$ | E_γ (keV) | I_γ (%) | Useful range (MeV) |
|---------------------------------------|-----------|------------------|----------------|--------------------|
| $^{27}\text{Al}(d,x)^{22}\text{Na}$ | 2.602 y | 1274.537 | 99.940 | 30–100 |
| $^{27}\text{Al}(d,x)^{24}\text{Na}$ | 14.997 h | 1368.626 | 99.9936 | 15–90 |
| $^{nat}\text{Ti}(d,xn)^{48}\text{V}$ | 15.9735 d | 983.525 | 99.98 | 5–50 |
| | | 1312.106 | 98.2 | |
| $^{nat}\text{Ti}(d,x)^{46}\text{Sc}$ | 83.79 d | 889.277 | 99.9840 | 5–75 |
| | | 1120.545 | 99.9870 | |
| $^{nat}\text{Cu}(d,xn)^{62}\text{Zn}$ | 9.193 h | 507.60 | 14.8 | 15–50 |
| | | 596.56 | 26.0 | |
| $^{nat}\text{Cu}(d,xn)^{63}\text{Zn}$ | 38.47 min | 669.62 | 8.2 | 8–50 |
| | | 962.06 | 6.5 | |
| $^{nat}\text{Cu}(d,xn)^{65}\text{Zn}$ | 243.93 d | 1115.539 | 50.04 | 5–50 |
| $^{nat}\text{Fe}(d,x)^{56}\text{Co}$ | 77.236 d | 846.770 | 99.9399 | 10–50 |
| | | 1238.288 | 66.46 | |
| $^{nat}\text{Ni}(d,x)^{61}\text{Cu}$ | 3.339 h | 282.956 | 12.2 | 3–50 |
| | | 656.008 | 10.8 | |
| $^{nat}\text{Ni}(d,x)^{56}\text{Co}$ | 77.236 d | 846.770 | 99.9399 | 5–50 |
| | | 1238.288 | 66.46 | |
| $^{nat}\text{Ni}(d,x)^{58}\text{Co}$ | 70.86 d | 810.759 | 99.450 | 5–50 |

relevant experimental cross-section data were identified in the literature [189–200], and are represented with uncertainties in Fig. 12(a). Ref. [190] contains two separate datasets that have been labelled (a) and (b). Six new references added after the previous update of the IAEA monitor reaction website in 2007 [10] are Refs. [189–194]. Two of the twelve studies were removed from further analysis, and the reasons for rejection are indicated in parentheses: Karpeles (1969) (energy shift visible below 50 MeV) [195], and Ring and Litz (1955) (discrepant data) [199].



(a) All experimental data are plotted with uncertainties.



(b) Selected data compared with evaluated Padé fit based on 21 parameters (solid) and including uncertainty bands (dashed) to give a $\chi^2=0.95$ up to 100 MeV.

FIG. 12. (Color online) Evaluated Padé fit and experimental data from Refs. [189–200] for the $^{27}\text{Al}(d,x)^{22}\text{Na}$ monitor reaction. Ref. [190] contains two datasets labelled (a) and (b).

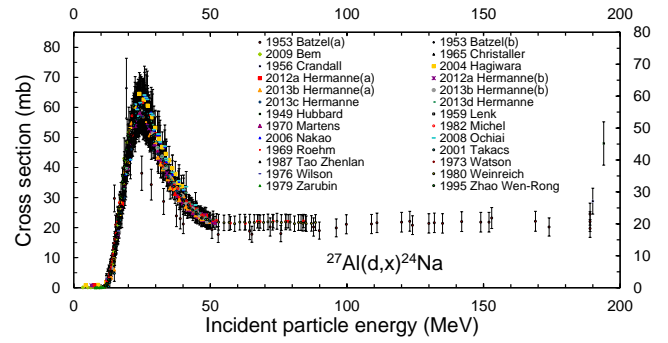
The datasets of the remaining ten papers were considered in the fitting process, as taken from Refs. [189–194, 196–198, 200]. Thus, a Padé function with 21 parameters was fitted to 185 selected data points with $\chi^2=0.95$ over the energy range from 20 to 100 MeV, as shown in Fig. 12(b). Uncertainties include a 4% systematic uncertainty, and decrease slowly from 60% near the reaction threshold, remain higher than 9% up to 45 MeV incident particle energy, and are of the order of 8% between 48 and 100 MeV. A slow rise of the excitation function up to 50 MeV arises from a combination of two reactions with cluster emissions: $^{27}\text{Al}(d,adn)^{22}\text{Na}$ (threshold of 24.19 MeV) and $^{27}\text{Al}(d,\alpha p2n)^{22}\text{Na}$ (threshold of 26.58 MeV). The plateau at higher energies also contains contributions from the $^{27}\text{Al}(d,3p4n)^{22}\text{Na}$ reaction with the emission of independent nucleons and a threshold of 56.99 MeV.

B. $^{27}\text{Al}(d,x)^{24}\text{Na}$

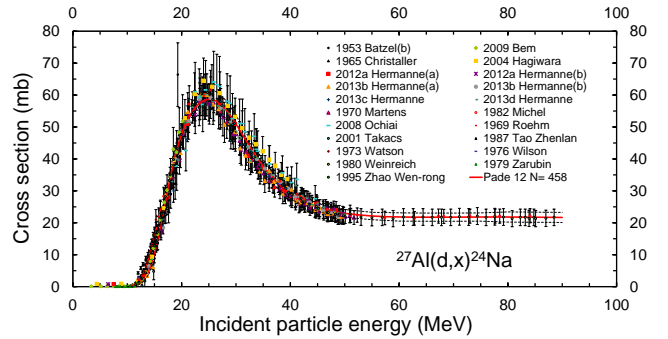
The formation of ^{24}Na ($T_{1/2}=14.997$ h) is easily quantified by means of the intense γ -ray line at 1368.626 keV (99.9936% intensity), and can be used in parallel with ^{22}Na to monitor deuterons over the energy range from 15 to 90 MeV range. However, ^{24}Na can also be produced from secondary-neutron interactions in the stacked foils, especially above 200 MeV. We suspect this effect causes the deviation of the measured data from the expected physical behaviour of the excitation function, and so actively discourages evaluations of $^{27}\text{Al}(d,x)^{24}\text{Na}$ as a monitor reaction above 100 MeV. As a continuation of the choices made in the 2007 update of the IAEA monitor reaction website [10], all datasets up to 200 MeV incident particle energy were included in the compilation while the fit and recommendation were limited to 90 MeV.

A total of twenty-three publications (twenty-six datasets) with experimental data up to 200 MeV were identified in the literature for the $^{27}\text{Al}(d,x)^{24}\text{Na}$ monitor reaction [189, 190, 192–194, 196–198, 200–214], and are represented with uncertainties in Fig. 13(a). Each of Refs. [190, 192, 201] contains two datasets that have been labelled (a) and (b). New references added after the previous update of the IAEA monitor website in 2007 [10] are as follows: Bém *et al.* (2009) [202], Hermanne *et al.* (2012a) [190], Hermanne *et al.* (2013b) [192], Hermanne *et al.* (2013c) [193], Hermanne *et al.* (2013d) [194], and Ochiai *et al.* (2008) [207]. Five datasets were removed and not considered for further analysis, and the reasons for their rejection are indicated in parentheses: Batzel *et al.* (1953)(a) (strange shape of the excitation function near the maximum for series-a) [201], Crandall *et al.* (1956) (only data above 100 MeV) [204], Hubbard (1949) (only data above 100 MeV) [205], Lenk and Slobodrian (1959) (arbitrary normalisation required) [206], and Nakao *et al.* (2006) (superseded by Ochiai *et al.* (2008) [207]) [198].

The remaining 21 datasets were analysed and evaluated



(a) All experimental data are plotted with uncertainties.



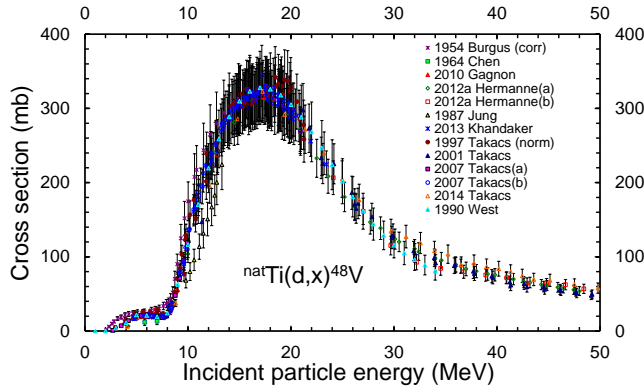
(b) Selected data compared with evaluated Padé fit based on 12 parameters (solid) and including uncertainty bands (dashed) to give a $\chi^2=2.60$ up to 90 MeV.

FIG. 13. (Color online) Evaluated Padé fit and experimental data from Refs. [189, 190, 192–194, 196–198, 200–214] for the $^{27}\text{Al}(d,x)^{24}\text{Na}$ monitor reaction. Each of Refs. [190, 192, 201] contains two datasets labelled (a) and (b).

further, as taken from Refs. [189, 190, 192–194, 196, 197, 200–203, 207–214]. A Padé function with 12 parameters was fitted to 458 selected data points with $\chi^2=2.60$ up to 90 MeV, and this fit is compared to the selected experimental data in Fig. 13(b). Uncertainties include a 4% systematic uncertainty, and range from 72% near the reaction threshold to below 6% between 20 and 75 MeV incident particle energy, before increasing slightly up to 7.3% at higher energies. Cluster emission is very important in this particular case, and the main contribution in the peak region arises from the $^{27}\text{Al}(d,\alpha p)$ reaction with a threshold at 5.76 MeV (any channel without the emission of an α -particle would have a threshold of at least 27.5 MeV).

C. $^{nat}\text{Ti}(d,xn)^{48}\text{V}$

The $^{nat}\text{Ti}(d,x)^{48}\text{V}$ reaction on readily available and corrosion resistant Ti is probably the most popular monitor for deuteron beams in the low and middle energy region (5–50 MeV). Activation product ^{48}V with $T_{1/2}=15.9735$ d decays with the emission of two intense γ -ray lines at 983.525 keV (99.98% intensity) and 1312.106 keV (98.2% intensity). Eleven publications with experimental cross-section data (thirteen datasets) at incident parti-



(a) All experimental data are plotted with uncertainties.

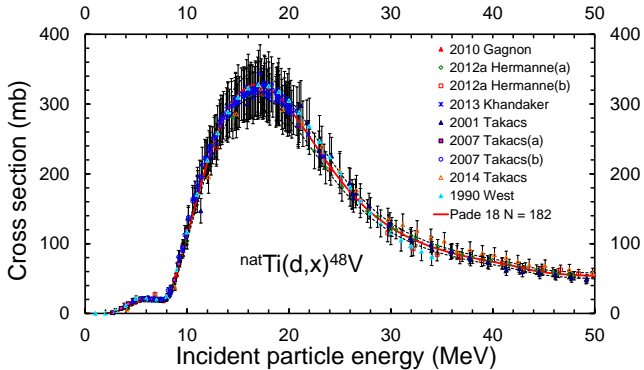
(b) Selected data compared with evaluated Padé fit based on 18 parameters (solid) and including uncertainty bands (dashed) to give a $\chi^2=1.04$ up to 50 MeV.

FIG. 14. (Color online) Evaluated Padé fit and experimental data from Refs. [104, 190, 200, 215–222] for the $^{nat}\text{Ti}(d,x)^{48}\text{V}$ monitor reaction. Both Refs. [190, 221] contain two datasets labelled (a) and (b).

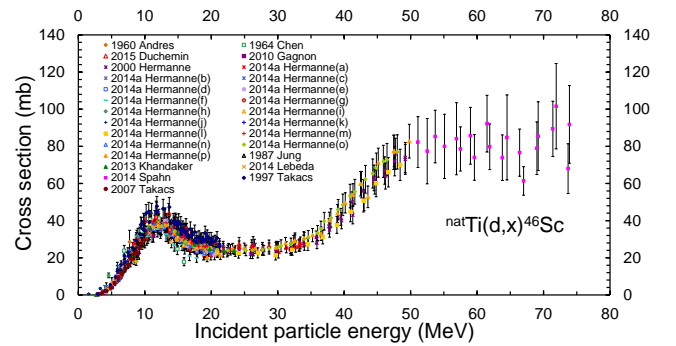
cle energies up to 50 MeV were identified in the literature [104, 190, 200, 215–222], and are shown with uncertainties in Fig. 14(a). Both of references [190, 221] contain two datasets labelled (a) and (b) that have been treated separately. Four new references added after the previous update of the IAEA monitor reaction website in 2007 [10] are listed in alphabetical order: Gagnon *et al.* (2010) [217], Hermanne *et al.* (2012a) [190], Khandaker *et al.* (2013) [219], and Takács *et al.* (2014) [222]. The results of four studies were removed from further analysis, and the reasons for their rejection are indicated in parentheses: Burgus *et al.* (1954) (normalised to natural composition, need correction for improved decay data, energy shift) [215], Chen and Miller (1964) (normalised and summed, large estimated uncertainties) [216], Jung (1987) (energy shift) [218], and Takács *et al.* (1997) (deviation near maximum) [220].

The datasets from the remaining seven papers were used in the least-squares evaluation [104, 190, 200, 217, 219, 221, 222]. A Padé function with 18 parameters was fitted to 182 selected data points with $\chi^2=1.04$ up to 50 MeV, as shown in Fig. 14(b). Uncertainties include a 4% systematic uncertainty, and range from 50% near

the reaction threshold to a minimum of 4.2% from 14 to 35 MeV incident particle energy that increases to 6.5% at higher energies. The broad maximum near 17 MeV ($\sigma_{max}=328$ mb) arises essentially from the $^{48}\text{Ti}(d,2n)^{48}\text{V}$ reaction on the stable and most naturally abundant ^{48}Ti isotope (threshold of 7.316 MeV). A small maximum at approximately 6 MeV is caused by the $^{47}\text{Ti}(d,n)^{48}\text{V}$ (Q -value of +4.604 MeV and ^{47}Ti natural abundance of 7.44%). We refer to Sec. II C for remarks on the presence of simultaneously formed ^{48}Sc ($T_{1/2}=43.67$ h).

D. $^{nat}\text{Ti}(d,x)^{46}\text{Sc}$

Reasons to include this additional reaction for the monitoring of deuteron beams along with the decay characteristics of ^{46}Sc are detailed in Sec. II D. Twelve publications with experimental cross-section data at incident particle energies up to 75 MeV were identified in the literature [107, 136, 216–221, 223–226], and are shown with uncertainties in Fig. 15(a). Table 2 of Ref. [107] contained sixteen sets of unpublished results for this reaction obtained in different experiments discussed in that paper. Since this reaction was not present earlier in the IAEA monitor reaction website [10], all references are new. Seven datasets were removed from further analysis, and the rea-



(a) All experimental data are plotted with uncertainties.

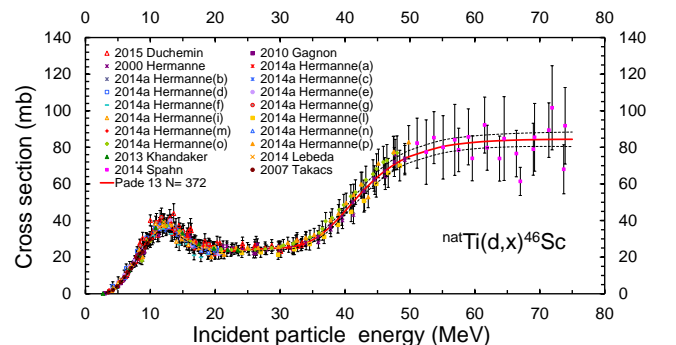
(b) Selected data compared with evaluated Padé fit based on 13 parameters (solid) and including uncertainty bands (dashed) to give a $\chi^2=0.78$ up to 75 MeV.

FIG. 15. (Color online) Evaluated Padé fit and experimental data from Refs. [107, 136, 216–221, 223–226] for the $^{nat}\text{Ti}(d,x)^{46}\text{Sc}$ monitor reaction. Ref. [107] contains 16 sets of data labelled 2014a Hermanne(a) to (p).

sons for rejection are indicated in parentheses: Andres and Meinke (1960) (energy shift) [223], Chen and Miller (1964) (energy shift) [216], Hermanne *et al.* (2014a)(h) (energy shift) [107], Hermanne *et al.* (2014a)(j) (energy shift) [107], Hermanne *et al.* (2014a)(k) (values too high) [107], Jung (1987) (values too low) [218], and Takács *et al.* (1997) (values scattered and too high near maximum) [220]. The remaining 20 datasets were used for further evaluation, as taken from Refs. [107, 136, 217, 219, 221, 224–226]. A Padé function with 13 parameters was fitted to 372 selected data points with $\chi^2=0.78$ up to 75 MeV, as shown in Fig. 15(b).

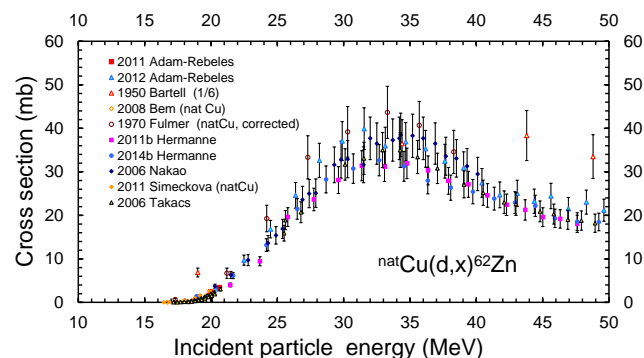
Uncertainties include a 4% systematic uncertainty, and range from 22% near the reaction threshold to a minimum of 4.2% from 12 to 32 MeV incident particle energy that increases to 4.8% at higher energies. The first maximum in the excitation function occurs at approximately 12 MeV, and arises from the $^{48}\text{Ti}(d,\alpha)^{46}\text{Sc}$ reaction on the stable and most naturally abundant ^{48}Ti isotope (Q-value of 3.979 MeV). A gradual rise starting around 32 MeV is dominated by the emission of separate nucleons ($^{48}\text{Ti}(d,2p2n)^{46}\text{Sc}$ reaction with a threshold of 25.34 MeV).

E. $^{nat}\text{Cu}(d,xn)^{62}\text{Zn}$

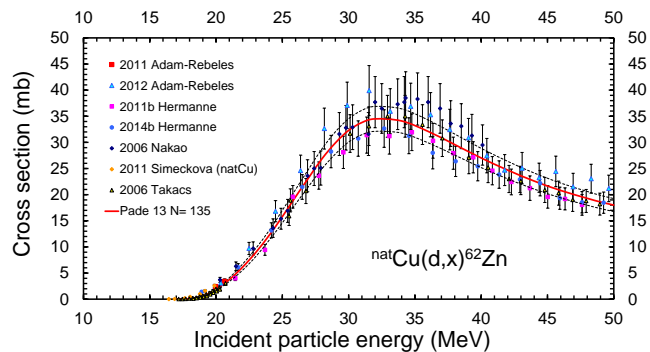
As already discussed in Sec. II, the three reactions on Cu were added to the list of deuteron monitors for reasons of completeness and their potential adoption because of the frequent use of electroplated targets with Cu-backing. The $^{nat}\text{Cu}(d,xn)^{62}\text{Zn}$ monitor reaction can be used over an energy range of 15 to 50 MeV. Decay characteristics of activation product ^{62}Zn ($T_{1/2}=9.193$ h) were discussed in Sec. II F. Ten publications with experimental cross-section data at incident particle energies up to 50 MeV were identified in the literature [198, 227–235], and are shown with uncertainties in Fig. 16(a).

Data in Refs. [230, 231, 234] were obtained with ^{63}Cu targets, and have been re-normalised to ^{nat}Cu . Additionally, the data of Ref. [231] were corrected for the outdated values adopted for the intensities of the γ -ray lines (15%). The original values of Ref. [227] are totally discrepant, and were only included in Fig. 16(a) after being divided arbitrarily by a factor of six. All references are new because the reaction was not present in the previous update of the IAEA monitor reaction website in 2007 [10]. Three references were removed prior to further analysis, and the reasons for their rejection are given in parentheses: Bartell *et al.* (1950) (discrepant data) [227], Fulmer and Williams (1970) (values too high after correction) [231], and Bém *et al.* (2008) (data superseded by values of Šimečková *et al.* (2011) [234]) [230].

The remaining seven datasets were considered in the fitting process, as taken from Refs. [198, 228, 229, 232–235]. A Padé function with 13 parameters was fitted to 135 selected data points with $\chi^2=1.57$ up to 50 MeV, as shown in Fig. 16(b). Uncertainties include a 4% sys-



(a) All experimental data are plotted with uncertainties.



(b) Selected data compared with evaluated Padé fit based on 13 parameters (solid) and including uncertainty bands (dashed) to give a $\chi^2=1.57$ up to 50 MeV.

FIG. 16. (Color online) Evaluated Padé fit and experimental data from Refs. [198, 227–235] for the $^{nat}\text{Cu}(d,xn)^{62}\text{Zn}$ monitor reaction.

tematic uncertainty, and range from nearly 40% near the reaction threshold to 7% above an incident particle energy of 25 MeV. The broad peak with a maximum at approximately 32 MeV arises from the $^{63}\text{Cu}(d,3n)^{62}\text{Zn}$ reaction with a threshold at 15.985 MeV, while the $^{65}\text{Cu}(d,5n)$ reaction can only contribute above 35 MeV and is responsible for the long tail.

F. $^{nat}\text{Cu}(d,xn)^{63}\text{Zn}$

The decay characteristics and specific problems associated with the use of ^{63}Zn as an activation product in a monitor reaction were discussed in Sec. II G. Eight publications with experimental cross-section data at incident particle energies up to 50 MeV were identified in the literature [207, 227, 230, 231, 234–237], and are shown with uncertainties in Fig. 17(a). Data in Refs. [230, 231, 234, 237] were obtained with ^{63}Cu targets, and have been re-normalised to ^{nat}Cu . The original values of Ref. [227] are totally discrepant, and remain represented in this form. All references are new as the reaction was not present in the previous update of the IAEA monitor reaction website in 2007 [10].

Two references were removed prior to further analysis, and the reasons for their rejection are indicated in

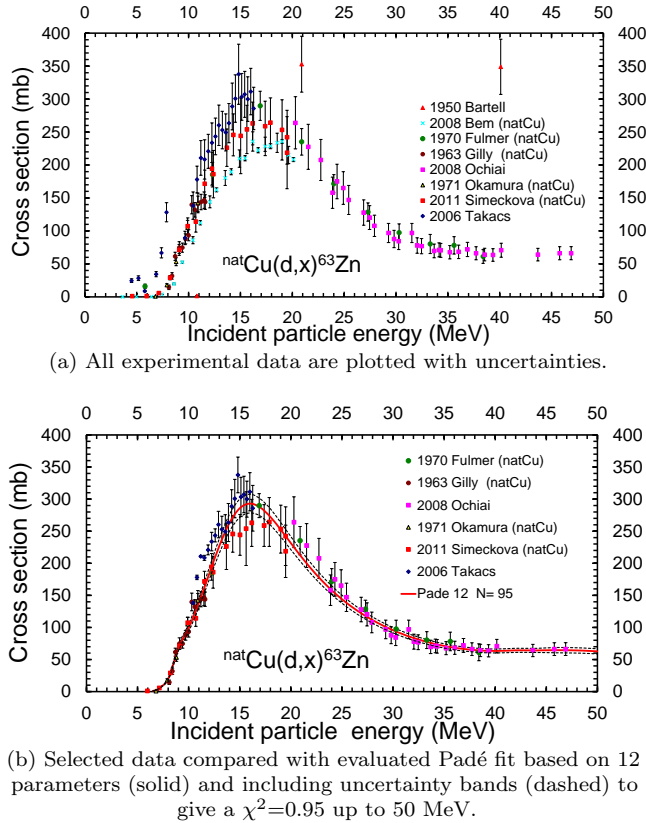


FIG. 17. (Color online) Evaluated Padé fit and experimental data from Refs. [207, 227, 230, 231, 234–237] for the $^{nat}\text{Cu}(d,xn)^{63}\text{Zn}$ monitor reaction.

parentheses: Bém *et al.* (2008) (superseded by Šimečková *et al.* (2011) [234]) [230], and Bartell *et al.* (1950) (discrepant) [227]. Data of Takács *et al.* (2006) [235] that seem too high near the maximum were included, but data points below 10 MeV were deleted. The lowest energy data points of Refs. [231, 234] were also not included in the fitting process.

The remaining six datasets were considered in the fitting process, as taken from Refs. [207, 231, 234–237]. A Padé function with 12 parameters was fitted to 95 selected data points with $\chi^2=0.95$ up to 50 MeV, as shown in Fig. 17(b). Uncertainties include a 4% systematic uncertainty, and range from 7.6% near the reaction threshold to a minimum of 4.3% from 20 to 30 MeV incident particle energy that increases to 6.4% at higher energies. The broad peak in the excitation function at approximately 16 MeV arises from the $^{63}\text{Cu}(d,2n)^{63}\text{Zn}$ reaction with a threshold at 6.577 MeV, while the $^{65}\text{Cu}(d,4n)$ reaction can only contribute above 26 MeV and is responsible for the slightly increasing long tail between 40 and 50 MeV.

G. $^{nat}\text{Cu}(d,xn)^{65}\text{Zn}$

The $^{nat}\text{Cu}(d,xn)^{65}\text{Zn}$ monitor reaction can be used over an incident particle energy range from 5 to 50 MeV. Decay characteristics of activation product ^{65}Zn were dis-

cussed in Sec. II H for proton monitoring. Fifteen publications with experimental cross-section data at incident particle energies up to 50 MeV were identified in the literature [84, 200, 218, 228–234, 237–241], and are shown with uncertainties in Fig. 18(a). Data in Refs. [230, 234, 237–240] were obtained with ^{65}Cu targets, and have been re-normalised to ^{nat}Cu . All references are new as the reaction was not present in the previous update of the IAEA monitor reaction website [10]. The dataset of Bém *et al.* (2008) [230] was rejected (superseded by values in Šimečková *et al.* (2011) [234]), and the four lowest energy data points of Ref. [239] were also discarded.

The remaining 14 datasets were considered in the fitting process, as taken from Refs [84, 200, 218, 228, 229, 231–234, 237–241]. A Padé function with 10 parameters was fitted to 242 selected data points with $\chi^2=1.10$ up to 50 MeV, as shown in Fig. 18(b). Uncertainties include a 4% systematic uncertainty, and range from nearly 10% near the reaction threshold to 4.5% above an incident particle energy of 12 MeV. Only the $^{65}\text{Cu}(d,2n)^{65}\text{Zn}$ reaction with a threshold at 4.493 MeV can contribute, and has a characteristic excitation function with a broad maximum at approximately 16 MeV.

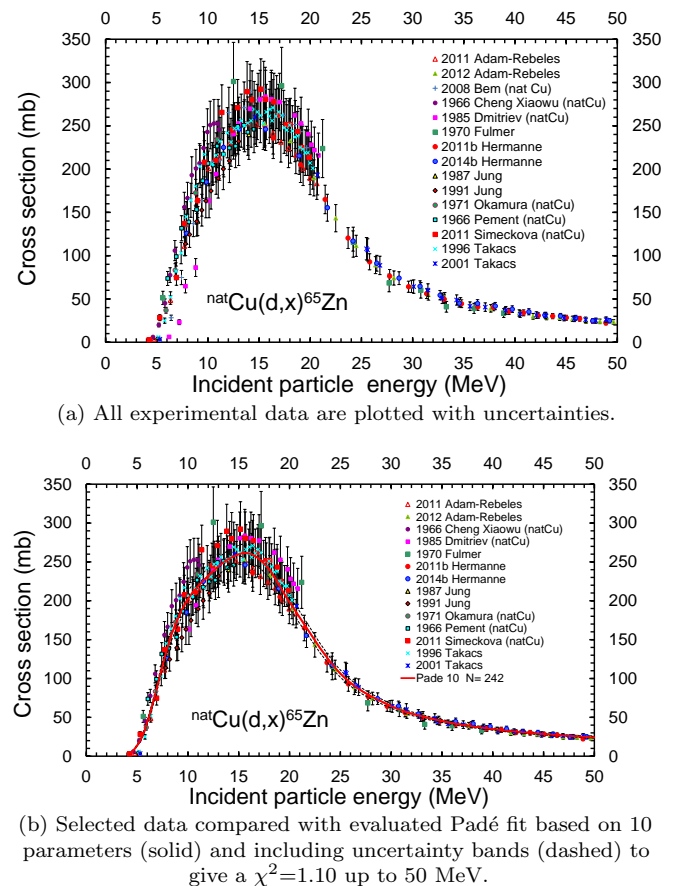


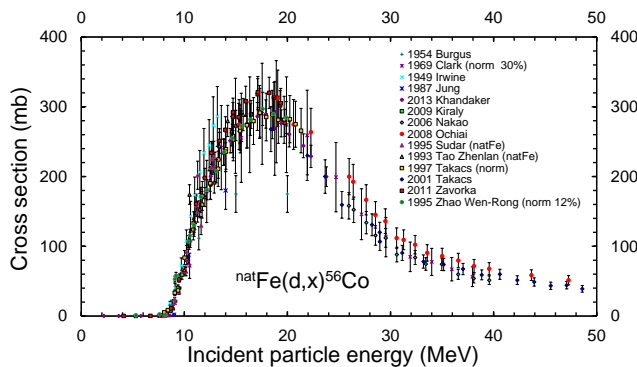
FIG. 18. (Color online) Evaluated Padé fit and experimental data from Refs. [84, 200, 218, 228–234, 237–241] for the $^{nat}\text{Cu}(d,xn)^{65}\text{Zn}$ monitor reaction.

H. $^{nat}\text{Fe}(d,x)^{56}\text{Co}$

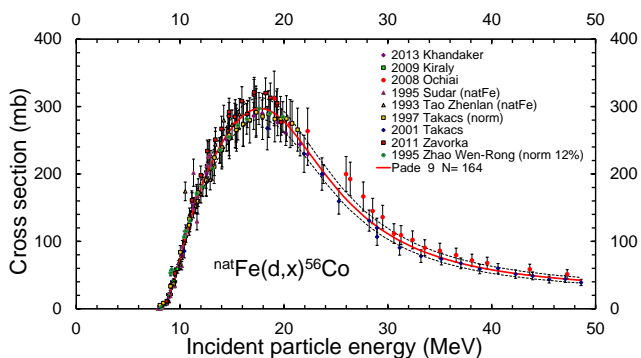
The $^{nat}\text{Fe}(d,x)^{56}\text{Co}$ monitor reaction can be used over an incident particle energy range from 10 to 50 MeV. Decay characteristics of activation product ^{56}Co ($T_{1/2} = 77.236$ d) were discussed in Sec. III for proton monitoring.

Fourteen publications with experimental cross-section data at incident particle energies up to 50 MeV were identified in the literature [198, 200, 207, 215, 218, 220, 242–247, 249, 250], and are shown with uncertainties in Fig. 19(a). Data in Refs. [246, 247] were originally published as studies of ^{56}Fe targets and have been converted to ^{nat}Fe . Adjustments were also made to outdated decay data adopted in Ref. [215], and the data of Refs. [242, 250] were normalised arbitrarily to agree better with the values of Ref. [200] by 30% and 12%, respectively.

Three new references were added after the previous update of the IAEA monitor reaction website in 2007 [10], and are listed in alphabetical order: Khandaker *et al.* (2013) [244], Ochiai *et al.* (2008) [207], and Zavorka *et al.* (2011) [249]. Five references were removed prior to further analysis, and the reasons for their rejection are given in parentheses: Burgus *et al.* (1954) (still exhibited significantly lower values after correction) [215], Clark *et al.* (1969) (arbitrarily normalised by 30%) [242], Irwine



(a) All experimental data are plotted with uncertainties.



(b) Selected data compared with evaluated Padé fit based on 9 parameters (solid) and including uncertainty bands (dashed) to give a $\chi^2=1.80$ up to 50 MeV.

FIG. 19. (Color online) Evaluated Padé fit and experimental data from Refs. [198, 200, 207, 215, 218, 220, 242–247, 249, 250] for the $^{nat}\text{Fe}(d,x)^{56}\text{Co}$ monitor reaction.

(1949) (shifted to lower energy) [243], Jung (1987) (values too low) [218], and Nakao *et al.* (2006) (superseded by Ochiai *et al.* (2008) [207]) [198]. Furthermore, all data points below 8 MeV in the datasets given by Refs. [244, 249, 250] were also rejected in the fitting process (see below for threshold of contributing reaction).

The remaining data points from nine datasets were subsequently considered in the fitting process, as taken from Refs [200, 207, 220, 244–247, 249, 250]. A Padé function with 9 parameters was fitted to 164 selected data points with $\chi^2=1.80$ up to 50 MeV, as shown in Fig. 19(b). Uncertainties include a 4% systematic uncertainty, and range from nearly 40% near the reaction threshold to 5.5% over an incident particle energy of 12 to 24 MeV, before reaching 10% at higher energies. Only the $^{56}\text{Fe}(d,2n)^{56}\text{Co}$ reaction with a threshold at 7.846 MeV contributes at the lower energies, and is responsible for the maximum at 17.6 MeV, while the $(d,3n)$ reaction on low natural abundance ^{57}Fe (2.2%) has a threshold of 15.757 MeV.

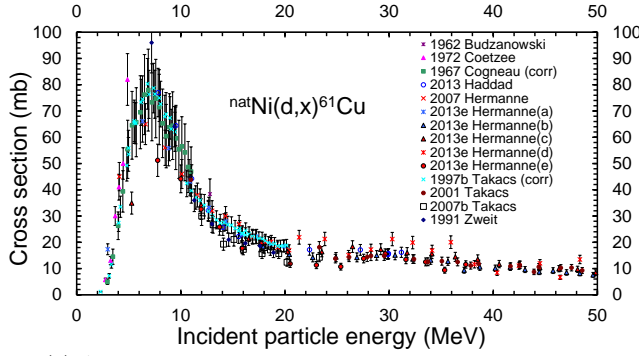
I. $^{nat}\text{Ni}(d,x)^{61}\text{Cu}$

The $^{nat}\text{Ni}(d,x)^{61}\text{Cu}$ monitor reaction is a production route for short-lived ^{61}Cu ($T_{1/2} = 3.339$ h) that can be used over an incident particle energy range of 3 to 50 MeV. Activity can be determined from the γ -ray lines at 282.956 keV (12.2% intensity) and 656.008 keV (10.8% intensity). Ten references with experimental cross-section data at incident particle energies up to 50 MeV were identified in the literature [200, 251–259], and are shown with uncertainties in Fig. 20(a).

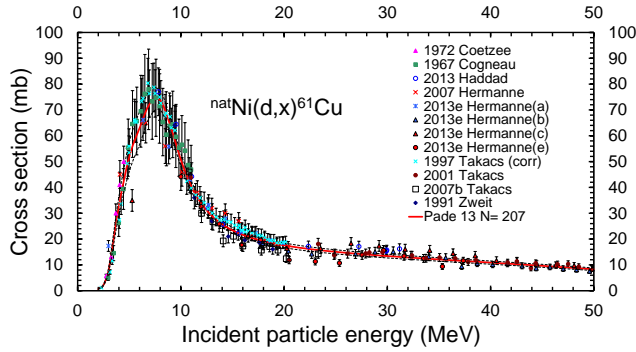
Ref. [256] contains five datasets labelled (a) to (e), and Ref. [258] contains data points published elsewhere in Refs. [255] and [200] that are represented separately here. The original data of [257] were corrected by 18% to achieve improved correspondence with [200] (re-estimation of beam current), while the values of Ref. [253] were arbitrarily decreased by 38% to give good agreement with all other data.

Three new references added after the previous update of the IAEA monitor reaction website in 2007 [10] are listed in alphabetical order: Haddad (2013) [254], Hermanne *et al.* (2013e) [256], and Takács *et al.* (2007) [258]. Two datasets were removed prior to further analysis, and the reasons for their rejection are given in parentheses: Budzanowski and Grotowski (1962) (only one point which is too high) [251], and Hermanne *et al.* (2013e)(d) (values too high) [256]. Three outlying data points near the threshold in the studies of Refs. [252, 256, 259] were also rejected from the fitting process.

The remaining 12 datasets were considered in the fitting process, as taken from Refs. [200, 252–259]. A Padé function with 13 parameters was fitted to 207 selected data points with $\chi^2=1.19$ up to 50 MeV, as shown in Fig. 20(b). Uncertainties include a 4% systematic uncertainty, and range from nearly 13% near the reaction threshold to between 5% and 5.5% over an incident particle energy



(a) All experimental data are plotted with uncertainties.

(b) Selected data compared with evaluated Padé fit based on 13 parameters (solid) and including uncertainty bands (dashed) to give a $\chi^2=1.19$ up to 50 MeV.FIG. 20. (Color online) Evaluated Padé fit and experimental data from Refs. [200, 251–259] for the $^{nat}\text{Ni}(d,x)^{61}\text{Cu}$ monitor reaction. Ref. [256] contains five datasets labelled (a) to (e).

range of 9 to 35 MeV, to reach 6% at higher energies. The only feasible contributor to the observed maximum in the excitation function is the $^{60}\text{Ni}(d,n)^{61}\text{Cu}$ reaction with a positive Q-value of 2.575 MeV, while reactions on low natural abundance $^{61,62}\text{Ni}$ are responsible for the long tail at high energies.

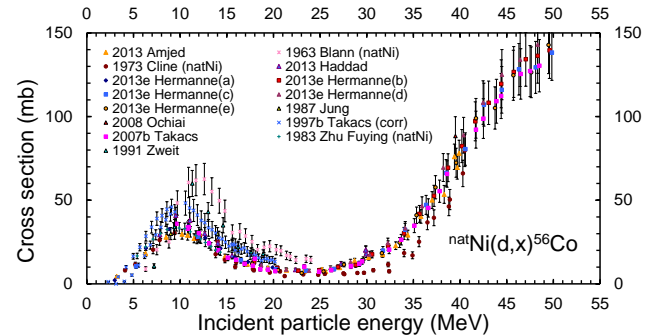
J. $^{nat}\text{Ni}(d,x)^{56}\text{Co}$

The $^{nat}\text{Ni}(d,x)^{56}\text{Co}$ reaction is proposed as an additional monitor that can be used over an incident particle energy range of 5 to 50 MeV. Decay characteristics of activation product ^{56}Co ($T_{1/2}=77.236$ d) were discussed in Sec. III. Eleven references with experimental cross-section data at incident particle energies up to 50 MeV were identified in the literature [207, 218, 254, 256–263], and are shown with uncertainties in Fig. 21(a). Ref. [256] contains five datasets labelled (a) to (e). Data in Refs. [261–263] were originally published as studies of ^{58}Ni targets and have been converted to ^{nat}Ni , while the original data of Ref. [257] were corrected by 18% to correspond better with [200] (based on a re-estimation of the beam current).

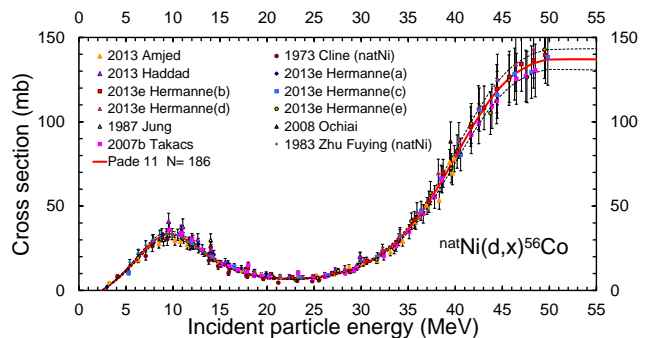
All data are new as this reaction was not present in the previous update of the IAEA monitor reaction website in 2007 [10]. Three datasets were removed prior to further analysis, and the reasons for their rejection are given in

parentheses: Blann and Merkel (1963) (values too high, even after normalisation) [261], Takács *et al.* (1997b) (values too high, even after correction) [257], and Zweit *et al.* (1991) (values too high) [259]. The data points of Cline (1973) [262] above 25 MeV were also removed because they did not include the contributions of reactions on ^{60}Ni , and therefore are too low. The remaining 12 datasets were considered in the fitting process, as taken from Refs. [207, 218, 254, 256, 258, 260, 262, 263]. A Padé function with 11 parameters was fitted to 186 selected data points with $\chi^2=1.02$ up to 50 MeV, as shown in Fig. 21(b).

The first maximum in the excitation function at 10 MeV arises from the $^{58}\text{Ni}(d,\alpha)^{56}\text{Co}$ reaction with a positive Q-value of 6.522 MeV, while the steep rise above 25 MeV originates from the emission of separate nucleons by the $^{58}\text{Ni}(d,2p2n)^{56}\text{Co}$ reaction with a threshold of 22.53 MeV. The $^{60}\text{Ni}(d,\alpha 2n)^{56}\text{Co}$ reaction at a threshold of 14.33 MeV on ^{60}Ni at 26.223% natural abundance would appear to be unimportant. As a result of the specific shape of the excitation function, uncertainties that include a systematic uncertainty of 4% are 5% in the region of the first maximum, rise slightly to 5.5% at an incident particle energy of 23 MeV, and are lower than 4.5% from 30 to 50 MeV.



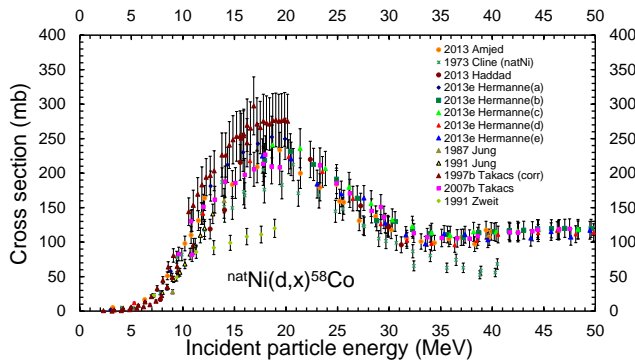
(a) All experimental data are plotted with uncertainties.

(b) Selected data compared with evaluated Padé fit based on 11 parameters (solid) and including uncertainty bands (dashed) to give a $\chi^2=1.02$ up to 50 MeV.FIG. 21. (Color online) Evaluated Padé fit and experimental data from Refs. [207, 218, 254, 256–263] for the $^{nat}\text{Ni}(d,x)^{56}\text{Co}$ monitor reaction.

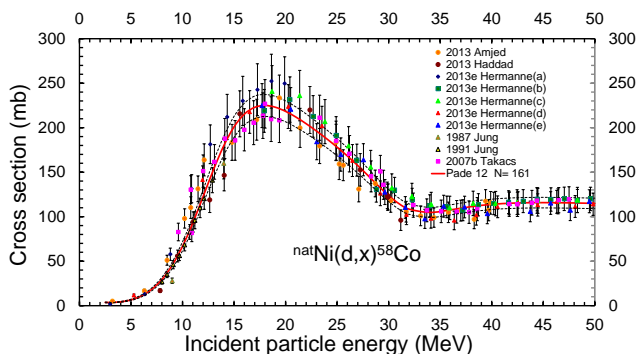
K. $^{nat}\text{Ni}(d,x)^{58}\text{Co}$

The $^{nat}\text{Ni}(d,x)^{58}\text{Co}$ monitor reaction is especially applicable in the deuteron energy range of 5–35 MeV. Decay characteristics of activation product ^{58}Co ($T_{1/2} = 70.86$ d) were discussed in Sec. II J. Nine references with experimental cross-section data at incident particle energies up to 50 MeV were identified in the literature [84, 218, 254, 256–260, 262], and are shown with uncertainties in Fig. 22(a). Ref. [256] contains five datasets labelled (a) to (e). Data in Ref. [262] were originally published as studies of ^{58}Ni targets and have been converted to ^{nat}Ni , while the original data of Takács [257] were corrected by 18% to correspond better with [200] (based on re-estimation of beam current).

All data are new as this reaction was not present in the previous update of the IAEA monitor reaction website in 2007 [10]. Three datasets were removed prior to further analysis, and the reasons for their rejection are given in parentheses: Cline (1973) (values too low, even after conversion, and not sure to which reaction these data refer) [262], Takács *et al.* (1997) (values too high, even after correction) [257], and Zweit *et al.* (1991) (values too low) [259]. The remaining 10 datasets were considered in the fitting process, as taken from Refs. [84, 218, 254, 256, 258,



(a) All experimental data are plotted with uncertainties.



(b) Selected data compared with evaluated Padé fit based on 12 parameters (solid) and including uncertainty bands (dashed) to give a $\chi^2=1.09$ up to 50 MeV.

FIG. 22. (Color online) Evaluated Padé fit and experimental data from Refs. [84, 218, 254, 256–260, 262] for the $^{nat}\text{Ni}(d,x)^{58}\text{Co}$ monitor reaction. Ref. [256] contains five datasets labelled (a) to (e).

260]. A Padé function with 12 parameters was fitted to 161 selected data points and $\chi^2=1.09$ up to 50 MeV, as shown in Fig. 22(b).

The broad maximum in the excitation function around 18 MeV arises from a combination of the $^{58}\text{Ni}(d,2p)^{58}\text{Co}$ reaction with a threshold at 1.887 MeV and the $^{60}\text{Ni}(d,\alpha)^{58}\text{Co}$ reaction with a positive $Q = +6.08$ MeV (Coulomb barrier for α emission shifts the effective threshold), while the small rise above 25 MeV originates from the emission of separate nucleons by the $^{60}\text{Ni}(d,2p2n)^{58}\text{Co}$ reaction with a threshold of 22.53 MeV. As a result of the specific shape of the excitation function, uncertainties which include a 4% systematic uncertainty are below 4.5% in the region of the first maximum and decrease to 4.2% at higher energies.

IV. MONITOR REACTIONS FOR ^3He BEAMS

TABLE IV. Reactions for monitoring ^3He beams and recommended decay data of the activation products ($T_{1/2}$ is the product half-life, and E_γ is the γ -ray energy in keV of the transition with intensity I_γ in %).

| Reaction | $T_{1/2}$ | E_γ (keV) | I_γ (%) | Useful range (MeV) |
|--|-----------|------------------|----------------|--------------------|
| $^{27}\text{Al}(^3\text{He},x)^{22}\text{Na}$ | 2.602 y | 1274.537 | 99.940 | 10–100 |
| $^{27}\text{Al}(^3\text{He},x)^{24}\text{Na}$ | 14.997 h | 1368.626 | 99.9936 | 20–130 |
| $^{nat}\text{Ti}(^3\text{He},x)^{48}\text{V}$ | 15.9735 d | 983.525 | 99.98 | 10–100 |
| | | 1312.106 | 98.2 | |
| $^{nat}\text{Cu}(^3\text{He},x)^{66}\text{Ga}$ | 9.49 h | 833.532 | 5.9 | 10–40 |
| | | 1039.22 | 37.0 | |
| $^{nat}\text{Cu}(^3\text{He},x)^{63}\text{Zn}$ | 38.47 min | 669.62 | 8.2 | 15–45 |
| | | 962.06 | 6.5 | |
| $^{nat}\text{Cu}(^3\text{He},x)^{65}\text{Zn}$ | 243.93 d | 1115.539 | 50.04 | 10–90 |

A. $^{27}\text{Al}(^3\text{He},x)^{22}\text{Na}$

The formation of long-lived ^{22}Na ($T_{1/2} = 2.602$ y) is easily quantified by means of the intense γ -ray line at 1274.537 keV (99.940% intensity), and the $^{27}\text{Al}(^3\text{He},x)^{22}\text{Na}$ reaction is widely used to monitor ^3He -particle beams over an energy range of 10 to 100 MeV.

Seven publications with experimental cross-section data were identified in the literature in the energy range under consideration [12, 264–267, 269, 270], and are represented with uncertainties in Fig. 23(a). Only the data measured by Lebeda (2016) [269] have been added since the previous update of the IAEA-NDS monitor reaction website in 2007 [10]. The study of Ref. [267] (data taken from [268]) contains three datasets represented separately as (a), (b) and (c). Dataset (a) of Ref. [267] was rejected because all values are a factor two lower than all other data.

All other datasets from seven papers [12, 264–267, 269, 270] were used as input for a least-squares Padé fit. A Padé function with 9 parameters was fitted to 147 selected data points with $\chi^2=1.14$ that covered the incident particle energy range from 10 to 100 MeV, as shown in Fig. 23(b). Uncertainties include a 4% systematic uncertainty, and decrease rapidly from 23% close to the reaction threshold to

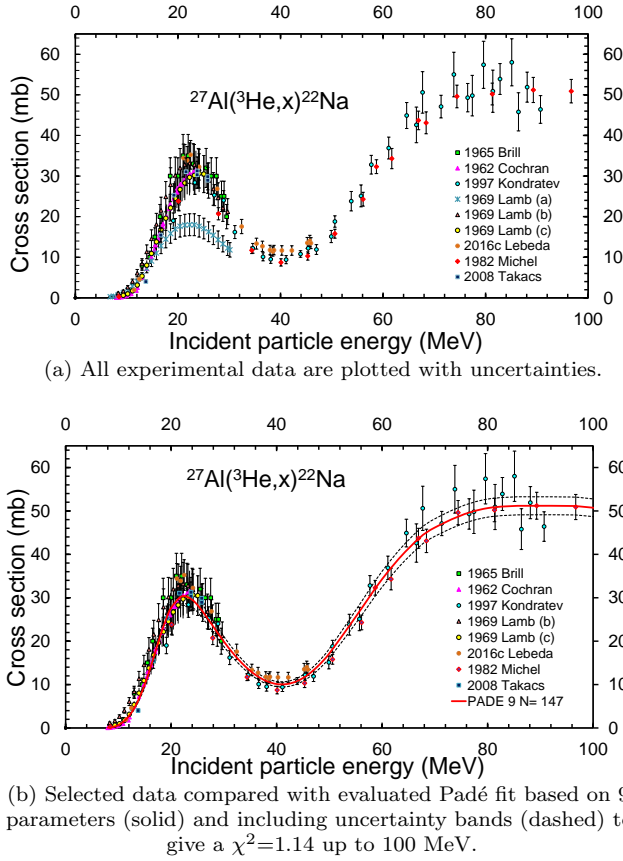


FIG. 23. (Color online) Evaluated Padé fit and experimental data from Refs. [12, 264–267, 269, 270] for the $^{27}\text{Al}(^3\text{He},x)^{22}\text{Na}$ monitor reaction. Ref. [267] contains three datasets labelled (a) to (c).

below 6% at an incident particle energy of 16 MeV, and are only 4% at 100 MeV. The rather sharp maximum in the excitation function at approximately 22 MeV arises from the clustered emission of the $^{27}\text{Al}(^3\text{He},2\alpha)^{22}\text{Na}$ reaction with an energy threshold of 2.149 MeV, while the increase and plateau at higher energies contains contributions from reactions that emit independent nucleons, for example $^{27}\text{Al}(^3\text{He},\alpha p2n)^{22}\text{Na}$ with a threshold of 33.608 MeV.

B. $^{27}\text{Al}(^3\text{He},x)^{24}\text{Na}$

The formation of ^{24}Na ($T_{1/2} = 14.997$ h) is easily quantified by means of the intense γ -ray line at 1368.626 keV (99.9936% intensity), and can be used in parallel with ^{22}Na to monitor ^3He -particle beams over an energy range of 20 to 130 MeV. As with the choices made during the course of the 2007 update [10], all datasets up to an incident particle energy of 180 MeV were included in the compilation, while the fit and recommendation were limited to below 130 MeV.

Six publications with experimental cross-section data that covered the energy range of interest were identified in the literature [264–266, 269–271], and are represented with uncertainties in Fig. 24(a). Only the data by Lebeda

(2016) [269] were added after the previous update of the IAEA monitor reaction website in 2007 [10].

The data of Frantsvog *et al.* (1982) [271] were not considered for further evaluation as they are clearly too low, while one low data point from Michel *et al.* (1982) [270] at an incident particle energy of 40 MeV was also removed from the fitting process. A Padé function with 9 parameters was fitted to 81 selected data points with a $\chi^2=1.44$ covering an energy range of 20 to 130 MeV, as shown in Fig. 24(b). Uncertainties include a 4% systematic uncertainty, and decrease from 20% near the reaction threshold to lower than 10% at an incident particle energy of 27 MeV and remain at approximately 7% between 44 and 130 MeV. The rather sharp maximum in the excitation function near 40 MeV arises from the $^{27}\text{Al}(^3\text{He},2\alpha p)^{24}\text{Na}$ reaction with an energy threshold of 12.063 MeV, while the plateau at higher energies contains contributions from reactions that emit a greater number of independent nucleons, for example the $^{27}\text{Al}(^3\text{He},4p2n)^{24}\text{Na}$ reaction with a threshold of 43.52 MeV.

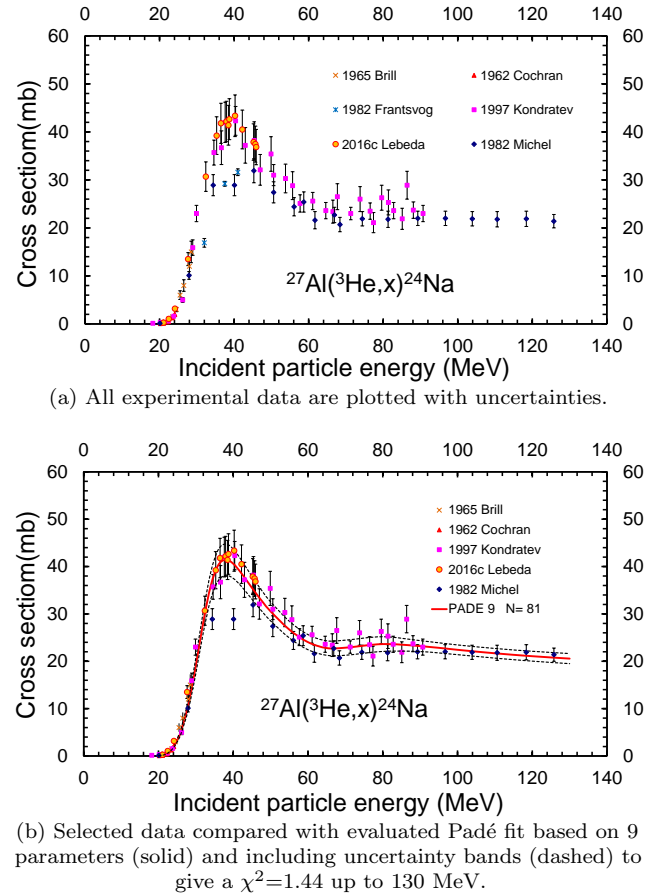
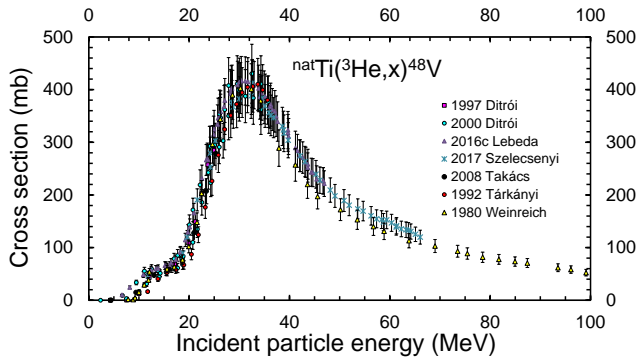


FIG. 24. (Color online) Evaluated Padé fit and experimental data from Refs. [264–266, 269–271] for the $^{27}\text{Al}(^3\text{He},x)^{24}\text{Na}$ monitor reaction.



(a) All experimental data are plotted with uncertainties.

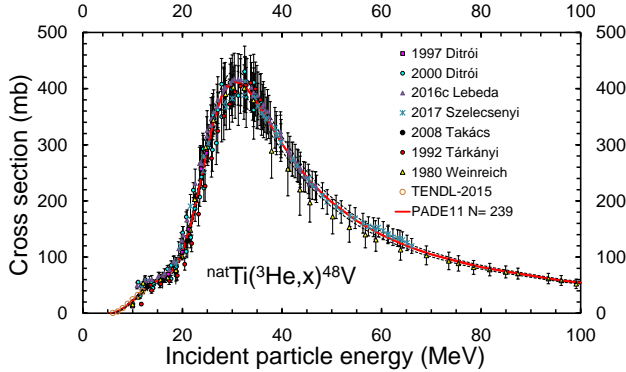
(b) Selected data compared with evaluated Padé fit based on 11 parameters (solid) and including uncertainty bands (dashed) to give a $\chi^2=1.25$ up to 100 MeV.

FIG. 25. (Color online) Evaluated Padé fit and experimental data from Refs. [12, 211, 269, 272–275] for the $^{nat}\text{Ti}(^3\text{He},x)^{48}\text{V}$ monitor reaction. The experimental data below 10 MeV were replaced by seven data points from TENDL-2015 [276].

C. $^{nat}\text{Ti}(^3\text{He},x)^{48}\text{V}$

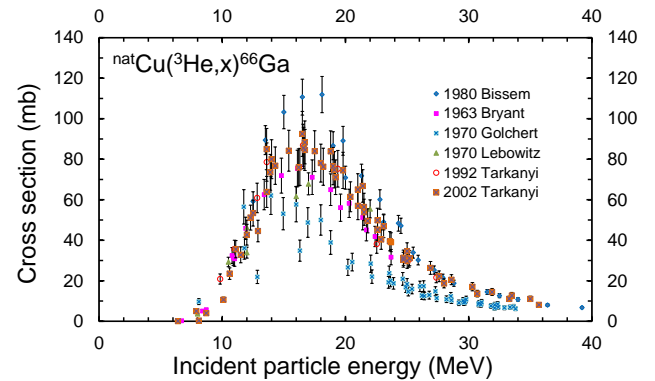
The $^{nat}\text{Ti}(^3\text{He},x)^{48}\text{V}$ reaction on readily available and corrosion resistant Ti is probably the most popular means of monitoring ^3He in the low and middle energy region of the beam (10–50 MeV). Activation product ^{48}V with $T_{1/2}=15.9735$ d decays via the emission of two intense γ -ray lines at 983.525 keV (99.98% intensity) and 1312.106 keV (98.2% intensity). Seven publications with relevant experimental cross-section data at incident particle energies up to 100 MeV were identified in the literature [12, 211, 269, 272–275], and are shown with uncertainties in Fig. 25(a). Two new references were added after the previous update of the IAEA monitor reaction website in 2007 [10]: Lebeda (2016) [269] and Szelecsényi *et al.* (2017) [274]. All datasets were used in the evaluation apart from values below an incident particle energy of 10 MeV that were deleted because of their large scatter and non-physical behaviour to be replaced by seven data points taken from the TENDL-2015 on-line database [276]. A Padé function with 11 parameters was fitted to 239 selected data points with $\chi^2=1.25$ up to 100 MeV, as shown in Fig. 25(b).

Uncertainties include a 4% systematic uncertainty, and

decrease from 45% near the reaction threshold to below 7% at 18 MeV, with variations between 4.5% and 4% within the 28–100 MeV energy range. The broad maximum near 32 MeV ($\sigma=400$ mb) arises essentially from the $^{48}\text{Ti}(^3\text{He},p2n)^{48}\text{V}$ reaction with a threshold at 13.3 MeV which involves the stable and most naturally abundant Ti isotope. A shoulder at lower energy arises from the $^{47}\text{Ti}(^3\text{He},n)^{48}\text{V}$ reaction, with a threshold of 9.45 MeV and ^{47}Ti natural abundance of 7.44%. We refer to Sec. II C for remarks on the presence of simultaneously formed ^{48}Sc ($T_{1/2}=43.67$ h).

D. $^{nat}\text{Cu}(^3\text{He},x)^{66}\text{Ga}$

A decision was taken to supplement the above monitors of ^3He beams with three additional reactions on ^{nat}Cu which is often used as the backing material for targets. Activation product ^{66}Ga with $T_{1/2}=9.49$ h decays via the emission of two γ -ray lines at 833.532 keV (5.9% intensity) and 1039.22 keV (37.0% intensity). Six publications with experimental cross-section data at incident particle energies up to 40 MeV were identified in the literature [275, 277–281], and are shown with uncertainties in Fig. 26(a). All references are new as this reaction was not



(a) All experimental data are plotted with uncertainties.

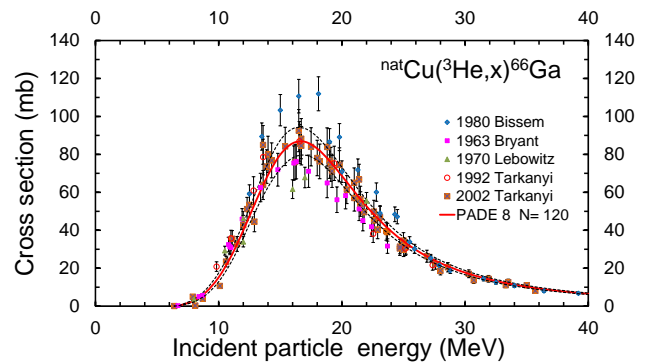
(b) Selected data compared with evaluated Padé fit based on 8 parameters (solid) and including uncertainty bands (dashed) to give a $\chi^2=1.69$ up to 40 MeV.

FIG. 26. (Color online) Evaluated Padé fit and experimental data from Refs. [275, 277–281] for the $^{nat}\text{Cu}(^3\text{He},x)^{66}\text{Ga}$ monitor reaction.

present in previous versions of the IAEA monitor reaction website [10]. The data of Golchert *et al.* (1970) [279] were removed prior to evaluation because the cross-section values are clearly lower than all other data.

A Padé function with 8 parameters was fitted to 120 selected data points with $\chi^2=1.69$ up to 40 MeV, as shown in Fig. 26(b). Uncertainties include a 4% systematic uncertainty, and decrease from 30% close to the reaction threshold to below 7% over an incident particle energy range of 18 to 40 MeV. The only contributor to the observed excitation function is the $^{65}\text{Cu}(^3\text{He},2n)^{66}\text{Ga}$ reaction with a threshold of 4.971 MeV that exhibits a broad maximum at approximately 17 MeV ($\sigma=86.5$ mb).

E. $^{nat}\text{Cu}(^3\text{He},x)^{63}\text{Zn}$

A second proposed monitor for ^3He -beams on Cu is the formation of short-lived ^{63}Zn ($T_{1/2}=38.47$ min.). Decay characteristics and specific problems associated with the use of this activation product were discussed in Sec. II G. Four publications with experimental cross-section data at incident particle energies up to 45 MeV were identified in the literature [277–280], and are shown with uncertainties in Fig. 27. The study of Bissem *et al.* (1980) [277] contains two datasets represented separately as (a) and (b). All references are new as this reaction was not present in previous versions of the IAEA monitor reaction website [10], and all of these data were included in the full evaluation.

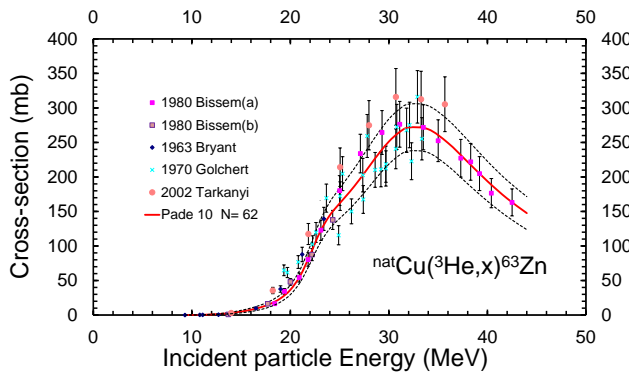


FIG. 27. (Color online) Evaluated Padé fit with 10 parameters (solid) and including uncertainty bands (dashed) to give a $\chi^2=1.78$ up to 45 MeV compared with experimental data from Refs. [277–280] for the $^{nat}\text{Cu}(^3\text{He},x)^{63}\text{Zn}$ monitor reaction. Ref. [277] contains two datasets represented as (a) and (b).

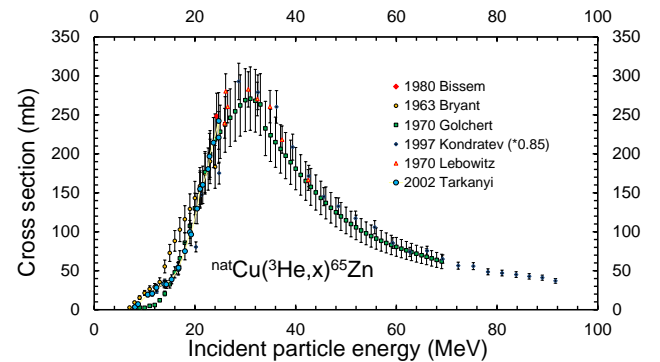
A Padé function with 10 parameters was fitted to 62 selected data points with $\chi^2=1.78$ up to 45 MeV, as shown in Fig. 27. Uncertainties include a 4% systematic uncertainty, and range from 45% close to the reaction threshold to less than 20% beyond an incident particle energy of 20 MeV with a minimum of 12.5% leading up to the maximum cross section considered. The only contribution within the energy domain under consideration is the $^{63}\text{Cu}(^3\text{He},p2n)^{63}\text{Zn}$ reaction with a threshold of 12.43 MeV which shows a broad maximum at approximately 32 MeV ($\sigma=271$ mb). The $^{65}\text{Cu}(^3\text{He},p4n)^{63}\text{Zn}$

reaction can only play a role at higher energies because the threshold is 31.072 MeV.

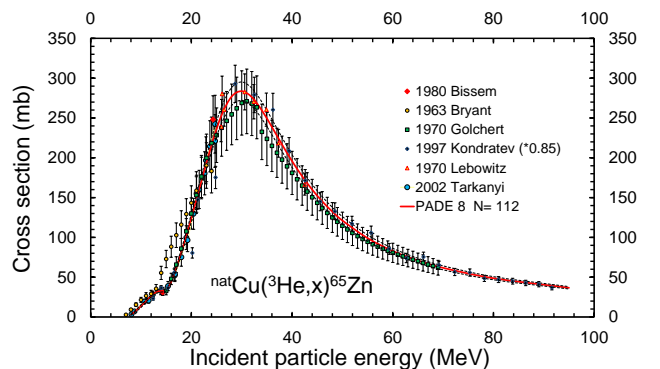
F. $^{nat}\text{Cu}(^3\text{He},x)^{65}\text{Zn}$

A third proposed monitor for ^3He -beams on Cu is the cumulative formation of long-lived ^{65}Zn ($T_{1/2}=243.93$ d) that includes the total decay of parent ^{65}Ga ($T_{1/2}=15.2$ min.). Decay characteristics of ^{65}Zn were discussed in Sec. II H. Six publications with experimental cross-section data at incident particle energies up to 95 MeV were identified in the literature as relevant [266, 277–281], and are shown with uncertainties in Fig. 28(a).

Bissem *et al.* (1980) [277] quantifies cross sections at only two energies (14.3 and 24.3 MeV), although cumulative formation on ^{nat}Cu could be derived from the original data (separate values for ^{65}Ga and ^{65}Zn formation on enriched $^{63,65}\text{Cu}$ targets). The published values of Kondratev *et al.* (1997) [266] were multiplied by a factor of 0.85 to obtain better agreement with much of the data from the other authors. Golchert *et al.* (1970) [279] considered only the contribution of reactions on ^{65}Cu , and therefore the low-energy region of the excitation function is underestimated. All references are new as this reaction



(a) All experimental data are plotted with uncertainties.



(b) Selected data compared with evaluated Padé fit based on 8 parameters (solid) and including uncertainty bands (dashed) to give a $\chi^2=0.62$ up to 90 MeV.

FIG. 28. (Color online) Evaluated Padé fit and experimental data from Refs. [266, 277–281] for the $^{nat}\text{Cu}(^3\text{He},x)^{65}\text{Zn}$ monitor reaction.

was not present in previous versions of the IAEA monitor reaction website [10].

Golchert *et al.* (1970) data below 15 MeV were removed prior to further evaluation because contributions from the ^{63}Cu -reactions are not included [279]. Although the values of Bryant *et al.* (1963) [278] exhibit a slight shift in the 14–19 MeV region, the dataset was still maintained within the selection. A Padé function with 8 parameters was fitted to 112 selected data points with $\chi^2=0.62$ up to 95 MeV, as shown in Fig. 28(b). Uncertainties include a 4% systematic uncertainty, and are approximately 20% close to the reaction threshold, decrease to less than 7% at an incident particle energy of 11 MeV and are constant at 4.1% from 17 MeV to the maximum energy studied. Four reactions are involved in the cumulative formation of ^{65}Zn . Only the exo-energetic reactions of $^{63}\text{Cu}(^3\text{He},p)^{65}\text{Zn}$ (Q value of +7.97 MeV) and $^{63}\text{Cu}(^3\text{He},n)^{65}\text{Ga}\rightarrow^{65}\text{Zn}$ (Q value of +3.937 MeV) contribute below 8 MeV, and their influence is dominant up to approximately 14 MeV. Around 15 to 16 MeV, the reactions of $^{65}\text{Cu}(^3\text{He},p2n)^{65}\text{Zn}$ with a threshold of 10.39 MeV and $^{65}\text{Cu}(^3\text{He},3n)^{65}\text{Ga}\rightarrow^{65}\text{Zn}$ with a threshold of 14.533 MeV begin to dominate, and are responsible for the high maximum of 283 mb at approximately 30 MeV.

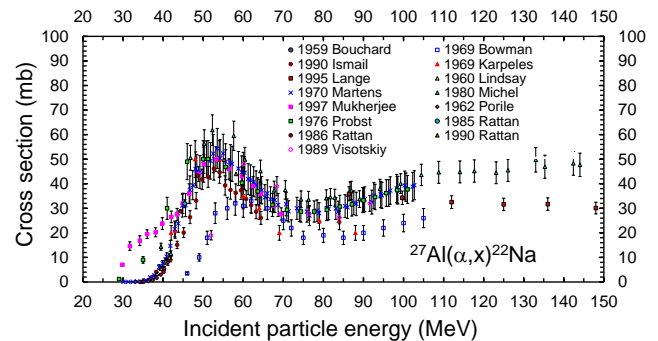
V. MONITOR REACTIONS FOR ^4HE BEAMS

TABLE V. Reactions for monitoring α beams and recommended decay data of the activation products ($T_{1/2}$ is the product half-life, and E_γ is the γ -ray energy in keV of the transition with intensity I_γ in %).

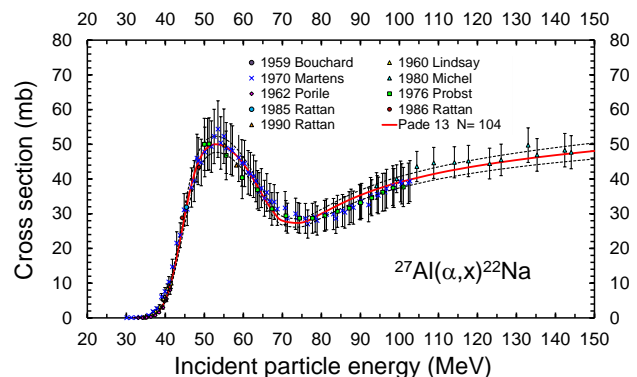
| Reaction | $T_{1/2}$ | E_γ (keV) | I_γ (%) | Useful range(MeV) |
|---|-----------|------------------|----------------|-------------------|
| $^{27}\text{Al}(\alpha,x)^{22}\text{Na}$ | 2.602 y | 1274.537 | 99.940 | 35–150 |
| $^{27}\text{Al}(\alpha,x)^{24}\text{Na}$ | 14.997 h | 1368.626 | 99.9936 | 40–160 |
| $^{nat}\text{Ti}(\alpha,x)^{51}\text{Cr}$ | 27.7010 d | 320.082 | 9.910 | 8–45 |
| $^{nat}\text{Cu}(\alpha,x)^{66}\text{Ga}$ | 9.49 h | 833.53 | 5.9 | 10–60 |
| | | 1039.22 | 37.0 | |
| $^{nat}\text{Cu}(\alpha,x)^{67}\text{Ga}$ | 3.2617 d | 184.576 | 21.410 | 10–45 |
| | | 300.217 | 16.64 | |
| $^{nat}\text{Cu}(\alpha,x)^{65}\text{Zn}$ | 243.93 d | 1115.539 | 50.04 | 10–45 |

A. $^{27}\text{Al}(\alpha,x)^{22}\text{Na}$

The formation of long-lived ^{22}Na ($T_{1/2} = 2.602$ y) is easily assessed by means of the intense γ -ray line at 1274.537 keV (99.940% intensity), and therefore the $^{27}\text{Al}(\alpha,x)^{22}\text{Na}$ reaction is widely used to monitor alpha-particle beams in the energy range of 35 to 150 MeV. Fifteen publications with experimental cross-section data within the incident particle energy range of interest were identified in the literature [195, 196, 282–294], and are shown with their uncertainties in Fig. 29(a). No new references were found following the previous update of the IAEA monitor reaction website in 2007 [10]. The results of six studies were removed prior to further analysis, and the reasons for their rejection are given in parentheses: Bowman and Blann (1969) (large energy shift, and values too low) [283], Ismail (1990) (values too low) [284],



(a) All experimental data are plotted with uncertainties.



(b) Selected data compared with evaluated Padé fit based on 13 parameters (solid) and including uncertainty bands (dashed) to give a $\chi^2=1.3$ up to 150 MeV.

FIG. 29. (Color online) Evaluated Padé fit and experimental data from Refs. [195, 196, 282–294] for the $^{27}\text{Al}(\alpha,x)^{22}\text{Na}$ monitor reaction.

Karpeles (1969) (values too low) [195], Lange *et al.* (1995) (only high energy values, lower than those of other authors) [285], Mukherjee *et al.* (1997) (discrepant data) [286], and Visotskiy *et al.* (1989) (energy shift, visible at lower energy) [294]. Additionally, the data points of Probst *et al.* (1976) [290] below 50 MeV (energy shift at the end of the stack foils) and the data points of Michel *et al.* (1980) [288] (end of the stack foils) were removed during the fitting process.

The remaining data from nine papers were used as input for a least-squares Padé fit [196, 282, 287–293]. Thus, a Padé function with 13 parameters was fitted to 104 selected data points with a $\chi^2=1.3$ covering the energy range from 35 to 150 MeV, as shown in Fig. 29(b). Uncertainties include a 4% systematic uncertainty, and decrease slowly from 30% near the reaction threshold, remain higher than 8% up to an incident particle energy of 46 MeV, and are of the order of 4.5% between 51 and 150 MeV. The rise of the excitation function up to 50 MeV results from the $^{27}\text{Al}(\alpha,2\alpha n)^{22}\text{Na}$ reaction with clustered emissions and a threshold of 25.850 MeV, while the slight increase and plateau at higher energies contains contributions from reactions that emit independent nucleons, for example $^{27}\text{Al}(\alpha,\alpha 2p 3n)^{22}\text{Na}$ with a threshold of 58.344 MeV.

B. $^{27}\text{Al}(\alpha, x)^{24}\text{Na}$

The formation of ^{24}Na ($T_{1/2} = 14.997$ h) is easily quantified by means of the intense γ -ray line at 1368.626 keV (99.9936% intensity), and therefore can be used in parallel with ^{22}Na to monitor α beams in the incident particle energy range of 40 to 160 MeV. Similar to the choice made in the 2007 update of Ref. [10], all datasets up to 180 MeV were included in the evaluation, while the fit and recommendations were limited to 160 MeV. Twenty publications with experimental cross-section data within the specified incident particle energy range of interest were identified in the literature [196, 282–300], and are shown with their uncertainties in Fig. 30(a). Data from eight publications were not included in the further evaluation, and the reason for their rejection are given in parentheses: Benzakin and Gauvin (1970)(values too high) [295], Bowman and Blann (1969) (low values and energy shift) [283], Gordon (1967) (values too high) [297], Lange *et al.* (1995) (values too low) [285], Lindner and Osborne (1953) (energy shift in region of study, very high primary α energy) [300], Mukherjee *et al.* (1997) (unusual shape of excitation function) [286], Probst *et al.* (1976) (energy shift) [290], and Visotskiy *et al.* (1989) (large energy shift) [294]. The low-energy data points of Porile (1962) [289] and Ismail

(1990) [284] were also removed prior to fitting.

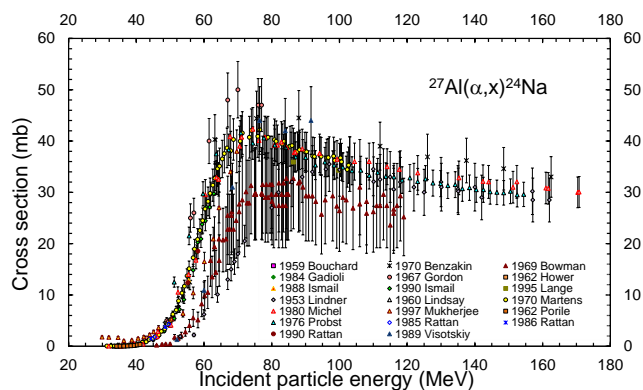
The remaining results from twelve publications were used for the least-squares data fitting [196, 282, 284, 287–289, 291–293, 296, 298, 299]. A Padé function with 12 parameters was fitted to 163 selected data points with a $\chi^2=1.44$ covering the energy range from 10 to 160 MeV, as shown in Fig. 30(b). Uncertainties include a 4% systematic uncertainty, and decrease slowly from 90% near the reaction threshold, remain higher than 6% up to an incident particle energy of 45 MeV, and are of the order of 4% between 70 and 160 MeV. The main contribution to the excitation function comes from the $^{27}\text{Al}(\alpha, \alpha 2pn)^{24}\text{Na}$ reaction with a threshold of 36.090 MeV. At higher energies, a plateau is formed by reactions with less cluster emission, for example the $^{27}\text{Al}(\alpha, 3dp)$ reaction has a threshold of 60.919 MeV, while the $^{27}\text{Al}(\alpha, 4p3n)^{24}\text{Na}$ reaction with the emission of individual nucleons has a threshold of 68.58 MeV. The small cross sections below 36 MeV are attributed to combinations of even stronger cluster emissions such as $^{27}\text{Al}(\alpha, \alpha^3\text{He})$ with a threshold of 27.23 MeV and $^{27}\text{Al}(\alpha, \alpha dp)$ with a threshold of 33.535 MeV.

C. $^{nat}\text{Ti}(\alpha, x)^{51}\text{Cr}$

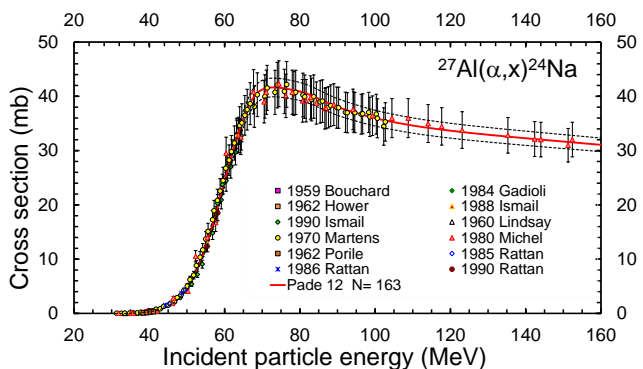
The preferred reaction for monitoring α beams with Ti foils involves the formation of relatively long-lived ^{51}Cr ($T_{1/2} = 27.7010$ d). Although the characteristic γ -ray decay line at 320.082 keV has only a moderate intensity of 9.910%, this emission allows an accurate assessment of the ^{51}Cr activity produced. Fifteen publications with experimental cross-section data within the specified incident particle energy range of interest were identified in the literature [86, 211, 275, 301–312], and are represented with their uncertainties in Fig. 31(a). The measurements by Hermanne *et al.* (1999b) constitute two datasets presented separately as (a) and (b) [303]. One new publication was found that is not present in the 2007 update of the IAEA monitor database [10]: Uddin and Scholten (2016) [310].

Datasets from eight publications were removed from further evaluation, and the reasons for their rejection are given in parentheses: Chang *et al.* (1973) (unusual shape of excitation function) [302], Hermanne *et al.* (1999b)(b) (values too low) [303], Iguchi *et al.* (1960) (energy shift) [304], Levkovskij (1991) (values too low) [86], Michel *et al.* (1983) (shifted to higher energies) [306], Tárkányi (1992) [275] (energy shift at lower energies), Weinreich *et al.* (1980) (energy shift at lower energies) [211], and Xiufeng Peng *et al.* (1998) (energy shift, data below threshold) [312].

Data points below 5 MeV of Király *et al.* (2008) [305] and Takács *et al.* (2007) [309] and the outlying value of Hermanne *et al.* (1999)(a) [303] at 18.7 MeV were not considered in the fitting process. The remaining eight datasets from eight publications were used for the least-squares fitting [301, 303, 305, 307–311]. A Padé function with 11 parameters was fitted to 242 selected data points with $\chi^2=1.50$ covering the energy range from 5 to 45 MeV,

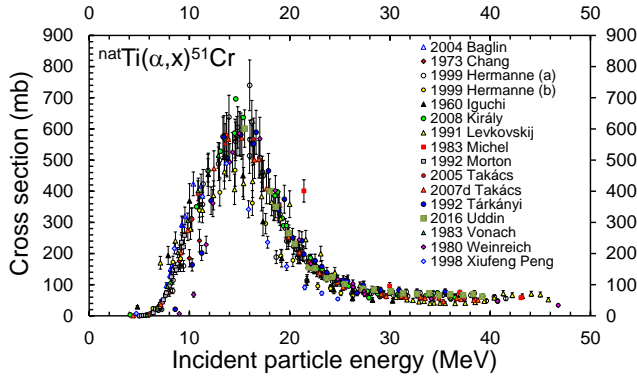


(a) All experimental data are plotted with uncertainties.



(b) Selected data compared with evaluated Padé fit based on 12 parameters (solid) and including uncertainty bands (dashed) to give a $\chi^2=1.44$ up to 160 MeV.

FIG. 30. (Color online) Evaluated Padé fit and experimental data from Refs. [196, 282–300] for the $^{27}\text{Al}(\alpha, x)^{24}\text{Na}$ monitor reaction.



(a) All experimental data are plotted with uncertainties.

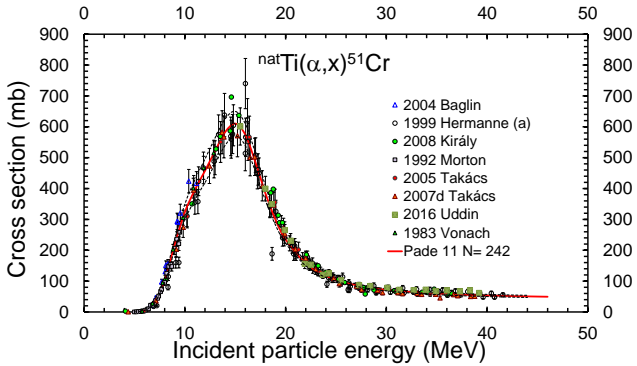
(b) Selected data compared with evaluated Padé fit based on 11 parameters (solid) and including uncertainty bands (dashed) to give a $\chi^2=1.50$ up to 45 MeV.

FIG. 31. (Color online) Evaluated Padé fit and experimental data from Refs. [86, 211, 275, 301–312] for the $^{nat}\text{Ti}(\alpha, x)^{51}\text{Cr}$ monitor reaction.

as shown in Fig. 31(b). Uncertainties include a 4% systematic uncertainty, and decrease from 10% near the reaction threshold to lower than 6% above an incident particle energy of 18 MeV. The main contribution to the maximum in the excitation function at approximately 15 MeV ($\sigma_{max}=610$ mb) arises essentially from the $^{48}\text{Ti}(\alpha, n)^{51}\text{Cr}$ reaction with a threshold at 9.911 MeV. Small contributions of reactions on less abundant Ti isotopes exist above 12 MeV, such as $^{49}\text{Ti}(\alpha, 2n)^{51}\text{Cr}$ with a threshold of 11.71 MeV and $^{50}\text{Ti}(\alpha, 3n)^{51}\text{Cr}$ with a threshold of 23.51 MeV.

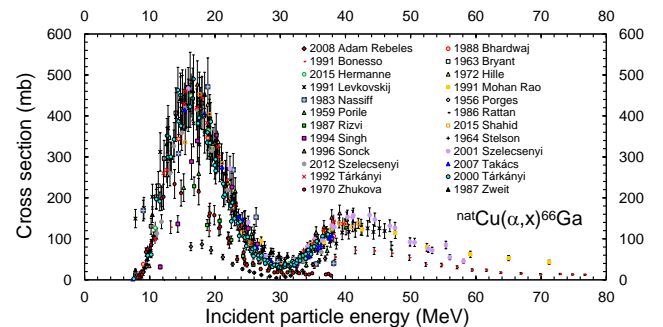
D. $^{nat}\text{Cu}(\alpha, x)^{66}\text{Ga}$

Several reactions on Cu as a backing material for electroplated or deposited targets are recommended to monitor α beams and other light-charged particles. Earlier evaluations of the three reactions discussed in the next three subsections have involved separating the known data into two groups defined as “high” and “low” with no satisfactory explanation (see [10]). Recent measurements supported by theoretical model calculations point towards the existence of only a “high” group of data.

The $^{nat}\text{Cu}(\alpha, xn)^{66}\text{Ga}$ reaction is preferred over the incident particle energy range from 10 to 30 MeV, result-

ing in an activation product with a half-life of 9.49 h that can be quantified by means of two γ -ray lines at 833.532 keV (5.9% intensity) and 1039.220 keV (37.0% intensity). Twenty-four publications with experimental cross-section data within the specified incident particle energy range of interest were identified in the literature [86, 275, 278, 292, 309, 313–331], and are represented with their uncertainties in Fig. 32(a). Three new publications were found that were not present in the 2007 update of the IAEA monitor database [10]: Hermanne *et al.* (2015) [316], Shahid *et al.* (2015) [323], and Szelecsényi *et al.* (2012) [328]. Datasets from eight publications were removed prior to further evaluation, and the reasons for their rejection are given in parentheses: Bonesso *et al.* (1993) (values too low) [315], Nassiff and Nassiff (1983) (data appear to be incorrect) [319], Porges (1956) (values too low) [320], Porile and Morrison (1959) (energy shift) [321], Rattan and Singh (1986) (only one point, value too low) [292], Rizvi *et al.* (1987) (energy shift) [322], Singh *et al.* (1994) (energy shift) [324], and Zhukova *et al.* (1970) (values too low) [330].

The five data points below 12 MeV of Levkovskij (1991) [86] and the lowest energy point of Shahid *et al.* (2015) [323] were removed prior to the fitting process because they were energy shifted or fell significantly below the main dataset. All remaining data points from sixteen publications were used for the least-squares fitting [86, 275, 278, 309, 313, 314, 316–318, 323, 325–



(a) All experimental data are plotted with uncertainties.

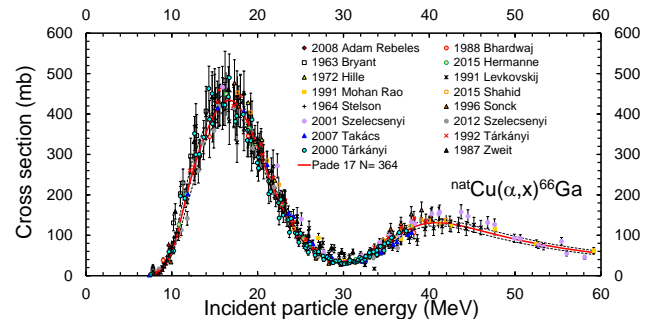
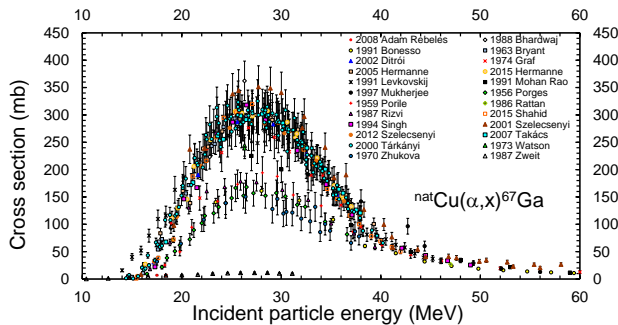
(b) Selected data compared with evaluated Padé fit based on 17 parameters (solid) and including uncertainty bands (dashed) to give a $\chi^2=1.53$ up to 60 MeV.

FIG. 32. (Color online) Evaluated Padé fit and experimental data from Refs. [86, 275, 278, 292, 309, 313–331] for the $^{nat}\text{Cu}(\alpha, x)^{66}\text{Ga}$ monitor reaction.

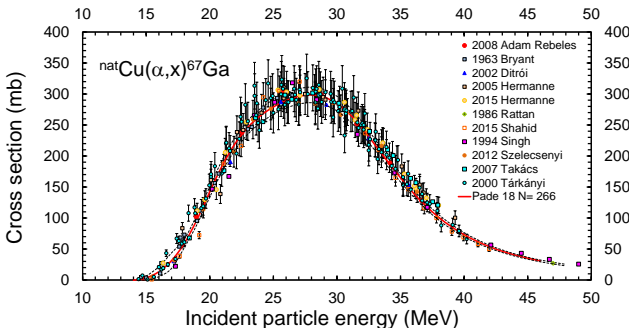
329, 331]. A Padé function with 17 parameters was fitted to 364 selected data points with a $\chi^2=1.53$ covering the energy range from 8 to 60 MeV, as shown in Fig. 32(b). Uncertainties include a 4% systematic uncertainty, and decrease from 10% near the reaction threshold to lower than 6% above an incident particle energy of 18 MeV. The main contribution to the first maximum in the excitation function at approximately 15 MeV ($\sigma_{max}=450$ mb) comes primarily from the $^{63}\text{Cu}(\alpha,n)^{66}\text{Ga}$ reaction with a threshold at 7.978 MeV. A second smaller maximum arises from the $^{65}\text{Cu}(\alpha,3n)^{66}\text{Ga}$ reaction on less naturally abundant ^{65}Cu with a threshold of 26.889 MeV.

E. $^{nat}\text{Cu}(\alpha,x)^{67}\text{Ga}$

The $^{nat}\text{Cu}(\alpha,x)^{67}\text{Ga}$ reaction constitutes a useful complement with Cu foils over the incident particle energy range from 15 to 40 MeV. Longer-lived activation product ^{67}Ga ($T_{1/2}=3.2617$ d) can be accurately quantified by means of the γ -ray lines at 184.576 keV (21.410% intensity) and 300.217 keV (16.64% intensity). Twenty-four publications with experimental cross-section data within the specified incident particle energy range of interest were identified in the literature [86, 210, 278, 286, 292, 309, 313–316, 318, 320–324, 327–334], and are represented with their uncertainties in Fig. 33(a). Three new publications were found that were not present in the 2007 update of the



(a) All experimental data are plotted with uncertainties.



(b) Selected data compared with evaluated Padé fit based on 18 parameters (solid) and including uncertainty bands (dashed) to give a $\chi^2=1.27$ up to 60 MeV.

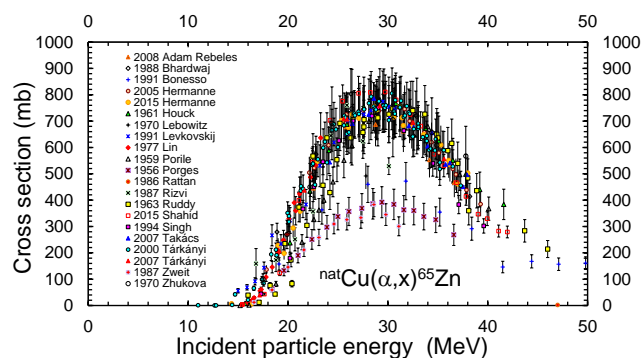
FIG. 33. (Color online) Evaluated Padé fit and experimental data from Refs. [86, 210, 278, 286, 292, 309, 313–316, 318, 320–324, 327–334] for the $^{nat}\text{Cu}(\alpha,x)^{67}\text{Ga}$ monitor reaction.

IAEA monitor database [10]: Hermanne *et al.* (2015) [316], Shahid *et al.* (2015) [323], and Szelecsényi *et al.* (2012) [328]. Datasets from thirteen publications were removed prior to further evaluation, and the reasons for their rejection are given in parentheses: Bhardwaj *et al.* (1988) (unusual shape of excitation function) [314], Bonesso *et al.* (1991) (values too low) [315], Graf and Munzel (1974) (values too low) [333], Levkovskij (1991) (energy shift, and values too low) [86], Mohan Rao *et al.* (1991) (values near maximum too low) [318], Mukherjee *et al.* (1997) (energy steps too large) [286], Porges (1956) (values too low) [320], Porile and Morrison (1959) (energy shift) [321], Rizvi *et al.* (1987) (energy shift, and values too low) [322], Szelecsényi *et al.* (2001) (values 10% too high) [327], Watson *et al.* (1973) (two outlying points too low) [210], Zhukova *et al.* (1970) (values too low) [330], and Zweit *et al.* (1987) (wrong data) [331].

All remaining results from eleven publications were used in the least-squares fitting process [278, 292, 309, 313, 316, 323, 324, 328, 329, 332, 334]. A Padé function with 18 parameters was fitted to 266 selected data points with a $\chi^2=1.27$ covering an energy range from 8 to 60 MeV, as shown in Fig. 33(b). Uncertainties include a 4% systematic uncertainty, and decrease from 100% near the reaction threshold to lower than 5% above an incident particle energy of 22 MeV to increase again at energies above 47 MeV (for example, 13.75% at 60 MeV). The only contribution to the maximum in the excitation function at approximately 28 MeV ($\sigma_{max}=298$ mb) arises from the $^{65}\text{Cu}(\alpha,2n)^{67}\text{Ga}$ reaction with a threshold of 14.971 MeV.

F. $^{nat}\text{Cu}(\alpha,x)^{65}\text{Zn}$

A third useful reaction on Cu with which to monitor α beams in the energy range from 20 to 45 MeV is $^{nat}\text{Cu}(\alpha,xn)^{65}\text{Zn}$ that results in long-lived activation product ^{65}Zn ($T_{1/2}=243.93$ d) with decay characteristics that have already been discussed in Sec. II H. Twenty-one publications with experimental cross-section data within the specified incident particle energy range of interest were identified in the literature [86, 281, 292, 309, 313–316, 320–324, 329–331, 334–338], and are represented with their uncertainties in Fig. 34(a). Two new publications were found that were not available during the 2007 update of the IAEA monitor database [10]: Hermanne *et al.* (2015) [316], and Shahid *et al.* (2015) [323]. Data from nine publications were discarded prior to further evaluation, and the reasons for their rejection are given in parentheses: Bonesso *et al.* (1991) (values too low) [315], Lebowitz and Greene (1970) (only one point, value too low) [281], Porges (1956) (values too low values) [320], Porile and Morrison (1959) (energy shift) [321], Rattan and Singh (1986) (values too low, noted as 1.987 mb in Table 4 of reference) [292], Rizvi *et al.* (1987) (values too low at higher energy) [322], Ruddy (1963) (data scattered at low energy) [337], Singh *et al.* (1994) (values too low at higher energy) [324], and Zweit *et al.* (1987) (values too low) [331]. The data



(a) All experimental data are plotted with uncertainties.

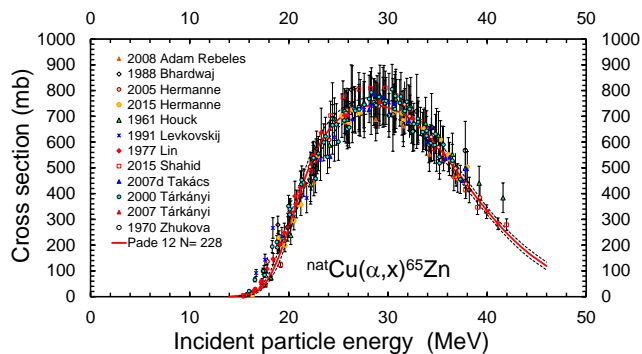
(b) Selected data compared with evaluated Padé fit based on 12 parameters (solid) and including uncertainty bands (dashed) to give a $\chi^2=1.48$ up to 45 MeV.

FIG. 34. (Color online) Evaluated Padé fit and experimental data from Refs. [86, 281, 292, 309, 313–316, 320–324, 329–331, 334–338] for the $^{nat}\text{Cu}(\alpha,x)^{65}\text{Zn}$ monitor reaction.

points below 16 MeV of Hermanne *et al.* (2015) [316], Levkovskij (1991) [86] and Tárkányi *et al.* (2000) [329] were also removed prior to the final fitting process.

All remaining datasets from twelve publications were used in the least-squares fitting process [86, 309, 313, 314, 316, 323, 329, 330, 334–336, 338]. A Padé function with 12 parameters was fitted to 228 selected data points with a $\chi^2=1.48$ covering the energy range from 16 to 45 MeV, as shown in Fig. 34(b). Uncertainties include a 4% systematic uncertainty, and decrease from 25% near the reaction threshold to lower than 5% over the incident particle energy range from 24 to 40 MeV to increase again to 12.5% at 45 MeV. The only contribution to the maximum in the excitation function at approximately 26 MeV ($\sigma_{max}=280$ mb) arises from the $^{63}\text{Cu}(\alpha,pn)^{65}\text{Zn}$ reaction with a threshold of 13.404 MeV. At higher energies, small contributions can originate from the $^{65}\text{Cu}(\alpha,p3n)^{65}\text{Zn}$ reaction with a threshold of 32.305 MeV; however, these potential sources are not visible in the measured excitation function.

VI. SUMMARY AND CONCLUSIONS

The IAEA Coordinated Research Project on “Nuclear Data for Charged-particle Monitor Reactions and Medical Isotope Production” galvanized nuclear cross-section research activities between 2012 and 2017 through the encouragement of highly relevant measurements at accelerators and comprehensive evaluations of the most relevant charged-particle induced reactions. The organisation of such a programme of work catalysed comprehensive technical discussions of the experimental and theoretical challenges in such measurements, theoretical modelling and evaluations in order to address cross-section reaction and decay data needs.

For the most part, investigations of evaluation methodology in this CRP remained firmly rooted within the realm of traditional least-squares techniques for merging experimental and model data. Nevertheless, previously unknown and ill-defined systematic uncertainties have been estimated on the basis of the considerable amount of data available for each of the selected beam-monitor reactions. Such estimated systematic uncertainties corresponds to the lowest achievable uncertainty for each monitor reaction at a given incident particle energy. This CRP galvanised the generation of new evaluations of charged-particle beam monitor reactions that for the first time include uncertainties for the most commonly used beam monitors relevant to accelerator applications.

Perhaps the most important contribution of the present CRP has been to provide significantly improved beam-monitor cross-section evaluations and evaluation methodology, and a timely road map for future work in this field. Thus, the CRP activities have served as a worthy and, in many respects, more comprehensive successor to the valuable pioneering efforts that produced IAEA-TECDOC-1211 some 20 years ago [1].

ACKNOWLEDGEMENTS

Our sincere thanks to all colleagues who have contributed to and worked on this project during the last five years. The preparation of this paper would not have been possible without the support, hard work and endless efforts of a large number of individuals and institutions.

First of all, the IAEA is grateful to all participant laboratories for their assistance in the work and for support of the CRP meetings and activities. The work described in this paper would not have been possible without IAEA Member State contributions. Work at ANL was supported by the U.S. Department of Energy, Office of Science, Office of Nuclear Physics, under contract no. DE-AC-06CH11357.

We much appreciate the valuable contributions made by I. Spahn during the various project meetings. Last but not least we are indebted to S.M. Qaim for his precedent work which is acknowledged as a source of inspiration.

- [1] K. Gul, A. Hermanne, M.G. Mustafa, F.M. Nortier, P. Obložinský, S.M. Qaim, B. Scholten, Y. Shubin, S. Takács, F.T. Tárkányi and Y. Zhuang, “Charged Particle Cross-section Database for Medical Radioisotope Production: Diagnostic Radioisotopes and Monitor Reactions”, IAEA Technical Report **IAEA-TECDOC-1211**, May 2001, Vienna, Austria. Available online at www-nds.iaea.org/publications/tecdocs/iaea-tecdoc-1211.pdf.
- [2] N. Otuka, E. Dupont, V. Semkova, B. Pritychenko *et al.*, “Towards a More Complete and Accurate Experimental Nuclear Reaction Data Library (EXFOR): International Collaboration Between Nuclear Reaction Data Centres (NRDC)”, *NUCL. DATA SHEETS* **120**, 272–276 (2014). Data available online (*e.g.*, at www-nds.iaea.org/exfor/).
- [3] K. Okamoto, Consultants’ Meeting on “Nuclear Data for Medical Radioisotope Production”, Vienna, April 1981, IAEA report **INDC(NDS)-123** (IAEA, Vienna, 1981). Available online at www-nds.iaea.org/publications/indc/indc-nds-123.pdf.
- [4] K. Okamoto, Consultants’ Meeting on “Data Requirements for Medical Radioisotope Production”, Tokyo, April 1987, IAEA report **INDC(NDS)-195** (IAEA, Vienna, 1988). Available online at www-nds.iaea.org/publications/indc/indc-nds-195.pdf.
- [5] O. Schwerer and K. Okamoto, “Status Report on Cross-sections of Monitor Reactions for Radioisotope Production” (IAEA, Vienna, 1989). Available online at www-nds.iaea.org/publications/indc/indc-nds-218.pdf.
- [6] N.P. Kocherov, Advisory Group Meeting on “Intermediate Energy Data for Applications, Working Group on Nuclear Data for Medical Applications” (IAEA, Vienna, 1990). Available online at www-nds.iaea.org/publications/indc/indc-nds-245.pdf.
- [7] P. Obložinský, First Research Coordination Meeting on “Development of Reference Charged Particle Cross-section Database for Medical Radioisotope Production”, IAEA report **INDC(NDS)-349** (IAEA, Vienna, 1995). Available online at www-nds.iaea.org/publications/indc/indc-nds-349.pdf.
- [8] P. Obložinský, Second Research Coordination Meeting on “Development of Reference Charged Particle Cross-section Database for Medical Radioisotope Production”, IAEA report **INDC(NDS)-371** (IAEA, Vienna, 1997). Available online at www-nds.iaea.org/publications/indc/indc-nds-371.pdf.
- [9] P. Obložinský, Third Research Coordination Meeting on “Development of Reference Charged Particle Cross-section Database for Medical Radioisotope Production”, IAEA report **INDC(NDS)-388** (IAEA, Vienna, 1998). Available online at www-nds.iaea.org/publications/indc/indc-nds-388.pdf.
- [10] IAEA reference data for charged-particle monitor reactions. Updated January–April 2007. Available online at www-nds.iaea.org/medical/monitor_reactions.html.
- [11] S. Takács, F. Tárkányi, M. Sonck, A. Hermanne, “New cross sections and intercomparison of proton monitor reactions on Ti, Ni and Cu”, *NUCL. INSTRUM. METHODS PHYS. RES.* **B188**, 106 (2002); EXFOR D4106.
- [12] S. Takács, F. Tárkányi, A. Hermanne, “Validation and upgrading of the recommended cross section data of charged particle monitor reactions”, *Proc. Int. Conf. Nuclear Data for Science and Technology*, Nice, France, 22–27 April, 2007. Eds.: O. Bersillon, F. Gunsing, E. Bange *et al.*, EDP Sciences, 1255–1258 (2008).
- [13] R. Capote and A.L. Nichols, Consultants’ Meeting on “High-precision beta-intensity measurements and evaluations for specific PET radioisotopes”, 3–5 Sept. 2008, IAEA report **INDC(NDS)-0535**, Dec. 2008, IAEA, Vienna, Austria. Available online at www-nds.iaea.org/publications/indc/indc-nds-0535.pdf.
- [14] E. Běták, A.D. Caldeira, R. Capote, B.V. Carlson, H.D. Choi, F.B. Guimarães, A.G. Ignatyuk, S.K. Kim, B. Király, S.F. Kovalev, E. Menapace, A.L. Nichols, M. Nortier, P. Pompeia, S.M. Qaim, B. Scholten, Yu.N. Shubin, J.-Ch. Sublet and F. Tárkányi, “Nuclear Data for the Production of Therapeutic Radionuclides”, **IAEA Technical Reports Series No. 473**, Eds: S.M. Qaim, F. Tárkányi and R. Capote, International Atomic Energy Agency, Vienna, Austria, 2011, ISBN 978-92-0-115010-3. Available online at www-nds.iaea.org/publications/tecdocs/technical-reports-series-473.pdf.
- [15] R. Capote and F.M. Nortier, Consultants’ Meeting on “Improvements in charged-particle monitor reactions and nuclear data for medical isotope production”, 21–24 June 2011, IAEA report **INDC(NDS)-0591**, Sept. 2011, IAEA, Vienna, Austria. Available online at www-nds.iaea.org/publications/indc/indc-nds-0591.pdf.
- [16] A.L. Nichols, S.M. Qaim and R. Capote, Technical Meeting on “Intermediate-term Nuclear Data Needs for Medical Applications: Cross Sections and Decay Data”, 22–26 August 2011, IAEA report **INDC(NDS)-0596**, Sept. 2011, IAEA, Vienna, Austria. Available online at www-nds.iaea.org/publications/indc/indc-nds-0596.pdf.
- [17] A.L. Nichols and R. Capote, Summary Report of First Research Coordination Meeting on Nuclear Data for Charged-particle Monitor Reactions and Medical Isotope Production, 3–7 Dec. 2012, IAEA report **INDC(NDS)-0630**, Feb. 2013, IAEA, Vienna, Austria. Available online at www-nds.iaea.org/publications/indc/indc-nds-0630.pdf.
- [18] H. Piel, S.M. Qaim, G. Stocklin, “Excitation Function of (p,xn) Reactions on ^{nat}Ni and Highly Enriched ^{62}Ni : Possibility of Production of Medically Important Radioisotope ^{62}Cu on a Small Cyclotron”, *RADIOCHIM. ACTA* **57**, 1–5 (1992).
- [19] F. Tárkányi, F. Szelescsenyi, S. Takács, “Determination of Effective Bombarding Energies and Fluxes Using Improved Stacked Foil Technique”, *ACTA RADIOL. SUPPL.* **376**, 72–73 (1991).
- [20] Evaluated Nuclear Structure Data File (ENSDF). Available online at www.nndc.bnl.gov/ensdf/. Developed and maintained by the International Network Of Nuclear Structure and Decay Data Evaluators (NSDD) (see www-nds.iaea.org/nsdd/).
- [21] **LiveChart of Nuclides**, IAEA decay data retrieval code available online at www-nds.iaea.org/medical/monitor_reactions.html.
- [22] **NuDat**, Brookhaven National Laboratory, USA. Decay data retrieval code available online at www.nndc.bnl.gov/nudat2/.

- [23] Decay Data Evaluation Project. Data available online at www.nucleide.org/DDEP.htm.
- [24] A.L. Nichols, F.M. Nortier and R. Capote, Summary Report of Second Research Coordination Meeting on “Nuclear Data for Charged-particle Monitor Reactions and Medical Isotope Production”, 8-12 December 2014, IAEA report **INDC(NDS)-0675**, April 2015, IAEA, Vienna, Austria. Available online at www-nds.iaea.org/publications/indc/indc-nds-0675.pdf.
- [25] M.-M. Bé, V. Chisté, C. Dulieu, M.A. Kellett, X. Mougeot, A. Arinc, V.P. Chechev, N.Z. Kuzmenko, T. Kibedi, A. Luca, A.L. Nichols, “Table of Radionuclides (Vol 8 – A=41 to 198)”, *MONOGRAPHIE BMIPM-5 Vol. 8* (2016), Bureau International des Poids et Mesures, Sévres, France: ^{63}Zn decay data.
- [26] H.E. Padé, “Sur la Représentation Approchée d’une Fonction par des Fractions Rationnelles”, *Supplement to ANN. SCI. L’ÉCOLE NORM. SUP.*, Series 3, vol. **9**, 3–93 (1892).
- [27] P.R. Graves-Morris (Ed.), “Padé Approximants and their Applications”, Academic Press, New York (1973).
- [28] G.A. Baker Jr., “Essentials of Padé Approximants”, Academic Press, New York (1975).
- [29] V.N. Vinogradov, E.V. Gai, and N.S. Rabotnov, “Analytical Approximation of Data in Nuclear and Neutron Physics”, *Energoatomizdat, Moscow* (1987) in Russian.
- [30] E.V. Gai, “Some Algorithms for the Nuclear Data Evaluation and Construction of the Uncertainty Covariance Matrices”, *Vopr. Atomnoy Nauki i Tekhniki, ser. Nuclear Constants*, Issues 1–2, 56–65 (2007).
- [31] S.A. Badikov and E.V. Gai, “Some Sources of the Underestimation of Evaluated Cross-section Uncertainties”, p. 117–129, IAEA report **INDC(NDS)-438** (IAEA, Vienna, 2003). Available online at www-nds.iaea.org/publications/indc/indc-nds-0438.pdf.
- [32] A.D. Carlson, V.G. Pronyaev, D.L. Smith, N.M. Larson, Chen Zhenpeng, G.M. Hale, F.-J. Hamsch, E.V. Gai, Soo-Youl Oh, S.A. Badikov, T. Kawano, H.M. Hofmann, H. Vonach, S. Tagesen, “International Evaluation of Neutron Cross Section Standards”, *NUCL. DATA SHEETS* **110**, 3215–3324 (2009).
- [33] E.V. Gai, A.V. Ignatyuk, “Uncertainties and Covariances of the Fission Cross Sections and the Fission Neutron Multiplicities for Actinides”, *NUCL. DATA SHEETS* **109**, 2890–2893 (2008).
- [34] R.E. Batzel and G.H. Coleman, “Cross Sections for Formation of ^{22}Na from Aluminum and Magnesium Bombarded with Protons”, *PHYS. REV.* **93**, 280–282 (1954); EXFOR D4101.
- [35] R. Bodemann, H. Busemann, M. Gloris, I. Leya, R. Michel, T. Schiekkel, U. Herpers, B. Holmqvist, H. Condé, P. Malmberg, B. Dittrich-Hannen, and M. Suter, “New Measurements of the Monitor Reactions $^{27}\text{Al}(p,x)^7\text{Be}$, $^{27}\text{Al}(p,3p3n)^{22}\text{Na}$, $^{27}\text{Al}(p,3pn)^{24}\text{Na}$ and $^{65}\text{Cu}(p,n)^{65}\text{Zn}$ ”, Progress Report on Nuclear Data Research in the Federal Republic of Germany, ed. S.M. Qaim, NEA report **NEA/NSC/DOC(95)10**, and p. 29–31, IAEA report **INDC(GER)-040** (IAEA, Vienna, 1995); EXFOR O0282. Contains part of the data.
- [36] E.Z. Buthelezi, F.M. Nortier, I.W. Schroeder, “Excitation Functions for the Production of ^{82}Sr by Proton Bombardment of ^{nat}Rb at Energies up to 100 MeV”, *APPL. RADIAT. ISOT.* **64**, 915–924 (2006); EXFOR O1424.
- [37] J.E. Cline and E.B. Nieschmidt, “Measurements of Spallation Cross Sections for 590 MeV Protons on Thin Targets of Copper, Nickel, Iron and Aluminum”, *NUCL. PHYS.* **A169**, 437–448 (1971).
- [38] J.B. Cumming, “Absolute Cross Section for the $^{12}\text{C}(p,pn)^{11}\text{C}$ Reaction at 50 MeV”, *NUCL. PHYS.* **49**, 417–423 (1963); EXFOR B0095.
- [39] B. Dittrich, U. Herpers, R. Bodemann, M. Lüpke, R. Michel, P. Signer, R. Wieler, H. Hofmann, and W. Woelfli, “Production of Short- And Medium-lived Radionuclides by Proton-induced Spallation Between 800 and 2600 MeV”, p. 46, Report to NEANDC No. **312,U** (1990) and *RADIOCHIM. ACTA* **50**, 11–18 (1990); EXFOR A0478.
- [40] M. Furukawa, S. Kume and S.K. Ogawa, “Excitation Functions for the Formation of ^7Be and ^{22}Na in Proton Induced Reactions on ^{27}Al ”, *NUCL. PHYS.* **69**, 362–368 (1965); EXFOR P0016.
- [41] H.R. Heydegger, A.L. Turkevich, A. Van Ginneken and P.H. Walpole, “Production of ^7Be , ^{22}Na and ^{28}Mg from Mg, Al and SiO_2 by Protons Between 82 and 800 MeV”, *PHYS. REV.* **C14**, 1506 (1976); EXFOR O0501.
- [42] M.U. Khandaker, K. Kim, M.W. Lee, K.S. Kim and G.N. Kim, “Excitation Functions for the $^{27}\text{Al}(p,x)^{22,24}\text{Na}$ Nuclear Reactions up to 40 MeV”, *J. KOREAN PHYS. SOC.* **59**, 1821–1824 (2011); EXFOR D7003.
- [43] M.C. Lagunas-Solar, O.F. Carvacho and R.R. Cima, “Cyclotron Production of PET Radionuclides: ^{18}F (109.77 min; β^+ 96.9%; EC 3.1%) from High-energy Protons on Metallic Aluminum Targets”, *APPL. RADIAT. ISOT.* **39**, 41–47 (1988); EXFOR A0445.
- [44] M. Lefort and X. Tarrago, “Emission of alpha Particles from the Spallation of Bismuth by Protons of 240 to 600 MeV”, *NUCL. PHYS.* **46**, 161–170 (1963); EXFOR D0465.
- [45] L. Marquez, and I. Perlman, “Observations on Lithium and Beryllium Nuclei Ejected from Heavy Nuclei by High Energy Particles”, *PHYS. REV.* **81**, 953 (1951); EXFOR C0259.
- [46] L. Marquez, “The Yield of F-18 from Medium and Heavy Elements with 420 MeV Protons”, *PHYS. REV.* **86**, 405 (1952); EXFOR C0250.
- [47] R. Michel, G. Brinkmann, and W. Herr, “Integral Excitation Functions for p-induced Reactions”, p. 68, IAEA report **INDC(GER)-21/L** (IAEA, Vienna, 1979); EXFOR A0151.
- [48] R. Michel, M. Gloris, H.-J. Lange, I. Leya, M. Lüpke, U. Herpers, B. Dittrich-Hannen, R. Rösel, Th. Schiekkel, D. Filges, P. Dragovitsch, M. Suter, H.-J. Hofmann, W. Wölfl, P.W. Kubik, H. Baur and R. Wieler, “Nuclide Production by Proton-induced Reactions on Elements ($6 < Z < 29$) in the Energy Range from 800 to 2600 MeV”, *NUCL. INSTRUM. METHODS PHYS. RES.* **B103**, 183–222 (1995); EXFOR O0277.
- [49] R. Michel, R. Bodemann, H. Busemann, R. Daunke, M. Gloris, L.H. Lange, B. Klug, A. Krins, I. Leya, M. Lüpke, S. Neumann, H. Reinhardt, M. Schnatz-Büttgen, U. Herpers, Th. Schiekkel, F. Sudbrock, B. Holmqvist, H. Condé, P. Malmberg, M. Suter, B. Dittrich-Hannen, P.W. Kubik, H.A. Synal and D. Filges, “Cross Sections for the Production of Residual Nuclides by Low- and Medium-energy Protons from the Target Elements C, N, O, Mg, Al, Si, Ca, Ti, V, Mn, Fe, Co, Ni, Cu, Sr, Y, Zr, Nb, Ba, and Au”, *NUCL. INSTRUM. METHODS PHYS. RES.* **B129**, 153–193 (1997); EXFOR O0276.

- [50] G.L. Morgan, K.R. Alrick, A. Saunders, F.C. Cverna, N.S.P. King, F.E. Merrill, L.S. Waters, A.L. Hanson, G.A. Greene, R.P. Liljestrand, R.T. Thompson and E.A. Henry, "Total Cross Sections for the Production of ^{22}Na and ^{24}Na in Proton-induced Reactions on ^{27}Al from 0.40 to 22.4 GeV", *NUCL. INSTRUM. METHODS PHYS. RES.* **B211**, 297–304 (2003); EXFOR C0950.
- [51] Th. Schiekkel, F. Sudbrock, U. Herpers, M. Gloris, H.-J. Lange, I. Leya, R. Michel, B. Dittrich-Hannen, H.-A. Synal, M. Suter, P.W. Kubik, M. Blann and D. Filges, "Nuclide Production by Proton-induced Reactions on Elements ($6 \leq Z \leq 29$) in the Energy Range from 200 MeV to 400 MeV", *NUCL. INSTRUM. METHODS PHYS. RES.* **B114**, 91–119 (1996); EXFOR O0284.
- [52] J.M. Sisterson, K. Kim, A. Beverding, P.A.J. Englert, M.W. Caffee, J. Vincent, C. Casteneda and R.C. Reedy, "Measuring Excitation Functions Needed to Interpret Cosmogenic Nuclide Production in Lunar Rocks", *Proc. of the 14th Int. Conf. Application of Accelerators in Research and Industry*, 6–9 November 1996, Denton, Texas, USA, Eds: J.L. Duggan and I.L. Morgan, AIP CONF. PROC. **392**, 811 (1997), AIP, Woodbury, New York.
- [53] G.F. Steyn, S.J. Mills, F.M. Nortier, B.R.S. Simpson and B.R. Meyer, "Production of ^{52}Fe via Proton-induced Reaction on Manganese and Nickel", *APPL. RADIAT. ISOT.* **41**, 315–325 (1990); EXFOR A0497.
- [54] T.N. Taddeucci, J. Ullmann, L.J. Rybarcyk and G.W. Butler, "Total Cross Sections for Production of ^7Be , ^{22}Na , and ^{24}Na in $p+^7\text{Li}$ and $p+^{27}\text{Al}$ Reactions at 495 and 795 MeV", *PHYS. REV.* **55**, 1551–1554 (1997); EXFOR O0985.
- [55] Yu.E. Titarenko, O.V. Shvedov, V.F. Batyaev, E.I. Karpikhin, V.M. Zhivun, A.B. Koldobsky, R.D. Mulambetov, A.N. Sosin, Yu.N. Shubin, A.V. Ignatyuk, V.P. Lunev, S.G. Mashnik, R.E. Prael, T.A. Gabriel and M. Blann, "Experimental and Theoretical Study of the Yields of Radioactive Product Nuclei in Tc-99 Thin Targets Irradiated with 100–2600 MeV Protons", p. 88, USSR report to the INDC No. **434** (2003). See also Yu.E. Titarenko, O.V. Shvedov, M.M. Igumov, S.G. Mashnik, E.I. Karpikhin, V.D. Kazaritsky, V.F. Batyaev, A.B. Koldobsky, V.M. Zhivun, A.N. Sosin, R.E. Prael, M.B. Chadwick, T.A. Gabriel and M. Blann, "Experimental and Computer Simulation Study of the Radionuclides Produced in Thin ^{209}Bi Targets by 130 MeV and 1.5 GeV Proton-induced Reactions", *NUCL. INSTRUM. METHODS PHYS. RES.* **A414**, 73–99 (1998); EXFOR O0902.
- [56] M.S. Uddin, M. Hagiwara, F. Tárkányi, F. Ditrói and M. Baba, "Experimental Studies on the Proton-induced Activation Reactions of Molybdenum in the Energy Range 22–67 MeV", *APPL. RADIAT. ISOT.* **60**, 911–920 (2004); EXFOR E1894.
- [57] V.N. Aleksandrov, M.P. Semenova and V.G. Semenov, "Cross Section of Radionuclide Production in the (p,x) Reactions of Al and Si", *ATOMIC ENERGY* **64**, 445–446 (1988); EXFOR A0340.
- [58] C. Brun, M. Lefort and X. Tarrago, "Détermination des Intensités de Faisceaux de Protons de 40 a 150 MeV", *J. PHYS. RADIUM* **23**, 371–377 (1962). Data from Ref. [339].
- [59] H. Gauvin, M. Lefort and X. Tarrago, "Emission d'Hélions dans les Reactions de Spallation", *NUCL. PHYS.* **39**, 447–463 (1962); EXFOR C0394.
- [60] A. Gruetter, "Excitation Functions for Radioactive Isotopes Produced by Proton Bombardment of Cu and Al in the Energy Range of 16 to 70 MeV", *NUCL. PHYS.* **A383**, 98–108 (1982); EXFOR A0178.
- [61] N.M. Hintz and N.F. Ramsey, "Excitation Functions to 100 MeV", *PHYS. REV.* **88**, 19 (1952); EXFOR B0076.
- [62] R.G. Korteling and A.A. Caretto, "Energy Dependence of ^{22}Na and ^{24}Na Production Cross Sections with 100–400 MeV Protons", *PHYS. REV.* **C1**, 1960 (1970); EXFOR C0253.
- [63] K. Miyano, "The ^7Be , ^{22}Na and ^{24}Na Production Cross Sections with 22–52 MeV Proton on ^{27}Al ", *J. PHYS. SOC. JAPAN* **34**, 853–856 (1973); EXFOR O0449.
- [64] P. Pulfer, "Determination of Absolute Production Cross Sections for Proton Induced Reactions in the Energy Range 15 to 72 MeV and at 1820 MeV", thesis, 1979, unpublished; EXFOR D0053.
- [65] Yu.E. Titarenko, S.P. Borovlev, M.A. Butko, V.M. Zhivun, K.V. Pavlov, V.I. Rogov, A.Yu. Titarenko, R.S. Tikhonov, S.N. Florya and A.B. Koldobskiy, "Cross Section of $^{27}\text{Al}(p,x)^{24}\text{Na}$, $^{27}\text{Al}(p,x)^{22}\text{Na}$, $^{27}\text{Al}(p,x)^7\text{Be}$ Monitor Reaction at Proton Energies 0.04–2.6 GeV", *PHYS. AT. NUCLEI* **74**, 507–522 (2011).
- [66] W.A. Vukolov and F.E. Chukreev, "Estimated Values of Reaction Cross Section Used at Proton Flux Monitoring in Nuclear Spectroscopy and Nuclear Structure", *YAD. SPEKTR. I STRUKTURA ATOMNOGO YADRA, Tezisy dokladov INIS-US-68 (INISSU68)* 560 (1988).
- [67] J.R. Walton, D. Heymann and A. Yaniv, "Cross Sections for He and Ne Isotopes in Natural Mg, Al, and Si, He Isotopes in CaF_2 , Ar Isotopes in Natural Al, Si, Ti, Cr and Stainless Steel Induced by 12 to 45 MeV Protons", *J. GEOPHYS. RES.* **81**, 5689 (1976); EXFOR O0350.
- [68] I.R. Williams and C.B. Fulmer, "Excitation Functions for Radioactive Isotopes Produced by Protons Below 60 MeV on Al, Fe and Cu", *PHYS. REV.* **162**, 1055 (1967); EXFOR B0073.
- [69] M. Lüpke, H.J. Lange, M. Schnatz-Buttgen, R. Michel, R. Rosel, U. Herpers, P. Cloth, D. Filger, "Proton-spallation at 1600 MeV", p. 50, Fed. Rep. Germany report to the INDC No. **037/LN** (1993); EXFOR A0519.
- [70] R.S. Gilbert, private communication in Ref. [71]. Data described as "excluded" on IAEA webpage because their values seem to be shifted to higher energies, although the maximal cross sections are in good agreement with the values of the selected group. However, these data are plotted in the tab labelled "selected" (see www-nds.iaea.org/medical/alp24na0.html)
- [71] H.G. Hicks, P.C. Stevenson, and W.C. Nervik, "Reaction $^{27}\text{Al}(p,3pn)^{24}\text{Na}$ ", *PHYS. REV.* **102**, 1390 (1956). Data from Ref. [339].
- [72] J.J. Hogan, E. Gadioli, "Production of ^{24}Na from ^{27}Al by 35–100 MeV Protons", *NUOVO CIM.* **A45**, 341–350 (1978); EXFOR B0131.
- [73] R. Holub, M. Fowler, L. Yaffe and A. Zeller, "Formation of ^{24}Na in Fission-Like Reactions", *NUCL. PHYS.* **A288**, 291–300 (1977); EXFOR T0128.
- [74] S. Meghir, "Excitation Functions of Some Monitor Reactions", thesis, McGill University, Canada, 1962: reported in J.H. Davies and L. Yaffe, *CAN. J. PHYS.* **41**, 762–783 (1963); EXFOR B0016.
- [75] Yu.E. Titarenko, V.F. Batyaev, R.D. Mulambetov, V.M. Zhivun, V.S. Barashenkov, S.G. Mashnik, Y.N. Shubin and A.V. Ignatyuk, "Excitation Functions

- of Product Nuclei from 40 to 2600 MeV Proton-irradiated $^{206,207,208, nat}\text{Pb}$ and ^{209}Bi ”, *NUCL. INSTRUM. METHODS PHYS. RES.* **A562**, 801–805 (2006); EXFOR O1728.
- [76] R. Michel, R. Stück and F. Peiffer, “Proton-induced Reaction on Ti, V, Mn, Fe, Co and Ni”, *NUCL. PHYS.* **A441**, 617–659 (1985); EXFOR A0100013.
- [77] A.G.C. Nair, S.S. Rattan, A. Ramaswami, R.J. Singh and R.H. Iyer, “Proton Induced Fission of ^{243}Am at 17.8 MeV: Formation Cross Section for the Fission Products”, *36th Symp. Nucl. Phys.*, 27–30 December 1993, Calicut, India, 188 (1993); EXFOR D6156.
- [78] R.J. Schneider, J.M. Sisterson, A.M. Koehler, J. Klein and R. Middleton, “Measurement of Cross Sections for Aluminum-26 and Sodium-24 Induced by Protons in Aluminum”, *NUCL. INSTRUM. METHODS PHYS. RES.* **B29**, 271–274 (1987); EXFOR C0199.
- [79] H. Yule, A. Turkevich, “Radiochemical Studies of the (p,pn) Reaction in Complex Nuclei in the 80–450 MeV Range”, *PHYS. REV.* **118**, 1591 (1960).
- [80] J.N. Barrandon, J.L. Debrun, A. Kohn, R.H. Spear, “Etude du Dosage de Ti, V, Cr, Fe, Ni, Cu et Zn par Activation avec des Protons d’Energie Limitée à 20 MeV”, *NUCL. INSTRUM. METHODS* **127**, 269–278 (1975); EXFOR O0086.
- [81] C. Birattari, M. Bonardi, I.F. Resmin, E.A. Salomon, “Status Report on Radioisotope Production for Biomedical Purposes at Milan AVF Cyclotron”, in *Proc. 9th Int. Conf. Cyclotrons and their Applications*, 7–10 September 1981, Caen, France, ed. G. Gendreau, Editions de Physique, 693 (1982). Experimental details are published in: E. Sabbioni, E. Marafante, L. Goetz, C. Birattari, “Cyclotron Production of Carrier Free ^{48}V and Preparation of Different ^{48}V Compounds for Metabolic Studies in Rats”, *RADIOCHEM. RADIOANAL. LETT.* **31**, 39–46 (1977).
- [82] R.L. Brodzinski, L.A. Rancitelli, J.A. Cooper, N.A. Wogman, “High-Energy Proton Spallation of Titanium”, *PHYS. REV.* **4**, 1250 (1971); EXFOR C0271.
- [83] E. Gadioli, E. Gadioli Erba, J.J. Hogan, K.I. Burns, “Emission of Alpha Particles in the Interaction of 10–85 MeV Protons with $^{48,50}\text{Ti}$ ”, *Z. PHYS.* **A301**, 289–300 (1981); EXFOR D4060.
- [84] P. Jung, “Cross Sections for the Production of Helium and Long-living Radioactive Isotopes by Protons and Deuterons”, *Proc. Int. Conf. on Nuclear Data for Science and Technology*, 13–17 May 1991, Jülich, Fed. Rep. of Germany, ed: S.M. Qaim, 352–354 (1992) Springer-Verlag, Berlin; EXFOR D4058.
- [85] M.U. Khandaker, K. Kim, M.W. Lee, K.S. Kim, G.N. Kim, Y.S. Cho, Y.O. Lee, “Investigations of the $^{nat}\text{Ti}(p,x)^{43,44m,44g,46,47,48}\text{Sc}$, ^{48}V Nuclear Processes up to 40 MeV”, *APPL. RADIAT. ISOT.* **67**, 1348–1354 (2009); EXFOR D0569.
- [86] V.N. Levkovskij, “Middle Mass Nuclides (A=40–100) Activation Cross Sections by Medium Energy (E=10–50 MeV) Protons and α -particles (Experiments and Systematics)”, *INTER-VESTI*, Moscow, (1991); EXFOR A0510.
- [87] S. Tanaka and M. Furukawa, “Excitation Functions for (p,n) Reactions with Titanium, Vanadium, Chromium, Iron and Nickel up to $E_p = 14$ MeV”, *J. PHYS. SOC. JAPAN* **14**, 1269–1275 (1959); EXFOR B0043.
- [88] J.R. Walton, D. Heymann, A. Yaniv, “He and Ne Cross Sections in Natural Mg, Al and Si Targets and Radionuclide Cross Sections in Natural Si, Ca, Ti and Fe Targets Bombarded with 14 to 45 MeV Protons”, *J. GEOPHYS. RES.* **78**, 6428–6442 (1973).
- [89] M.E. Bennett, D.A. Mayorov, K.D. Chapkin, M.C. Alfonso, T.A. Werke, C.M. Folden III, “Measurement of the $^{nat}\text{Lu}(p,x)^{175}\text{Hf}$ Excitation Function”, *NUCL. INSTRUM. METHODS PHYS. RES.* **B276**, 62–65 (2012); EXFOR C1909.
- [90] B. Dittrich, “Radiochemische Untersuchung protonen- und α -Induzierter Spallations- und Fragmentations Reaktionen mit Hilfe der Gamma- und Beschleunigermassen-Spektrometrie”, dissertation, Universität zu Köln, Köln, 1990.
- [91] D. Fink, J. Sisterson, S. Vogt, G. Herzog, J. Klein, R. Middleton, A. Koehler, A. Magliss, “Production of ^{41}Ca and K, Sc and V Short-lived Isotopes by the Irradiation of Ti with 35 to 150 MeV Protons: Applications to Solar Cosmic Ray Studies”, *NUCL. INSTRUM. METHODS PHYS. RES.* **B52**, 601–607 (1990); EXFOR C0430.
- [92] E. Garrido “Production de Radio-isotopes: de la Mesure de la Section Efficace à la Production”, thesis, Annexe B: Valeurs de Sections Efficaces de Production, Université de Nantes, 2011.
- [93] E. Garrido, C. Duchemin, A. Guertin, F. Hadad, N. Michel, V. Métivier, “New Excitation Functions for Proton Induced Reactions on Natural Titanium, Nickel and Copper up to 70 MeV”, *NUCL. INSTRUM. METHODS PHYS. RES.* **B383**, 191–212 (2016); EXFOR O2315.
- [94] A. Hermanne, R. Adam Rebeles, F. Tárkányi, S. Takács, B. Király, A.V. Ignatyuk, “Cross Sections for Production of Longer Lived $^{170,168,167}\text{Tm}$ in 16 MeV Proton Irradiation of ^{nat}Er ”, *NUCL. INSTRUM. METHODS PHYS. RES.* **B269**, 695–699 (2011).
- [95] A. Hermanne, F. Tárkányi, S. Takács, “Experiments on Ti, Cu and Ni Foils with Protons of 36, 25 and 17 MeV at VUB Cyclotron”, private communication, 2013.
- [96] P. Kopecky, F. Szelecsényi, T. Molnár, P. Mikecz, F. Tárkányi, “Excitation Functions of (p,xn) Reactions on ^{nat}Ti : Monitoring of Bombarding Proton Beams”, *APPL. RADIAT. ISOT.* **44**, 687–692 (1993); EXFOR D4001.
- [97] O. Lebeda, “New Cross-sections for the $^{nat}\text{Ti}(p,x)^{48}\text{V}$ - ^{46}Sc Reactions”, private communication, 2016.
- [98] R. Michel and G. Brinkmann, “On the Depth-Dependent Production of Radionuclides ($44 < A < 59$) by Solar Protons in Extraterrestrial Matter”, *J. RADIOANAL. NUCL. CHEM.* **59**, 467–510 (1980); EXFOR A0145.
- [99] R. Stück, “Protonen- induzierte Reaktionen an Ti, V, Mn, Fe, Co und Ni. Messung und Hybrid Modell Analyse Integraler Anregungsfunktionen und ihre Anwendung in Modellrechnungen zur Produktion Kosmogener Nuklide”, dissertation, Universität zu Köln, Köln, 1983; EXFOR A0100.
- [100] F. Szelecsényi, F. Tárkányi, S. Takács, A. Hermanne, M. Sonck, Yu.N. Shubin, M.G. Mustafa, Zhuang Youxiang, “Excitation Function for the $^{nat}\text{Ti}(p,x)^{48}\text{V}$ Nuclear Process: Evaluation and New Measurements for Practical Applications”, *NUCL. INSTRUM. METHODS PHYS. RES.* **B174**, 47–64 (2001); EXFOR D4083.
- [101] S. Takács, F. Tárkányi, A. Hermanne, R. Adam Rebeles, “Activation Cross Sections of Proton Induced Nuclear Reactions on Natural Hafnium”, *NUCL. INSTRUM.*

- METHODS PHYS. RES. **B269**, 2824-2834 (2011).
- [102] S. Takács, M.P. Takács, A. Hermanne, F. Tárkányi, R. Adam Rebeles, "Cross Sections of Proton-induced Reactions on ^{nat}Sb ", NUCL. INSTRUM. METHODS PHYS. RES. **B297**, 44-57 (2013).
- [103] F. Tárkányi, F. Ditrói, A. Hermanne, S. Takács, A.V. Ignatyuk, "Investigation of Activation Cross-sections of Proton Induced Nuclear Reactions on ^{nat}Mo up to 40 MeV: New Data and Evaluation", NUCL. INSTRUM. METHODS PHYS. RES. **B280**, 45-73 (2012).
- [104] H.I. West, R.G. Lanier Jr., M.G. Mustafa, "Excitation Functions for the Nuclear Reactions on Titanium Leading to the Production of ^{48}V , ^{44}Sc and ^{47}Sc by Proton, Deuteron and Triton Irradiations at 0-35 MeV", UCLR-ID-115738, November 1993, PHYS. REV. **C42**, 683 (1990).
- [105] K. Zarie, N. Al Hammad, A. Azzam, "Experimental Study of Excitation Functions of Some Proton Induced Reactions on ^{nat}Ti for Beam Monitoring", RADIOCHIM. ACTA **94**, 795-799 (2006); EXFOR D0433.
- [106] R. Michel, G. Brinkmann, H. Weigel, W. Herr, "Proton-induced Reactions on Titanium with Energies Between 13 and 45 MeV", J. INORG. NUCL. CHEM. **40**, 1845-1851 (1978); EXFOR B0100.
- [107] A. Hermanne, F. Tárkányi, S. Takács, F. Ditrói, N. Amjed, "Excitation Functions for Production of ^{46}Sc by Deuteron and Proton Beams in ^{nat}Ti : A Basis for Additional Monitor Reactions", NUCL. INSTRUM. METHODS PHYS. RES. **B338**, 31-41 (2014); EXFOR D4310.
- [108] S. Neumann, "Activation Experiments with Medium-energy Neutrons and the Production of Cosmogenic Nuclides in Extraterrestrial Matter", thesis, Universität Hannover, 1999; EXFOR O1882.
- [109] V.N. Aleksandrov, M.P. Semenova, V.G. Semenov, "Production Cross Section of Radionuclides in (p,x) Reactions on Copper and Nickel Nuclei", ATOMIC ENERGY **62**, 411 (1987); EXFOR A0351.
- [110] A.A. Alharbi, J. Alzahrani, A. Azzam, "Activation Cross-section Measurements of Some Proton Induced Reactions on Ni, Co and Mo for Proton Analysis (PAA) purposes", RADIOCHIM. ACTA **99**, 763-770 (2011); EXFOR D0673003.
- [111] F.S. Al-Saleh, K.S. Al Mugren, A. Azzam, "Excitation Functions of (p,x) Reactions on Natural Nickel Between Proton Energies of 2.7 and 27.5 MeV", APPL. RADIAT. ISOT. **65**, 104-113 (2007); EXFOR O1503005.
- [112] N.F. Amjed, F. Tárkányi, A. Hermanne, F. Ditrói, S. Takács, M. Hussain, M., "Activation Cross-sections of Proton Induced Reactions on Natural Ni up to 65 MeV", APPL. RADIAT. ISOT. **92**, 73-84 (2014); EXFOR 4301.
- [113] G.A. Brinkman, J. Helmer, L. Lindner, "Nickel and Copper Foils as Monitors for Cyclotron Beam Intensities", RADIOCHEM. RADIOANAL. LETT. **28**, 9-19 (1977)
- [114] G. Brinkmann, "Integrale Anregungsfunktionen für Protonen- und Alpha-induzierte Reaktionen an Targetelementen $22 < Z < 28$ ", dissertation, Universität zu Köln, Köln, 1979.
- [115] B.L. Cohen, E. Newman, T.H. Handley, "(p,pn)+(p,2n) and (p,2p) Cross Sections in Medium Weight Elements", PHYS. REV. **99**, 723 (1955); EXFOR B0049.
- [116] H.A. Ewart and M. Blann, "Nuclear Cross Section for Charged Particle Induced Reactions", ORNL preprints **CPX-1**, **CPX-2**, Oak Ridge National Laboratory (1964). Numerical data are taken from [248].
- [117] M. Furukawa, A. Shinohara, M. Narita, S. Kojima, "Production of $^{59,63}\text{Ni}$ from Natural Ni Irradiated with Protons up to $E_p=40$ MeV and Decay of ^{56}Ni ", p. 35, Annual report 1990, Inst. Nucl. Study, University of Tokyo (1990). Numerical data are taken from [248]; EXFOR E1864.
- [118] F.J. Haasbroek, J. Steyn, R.D. Neirinckx, G.F. Burdzik, M. Cogneau, P. Wanet, "Excitation Functions and Thick Target Yields for Radioisotopes Induced in Natural Mg, Co, Ni and Ta by Medium Energy Protons", CSIR report **CSIR-FIS-89** (1976), and INT. J. APPL. RADIAT. ISOT. **28**, 533-534 (1977); EXFOR B0098.
- [119] S. Kaufman, "Reactions of Protons with Ni-58 and Ni-60", PHYS. REV. **117**, 1532 (1960), EXFOR B0055.
- [120] M.U. Khandaker, K.S. Kim, M.W. Lee, G.N. Kim, "Excitation Functions of (p,x) Reactions on Natural Nickel up to 40 MeV", NUCL. INSTRUM. METHODS PHYS. RES. **B269**, 1140-1149 (2011); EXFOR D7002007.
- [121] H. Piel, "Bestimmung der Anregungsfunktionen von (p,xn)-Reaktionen an Ni-Isotopen", Diplomarbeit, Universität zu Köln, Köln, 1991.
- [122] M. Sonck, A. Hermanne, J. Van Hoyweghen, F. Szelecsényi, S. Takács, F. Tárkányi, "Study of the $^{nat}\text{Ni}(p,x)^{57}\text{Ni}$ process up to 44 MeV for monitor purposes", APPL. RADIAT. ISOT. **49**, 1533-1536 (1998); EXFOR D4062.
- [123] G.F. Steyn, S.J. Mills, F.M. Nortier, private communication, 1996.
- [124] S. Tanaka, M. Furukawa, M. Chiba, "Nuclear Reactions of Nickel with Protons up to 56 MeV", J. INORG. NUCL. CHEM. **34**, 2419-2426 (1972); EXFOR B0020.
- [125] F. Tárkányi, F. Szelecsényi, P. Kopecky, "Excitation Functions of Proton Induced Nuclear Reactions on Natural Nickel for Monitoring Beam Energy and Intensity", APPL. RADIAT. ISOT. **42**, 513-517 (1991); EXFOR D4002.
- [126] Yu.E. Titarenko, V.F. Batyaev, A.Yu. Titarenko, M.A. Butko, K.V. Pavlov, S.N. Florya, R.S. Tikhonov, V.M. Zhivun, A.V. Ignatyuk, S.G. Mashnik, S. Leray, A. Boudard, J. Cugnon, D. Mancusi, Y. Yariv, K. Nishihara, N. Matsuda, H. Kumawat, G. Mank, W. Gudowski, "Measurement and Simulation of the Cross Sections for Nuclide Production in Nb-93 and Ni-nat Targets Irradiated with 0.04- to 2.6-GeV Protons", YAD. FIZ. **74**, 561 (2011); EXFOR A0906002.
- [127] B.V. Zhuravlev, O.V. Grusha, S.P. Ivanova, V.I. Trykova, Yu.N. Shubin, "Analysis of Neutron Spectra in 22-MeV Proton Interactions with Nuclei", YAD. FIZ. **39**, 264 (1984); EXFOR A0271.
- [128] F.S. Al-Saleh, A.A. Al-Harbi, A. Azzam, "Excitation Functions of Proton Induced Nuclear Reactions on Natural Copper Using a Medium-sized Cyclotron", RADIOCHIM. ACTA **94**, 394-396 (2006); EXFOR D0422.
- [129] G.H. Coleman and H.A. Tewes, "Nuclear Reactions of Copper with Various High-energy Particles", PHYS. REV. **99**, 288-289 (1955); EXFOR C0283.
- [130] S.N. Ghoshal, "An Experimental Verification of the Theory of Compound Nucleus", PHYS. REV. **80**, 939-942 (1950); EXFOR B0017.
- [131] M.W. Green and E. Lebowitz, "Proton Reactions with Copper for Auxiliary Cyclotron Beam Monitoring", INT. J. APPL. RADIAT. ISOT. **23**, 342-344 (1972);

- EXFOR B0074.
- [132] L.R. Greenwood and R.K. Smither, “Measurement of Cu Spallation Cross Sections at IPNS”, p. 11-17, DOE report **DOE/ER-0046/18** (1984), EXFOR C0537.
- [133] A. Hermanne, F. Szelecsényi, M. Sonck, S. Takács, F. Tárkányi, P. Van den Winkel, “New Cross Section Data on $^{68}\text{Zn}(p,2n)^{67}\text{Ga}$ and $^{nat}\text{Zn}(p,xn)^{67}\text{Ga}$ Nuclear Reactions for the Development of a Reference Data Base”, *J. RADIOANAL. NUCL. CHEM.* **240**, 623–630 (1999); EXFOR A088.
- [134] M.U. Khandaker, M.S. Uddin, K.S. Kim, Y.S. Lee, G.N. Kim, “Measurement of cross-sections for the (p,xn) reactions in natural molybdenum”, *NUCL. INSTRUM. METHODS PHYS. RES.* **B262**, 171–181 (2007); EXFOR D04461.
- [135] P. Kopecky, “Proton beam monitoring via the $\text{Cu}(p,x)^{58}\text{Co}$, $^{63}\text{Cu}(p,2n)^{62}\text{Zn}$ and $^{65}\text{Cu}(p,n)^{65}\text{Zn}$ reactions in copper”, *INT. J. APPL. RADIAT. ISOT.* **36**, 657-661 (1985); EXFOR A0333.
- [136] O. Lebeda, “Cross-section values for proton and deuteron beam monitoring”, private communication at Second Research Coordination Meeting, IAEA, Vienna, 2014. See also Ref. [23].
- [137] S.J. Mills, G.F. Steyn, F.M. Nortier, “Experimental and theoretical excitation functions of radionuclides produced in proton bombardment of copper up to 200 MeV”, *APPL. RADIAT. ISOT.* **43**, 1019-1030 (1992); EXFOR A0507.
- [138] M. Shahid, K. Kim, H. Naik, M. Zaman, S.C. Yang, G.N. Kim, “Measurement of excitation functions in proton induced reactions on natural copper from their threshold to 43 MeV”, *NUCL. INSTRUM. METHODS PHYS. RES.* **B342**, 305-313 (2015); EXFOR D7015.
- [139] T. Siiskonen, J. Huikari, T. Haavisto, J. Bergman, S.-J. Heselius, J.-O. Lill, T. Lonroth, K. Perajarvi, “Excitation functions of proton-induced reactions in ^{nat}Cu in the energy range 7–17 MeV”, *APPL. RADIAT. ISOT.* **67**, 2037–2039 (2009); EXFOR D0549001.
- [140] R.D. Albert and L.F. Hansen, “10-MeV proton reaction cross sections for ^{63}Cu and ^{65}Cu ”, *PHYS. REV. LETT.* **6**, 13-14 (1961).
- [141] A.E. Antropov, V.P. Gusev, P.P. Zarubin, P.D. Ioannu, V.Yu. Padalko, “Measurements of total cross sections for the (p,n) reaction on medium weight nuclei at the proton energy 6 MeV”, *30th Annual Conf. Nucl. Spectrosc. Nucl. Structure*, 18–21 March 1980, Leningrad, p. 316 (1980); EXFOR A0072.
- [142] J.P. Blaser, F. Boehm, P. Marmier, D.C. Peaslee, “Fonctions d’excitation de la Réaction (p,n) (I)”, *HELV. PHYS. ACTA* **24**, 3-38 (1951); EXFOR B0048.
- [143] K.F. Chackett, G.A. Chackett, L. Ismail, “The (p,n) Reaction Cross Section of Copper for 9.3 MeV Protons”, *PROC. PHYS. SOC. (LONDON)* **80**, 738-740 (1962); EXFOR B0070.
- [144] R. Collé, R. Kishore, J.B. Cumming, “Excitation Functions for (p,n) Reactions to 25 MeV on ^{63}Cu , ^{65}Cu and ^{107}Ag ”, *PHYS. REV.* **C9**, 1819 -1830 (1974); EXFOR B0057.
- [145] G.F. Dell, W.D. Ploughe, H.J. Hausman, “Total Reaction Cross Sections in the Mass Range 45 to 65”, *NUCL. PHYS.* **64**, 513–523 (1965); EXFOR B0064.
- [146] L.F. Hansen and R.D. Albert, “Statistical theory predictions for 5- to 11-MeV (p,n) and (p,p') nuclear reactions in ^{51}V , ^{59}Co , ^{63}Cu , ^{65}Cu , and ^{103}Rh ”, *PHYS. REV.* **128**, 291-299 (1962); EXFOR B0066.
- [147] M. Hille, P. Hille, M. Uhl, W. Weisz, “Excitation Functions of (p,n) and (α,n) Reactions on Ni, Cu and Zn”, *NUCL. PHYS.* **A198**, 625-640 (1972).
- [148] H.A. Howe, “ (p,n) Cross-sections of Copper and Zinc”, *PHYS. REV.* **109**, 2085–2085 (1958); EXFOR B0060.
- [149] R.M. Humes, G.F. Dell, W.D. Ploughe, J.J. Hausman, “ (p,n) Cross-sections at 6.75 MeV”, *PHYS. REV.* **130**, 1522 (1963); EXFOR B0061.
- [150] C.H. Johnson, A. Galonsky, C.N. Inskeep, “Cross Sections for (p,n) Reactions in Intermediate-Weight Nuclei”, p. 25-28, ORNL Progress Report **ORNL-2910** (1960); EXFOR B0068.
- [151] G.A. Jones, J.P. Schiffer, J.R. Huizenga, J. Wing, “Measurements of (p,n) Cross Sections on Cu at 9.85 MeV”, TID report **TID-12696** (1961); EXFOR: B0063.
- [152] V. Meyer and N.M. Hintz, “Charged Particle and Total Reaction Cross Sections for Protons at 9.85 MeV”, *PHYS. REV. LETT.* **5**, 207-209 (1960); EXFOR C1042.
- [153] H. Taketani and W.P. Alford, “ (p,n) Cross Sections on Ti-47, V-51, Cr-52, Co-59 and Cu-63 from 4 to 6.5 MeV”, *PHYS. REV.* **125**, 291-294 (1962).
- [154] J. Wing and J.R. Huizenga, “ (p,n) cross sections of ^{51}V , ^{52}Cr , ^{63}Cu , ^{65}Cu , ^{107}Ag , ^{109}Ag , ^{111}Cd , ^{114}Cd and ^{139}La from 5 to 10.5 MeV”, *PHYS. REV.* **128**, 280-290 (1962); EXFOR B0065.
- [155] Y. Yoshizawa, H. Noma, T. Horiguchi, T. Katoh, A. Amemiya, M. Itoh, K. Hisatake, M. Sekikawa, K. Chida, “Isotope Separator on-line at INS FM Cyclotron”, *NUCL. INSTRUM. METHODS* **134**, 93-100 (1976); EXFOR E 1866.
- [156] G. Albouy, M. Gusakow, N. Poffi, H. Sergolle, L. Valentin, “Réaction (p,n) a Moyenne Énergie”, *J. PHYS. RADIUM* **23**, 1000–1002 (1962); EXFOR B0106.
- [157] P.P. Dmitriev, I.S. Konstantinov, N.N. Krasnov, “Excitation function for the $^{65}\text{Cu}(p,n)^{65}\text{Zn}$ reaction”, *ATOMIC ENERGY* **24**, 279-280 (1968); EXFOR O0419.
- [158] E. Gadioli, A.M. Grassi Strini, G. Lo Bianco, G. Strini, G. Tagliaferri, “Excitation functions of ^{51}V , ^{56}Fe , $^{65}\text{Cu}(p,n)$ reactions between 10 and 45 MeV”, *NUOVO CIM.* **A22**, 547-558 (1974); EXFOR B0027.
- [159] H.R. Heydegger, C.K. Garrett, A. Van Ginneken, “Thin-target cross sections for some Cr, Mn, Fe, Co, Ni, and Zn nuclides produced in copper by 82- to 416-MeV protons”, *PHYS. REV.* **C6**, 1235–1240 (1972); EXFOR O0416.
- [160] C.H. Johnson, A. Galonsky, J.P. Ulrich, “Proton strength functions from (p,n) cross sections”, *PHYS. REV.* **109**, 1243 (1958); EXFOR B0046.
- [161] S.M. Kormali, D.L. Swindle, E.A. Schweikert, “Charged particle activation of medium Z elements. II. Proton excitation functions”, *J. RADIOANAL. CHEM.* **31**, 437–450 (1976); EXFOR D4073.
- [162] J. Kuhnhehn, “Protonen-induzierte Erzeugung Radioaktiver Restkerne in Blei und Bismut bei Energien bis 71 MeV”, thesis, Universität zu Köln, Köln, 2001; EXFOR O0920.
- [163] B.W. Shore, N.S. Wall, J.W. Irvine Jr., “Interactions of 7.5 MeV protons with copper and vanadium”, *PHYS. REV.* **123**, 276–283 (1961); EXFOR B0067.
- [164] Z.E. Switkowski, J.C.P. Heggie, F.M. Mann, “Threshold effects in proton-induced reactions on copper”, *AUSTRALIAN J. PHYS.* **31**, 253-265 (1978); EX-

- FOR D0118.
- [165] E. Acerbi, C. Birattari, M. Castiglioni, F. Resmini, "Nuclear applied physics at the Milan cyclotron", *J. RADIOANAL. CHEM.* **34**, 191–217 (1976); EXFOR D0260.
- [166] Yu.V. Aleksandrov, A.I. Bogdanov, S.K. Vasilev, R.B. Ivanov, M.A. Mikhailova, T.I. Popova, V.P. Prikhodtseva, "Cross Section for the Production of Radioactive Nuclides Under Bombardment of Intermediate-Mass Nuclei with 1-GeV Protons", *IZV. ROSS. AKAD. NAUK, SER. FIZ.* **54**, 2249 (1990); EXFOR A0501.
- [167] M. Fassbender, Yu.N. Shubin, V.P. Lunev, S.M. Qaim, "Experimental Studies and Nuclear Model Calculations on the Formation of Radioactive Products in Interactions of Medium Energy Protons with Copper, Zinc and Brass: Estimation of collimator activation in proton therapy facilities", *APPL. RADIAT. ISOT.* **48**, 1221–1230 (1997); EXFOR O0722.
- [168] S.A. Graves, P.A. Ellison, T.E. Barnhart, H.F. Valdovinos, E.R. Birnbaum, F.M. Nortier, R.J. Nickles, J.W. Engle, "Nuclear Excitation Functions of Proton-induced Reactions ($E_p = 35 - 90$ MeV) from Fe, Cu and Al", *NUCL. INSTRUM. METHODS PHYS. RES.* **B386**, 44–53 (2016).
- [169] T. Ido, A. Hermanne, F. Ditróí, Z. Szucs, I. Mahunka, F. Tárkányi, "Excitation functions of proton induced nuclear reactions on ^{nat}Rb from 30 to 70 MeV. Implication for the production of ^{82}Sr and other medically important Rb and Sr radioisotopes", *NUCL. INSTRUM. METHODS PHYS. RES.* **B194**, 369–388 (2002); EXFOR D4414.
- [170] O. Lebeda, Cross Sections for the $^{nat}\text{Cu}(p,x)^{58}\text{Co}$ Reaction, private communication, 2015.
- [171] R. Michel, B. Dittrich, U. Herpers, F. Peiffer, T. Schiffmann, P. Cloth, P. Dragovitsch, D. Filges, "Proton-induced spallation at 600 MeV", *ANALYST (LONDON)* **114**, 287–298 (1989); EXFOR O0078
- [172] C.J. Orth, B.J. Dropesky, R.A. Williams, G.C. Giesler, J. Hudis, "Pion-Induced Spallation of Copper Across the (3,3) Resonance", *PHYS. REV.* **C18**, 1426 (1978) EXFOR O0418.
- [173] J.M. Sisterson, "Selected Radiation Safety Issues at Proton Therapy Facilities", *Proc. 12th Biannual Topical Meeting of the Radiation Protection and Shielding Division of the American Nuclear Society*, 14–18 April 2002, Santa Fe, New Mexico, USA, p. 01-28-02 (2002); EXFOR C0879.
- [174] Yu.E. Titarenko, E.I. Karpikhin, A.F. Smolyakov, M.M. Igumnov, O.V. Shvedov, N.V. Stepanov, V.D. Kazaritsky, V.F. Batyaev, S.G. Mashnik, T.A. Gabriel, "Experimental and Calculative Research of Radioactive Nuclei Formation- Products of Target and Constructional Materials of Electronuclear Facilities Irradiated by Protons with Energies 1.5 GeV and 130 MeV", *Workshop on Exact Measurements in Nucl. Spectrosc.*, Sarov, Russia, p. 184 (1996).
- [175] Yu.E. Titarenko, V.F. Batyaev, V.M. Zhivun, A.B. Koldobsky, Yu.V. Trebukhovskiy, E.I. Karpikhin, R.D. Mulambetov, S.V. Mulambetova, Yu.A. Nekrasov, A.Yu. Titarenko, K.A. Lipatov, B.Yu. Sharkov, I.V. Roudskoy, G.N. Smirnov, V.S. Barashenkov, K.K. Gudima, M.I. Baznat, S.G. Mashnik, R.E. Prael, "Nuclide production cross sections for Co-59 and Cu-nat irradiated with 0.2-GeV and 2.6-GeV protons and 0.2-GeV/nucleon carbon ions", *Int. Meeting Nucl. Appl. of Accelerator Technol.*, San Diego, CA, USA, p. 59 (2003); EXFOR O1342.
- [176] H. Yashima, Y. Uwamino, H. Sugita, T. Nakamura, S. Ito, A. Fukumura, "Projectile dependence of radioactive spallation products induced in copper by high-energy heavy ions", *PHYS. REV.* **C66**, 044607 (2002); EXFOR O1003.
- [177] H. Yashima, Y. Uwamino, H. Iwase, H. Sugita, T. Nakamura, S. Ito, A. Fukumura, "Measurement and calculation of radioactivities of spallation products by high-energy heavy ions", *RADIOCHIM. ACTA* **91**, 689–696 (2003); EXFOR E1829.
- [178] S. Takács, F. Tárkányi, M. Sonck, A. Hermanne, "Investigation of the $^{nat}\text{Mo}(p,x)^{96m,g}\text{Tc}$ nuclear reaction to monitor proton beams: New measurements and consequences on the earlier reported data", *NUCL. INSTRUM. METHODS PHYS. RES.* **B198**, 183–196 (2002); EXFOR D4110
- [179] S.M. Qaim, S. Sudar, B. Scholten, A.J. Koning, H.H. Coenen, "Evaluation of excitation functions of $^{100}\text{Mo}(p,d,pn)^{99}\text{Mo}$ and $^{100}\text{Mo}(p,2n)^{99m}\text{Tc}$ reactions. Estimation of long-lived ^{99g}Tc impurity and its implication on the specific activity of cyclotron produced ^{99m}Tc ", *APPL. RADIAT. ISOT.* **85**, 101–113 (2014).
- [180] A.A. Alharbi A. Azzam, M. McCleskey, B. Roeder, A. Spiridon, E. Simmons, V.Z. Goldberg, A. Banu, L. Trache, R.E. Tribble, "Medical Radioisotopes Production: A Comprehensive Cross-section Study for the Production of Mo and Tc Radioisotopes via Proton Induced Nuclear Reactions on ^{nat}Mo ." *Radioisotopes – Applications in Bio-Medical Science*, Ed: Nirmal Singh (2011) ISBN:978-953-307-748-2; EXFOR C2157.
- [181] J. Cervenák and O. Lebeda, "Experimental cross-sections for proton-induced nuclear reactions on ^{nat}Mo ", *NUCL. INSTRUM. METHODS PHYS. RES.* **B380**, 32–49 (2016); EXFOR D0805
- [182] M.B. Challan, M.N.H. Comsan, M.A. Abou-Zeid, "Thin target yields and EMPIRE-II predictions on the accelerator production of technetium-99m", *J. NUCL. RADIAT. PHYS.* **2**, 1–12 (2007); EXFOR O1737.
- [183] M.U. Khandaker, A.K.M.M.H. Meaze, K. Kim, D. Son, G. Kim, L.S. Lee, "Measurements of the Proton-Induced Reaction Cross-sections of ^{nat}Mo by Using the MC50 Cyclotron at the Korea Institute of Radiological and Medical Sciences", *J. KOREAN PHYS. SOC.* **48**, 821–826 (2006); EXFOR D4120
- [184] O. Lebeda and M. Pruszyński, "New measurement of excitation functions for (p,x) reactions on ^{nat}Mo with special regard to the formation of ^{95m}Tc , $^{96m+g}\text{Tc}$, ^{99m}Tc and ^{99}Mo ", *APPL. RADIAT. ISOT.* **68**, 2355–2365 (2010); EXFOR D0615.
- [185] E.A. Skakun, V.S. Batij, Y.N. Rakivnenko, O.A. Rastrepin, "Excitation functions and isomeric ratios for the interaction of protons of less than 9-MeV with Zr and Mo isotopes", *SOV. J. NUCL. PHYS.* **46**, 17–24 (1987); EXFOR A0338
- [186] S. Takács, A. Hermanne, F. Ditróí, F. Tárkányi, M. Aikawa, "Reexamination of cross sections of the $^{100}\text{Mo}(p,2n)^{99m}\text{Tc}$ reaction", *NUCL. INSTRUM. METHODS PHYS. RES.* **B347**, 26–38 (2015); EXFOR D4322.
- [187] W. Zhao, W. Yu, X. Han, H. Lu, "Excitation functions of reactions from $d + \text{Ti}$, $d + \text{Mo}$, $p + \text{Ti}$ and $p + \text{Mo}$ ", pp. 17–20 in *COMM. NUCLEAR DATA PROGRESS*

- 19, INDC(CPR)-044/L**, China Nuclear Data Centre, Atomic Energy Press, Beijing (1998).
- [188] M. Bonardi, C. Groppi, F. Sabbioni, “Thin target excitation functions, cross sections and optimized thick-target yields for $^{nat}\text{Mo}(p,xn)^{94g}\text{Tc}$, $^{95m,g}\text{Tc}$, $^{96m,g}\text{Tc}$ nuclear reactions induced by protons from threshold up to 44 MeV”, *APPL. RADIAT. ISOT.* **57**, 617-635 (2002); EXFOR O 0845
- [189] M. Hagiwara, T. Itoga, M. Baba, M.S. Uddin, N. Hirabayashi, T. Oishi, T. Yamaguchi, “Experimental studies on the neutron emission spectrum and activation cross section for 40 MeV deuterons in IFMIF accelerator structural elements”, *J. NUCL. MATER.* **329**, 218–222 (2004); EXFOR E1985.
- [190] A. Hermanne, S. Takács, F. Tárkányi, R. Adam Rebeles, A. Ignatyuk, “Excitation functions for ^7Be , $^{22,24}\text{Na}$ in Mg and Al by deuteron irradiations up to 50 MeV”, *APPL. RADIAT. ISOT.* **70**, 2763–2772 (2012); EXFOR D4253.
- [191] A. Hermanne, S. Takács, F. Tárkányi, R. Adam Rebeles, A. Ignatyuk, “Activation cross sections for deuteron induced reactions on Si up to 50 MeV”, *NUCL. INSTRUM. METHODS PHYS. RES.* **B285**, 43-48 (2012).
- [192] A. Hermanne, R. Adam Rebeles, F. Tárkányi, S. Takács, M.P. Takács, A.V. Ignatyuk, M.S. Uddin, “Excitation functions of deuteron induced reactions on ^{nat}Os up to 50 MeV: Experiments and comparison with theoretical codes”, *NUCL. INSTRUM. METHODS PHYS. RES.* **B297**, 75-85 (2013).
- [193] A. Hermanne, R. Adam Rebeles, F. Tárkányi, S. Takács, J. Csikái, M.P. Takács, A. Ignatyuk, “Deuteron induced reactions on Ho and La: Experimental excitation functions and comparison with code results”, *NUCL. INSTRUM. METHODS PHYS. RES.* **B311**, 102-111 (2013).
- [194] A. Hermanne, S. Takács, R. Adam Rebeles, F. Tárkányi, M.P. Takács, “New measurements and evaluation of database for deuteron induced reaction on Ni up to 50 MeV”, *NUCL. INSTRUM. METHODS PHYS. RES.* **B299**, 8–23 (2013).
- [195] A. Karpeles, “Anregungsfunktionen für die Bildung von ^{68}Ge , ^{65}Zn und ^{22}Na bei der Deuteronenbestrahlung von Gallium und Aluminium”, *RADIOCHIM. ACTA* **12**, 212–213 (1969); EXFOR D0073.
- [196] U. Martens and G.W. Schweimer, “Production of ^7Be , ^{22}Na , ^{24}Na and ^{28}Mg by irradiation of ^{27}Al with 52 MeV deuterons and 104 MeV alpha particles”, *Z. PHYS.* **233**, 170–177 (1970); EXFOR B0142.
- [197] R. Michel, G. Brinkmann, M. Galas, R. Stuck, “Production of ^{24}Na and ^{22}Na by ^2H -induced reactions on aluminium”, private communication, R. Michel, August 1982; EXFOR A0158.
- [198] N. Nakao, J. Hori, K. Ochiai, N. Kubota, S. Sato, M. Yamauchi, N.S. Ishioka, T. Nishitani, “Measurements of deuteron-induced activation cross-sections for IFMIF accelerator structural materials”, *NUCL. INSTRUM. METHODS PHYS. RES.* **A562**, 785–788 (2006); EXFOR E1988.
- [199] O. Ring and L.M. Litz, “Excitation Function for ^{22}Na from Deuterons on Aluminum”, *PHYS. REV.* **97**, 427–428 (1955); EXFOR C0990.
- [200] S. Takács, F. Szelecsényi, F. Tárkányi, M. Sonck, A. Hermanne, Yu.N. Shubin, A. Dityuk, M.G. Mustafa, Zhuang Youxiang, “New Cross Sections and Intercomparison of Deuteron Monitor Reactions on Al, Ti, Fe, Ni and Cu”, *NUCL. INSTRUM. METHODS PHYS. RES.* **B174**, 235–258 (2001); EXFOR: D4081. See also [225]
- [201] R.E. Batzel, W.W.T. Crane, G.D. O’Kelley, “The excitation function for the $^{27}\text{Al}(d,\rho\alpha)^{24}\text{Na}$ reaction”, *PHYS. REV.* **91**, 939 (1953); EXFOR P0067.
- [202] P. Bém, E. Šimečková, M. Honusek, U. Fisher, S.P. Simakov, R.A. Forrest, M. Avrigeanu, A.C. Obreja, F.L. Roman, V. Avrigeanu “Low and medium energy deuteron-induced reactions on ^{27}Al ”, *PHYS. REV.* **C79**, 044610 (2009), EXFOR D0453.
- [203] G. Christaller, *Europium Colloquium on AVF Cyclotrons*, Eindhoven (1965). Data from J. Tobailem *et al.* [339].
- [204] W.E. Crandall, G.P. Milburn, R.V. Pyle, W. Birnbaum, “ $^{12}\text{C}(x,xn)^{11}\text{C}$ and $^{27}\text{Al}(x,x2pn)^{24}\text{Na}$ cross sections at high energies”, *PHYS. REV.* **101**, 329 (1956); EXFOR B0101.
- [205] H.W. Hubbard, “ $^{27}\text{Al}(d,\rho\alpha)^{24}\text{Na}$ cross section”, *PHYS. REV.* **75**, 1470 (1949); EXFOR D4103.
- [206] P.A. Lenk and R.J. Slobodrian, “Excitation function for the $^{27}\text{Al}(d,\rho\alpha)^{24}\text{Na}$ reaction between 0 and 28.1 MeV”, *PHYS. REV.* **116**, 1229 (1959); EXFOR P0124.
- [207] K. Ochiai, M. Nakao, N. Kubota, S. Sato, Y. Yamaguchi, N.H. Ishioka, T. Nishitani, C. Konno, “Deuteron induced activation cross section measurement for IFMIF”, *Proc. Int. Conf. on Nuclear Data for Science and Technology*, 22–27 April 2007, Nice, France. eds: O. Bersillon, F. Gunsing, E. Bange *et al.*, Volume **2**, 1011–1013 (2008) EDP Sciences; EXFOR E2121.
- [208] H.F. Roehm, C.J. Verwey, J. Steyn, W.L. Rautenbach, “Excitation functions for the $^{24}\text{Mg}(d,\alpha)^{22}\text{Na}$, $^{26}\text{Mg}(d,\alpha)^{24}\text{Na}$ and $^{27}\text{Al}(d,\rho\alpha)^{24}\text{Na}$ reactions”, *J. INORG. NUCL. CHEM.* **31**, 3345–3356 (1969); EXFOR B0099.
- [209] Tao Zhenlan, Zhu Fuying, Wang Gongqing, “Measurements of excitation function for $^{27}\text{Al}(d,\rho\alpha)$ ”, *CANADIAN NUCL. TECHNOL.* **2**, 45 (1987); EXFOR S0011.
- [210] I.A. Watson, S.L. Waters, D.K. Bewley, D.J. Silvester, “A method for the measurement of the cross sections for the production of radioisotopes by charged particles from a cyclotron”, *NUCL. INSTRUM. METHODS* **106**, 231–235 (1973); EXFOR D0070.
- [211] R. Weinreich, H.J. Probst, S.M. Qaim, “Production of ^{48}Cr for application in life science”, *INT. J. APPL. RADIAT. ISOT.* **31**, 223–232 (1980); EXFOR A0169.
- [212] R.L. Wilson, D.J. Frantsvog, A.R. Kunselman, C. Détraz, C.S. Zaidins, “Excitation functions of reactions induced by ^1H and ^2H ions on natural Mg, Al and Si”, *PHYS. REV.* **C13**, 976 (1976); EXFOR D4104.
- [213] P.P. Zarubin, “Excitation function of $^{27}\text{Al}(d,\rho\alpha)^{24}\text{Na}$ ”, *29th Ann. Conf. Nucl. Spectrosc. and Nucl. Struct.*, Riga, 314 (1979), data taken from [5]; EXFOR A0667.
- [214] Zhao Wen-Rong, Lu Han-Lin, Yu Wei-Xiang, Cheng Jiang-Tao, “Excitation function of $^{27}\text{Al}(d,\rho\alpha)^{24}\text{Na}$ ”, *CHIN. J. NUCL. PHYS.* **17**, 160–163 (1995); EXFOR S0043.
- [215] H.W. Burgus, G.A. Cowan, J. Hadley, W. Hess, T. Shull, M.L. Stevenson, H. York, “Cross Sections for the Reactions $^{48}\text{Ti}(d,2n)^{48}\text{V}$, $^{52}\text{Cr}(d,2n)^{52}\text{Mn}$, $^{56}\text{Fe}(d,2n)^{56}\text{Co}$ ”, *PHYS. REV.* **95**, 750 (1954); EXFOR D4102.
- [216] K.L. Chen and J.M. Miller, “Comparison between Reactions of Alpha Particles with Scandium-45 and Deuterons with Titanium-47”, *PHYS. REV.* **B134**, 1269 (1964); EXFOR D4105.

- [217] K. Gagnon, M.A. Avila-Rodriguez, J. Wilson, S.A. Mcquarrie, “Experimental deuteron cross section measurements using single natural titanium foils from 3 to 9 MeV with special reference to the production of ^{47}V and ^{51}Ti ”, *NUCL. INSTRUM. METHODS PHYS. RES.* **B268**, 1392–1398 (2010); EXFOR C1801.
- [218] P. Jung, “Helium production and long-term activation by protons and deuterons in metals for fusion reactor application”, *J. NUCL. MATER.* **144**, 43–50 (1987).
- [219] M.U. Khandaker, H. Haba, J. Kanaya, N. Otuka, “Excitation functions of the (d,x) nuclear reactions on natural titanium up to 24 MeV”, *NUCL. INSTRUM. METHODS PHYS. RES.* **B296**, 14–21 (2013); EXFOR E2404.
- [220] S. Takács, M. Sonck, B. Scholten, A. Hermanne, F. Tárkányi, “Excitation Functions of Deuteron Induced Reactions on ^{nat}Ti up to 20 MeV for Monitoring Deuteron Beams”, *APPL. RADIAT. ISOT.* **48**, 657–665 (1997); corrected by 18 percent; EXFOR D4046.
- [221] S. Takács, B. Király, F. Tárkányi, A. Hermanne, “Evaluated activation cross sections of longer-lived radionuclides produced by deuteron induced reactions on natural titanium”, *NUCL. INSTRUM. METHODS PHYS. RES.* **B262**, 7–12 (2007); EXFOR D4168.
- [222] S. Takács, M.P. Takács, A. Hermanne, F. Tárkányi, R. Adam-Rebeles, “Excitation functions of longer lived radionuclides formed by deuteron irradiation of germanium”, *NUCL. INSTRUM. METHODS PHYS. RES.* **B336**, 81–95 (2014).
- [223] O.U. Andres and W.W. Meinke, “Absolute (d,n) -reaction cross sections of zirconium, molybdenum, titanium and sulfur”, *PHYS. REV.* **120**, 2114 (1960); EXFOR D4057.
- [224] V. Duchemin, “Deuteron monitoring through $^{nat}\text{Ti}(d,x)^{46}\text{Sc}$ at Arronax”, private communication, 2015.
- [225] A. Hermanne, M. Sonck, S. Takács, F. Tárkányi, “Experimental Study of Excitation Function for Some Reactions Induced by Deuterons (10–50 MeV) on Natural Fe and Ti”, *NUCL. INSTRUM. METHODS PHYS. RES.* **B161–163**, 178–185 (2000); EXFOR D4082.
- [226] I. Spahn, “Monitoring of deuterons beams by $^{nat}\text{Ti}(d,x)$ and $^{nat}\text{Cu}(d,x)$ reactions in Jülich”, private communication, 2014.
- [227] F.O. Bartell, A.C. Helmholz, S.D. Softky, D.B. Stewart, “Excitation Functions for Spallation Reactions on Cu”, *PHYS. REV.* **80**, 1006–1010 (1950); EXFOR P0069.
- [228] R. Adam Rebeles, P. Van den Winkel, A. Hermanne, S. Takács, “Experimental excitation functions of deuteron induced reactions on natural thallium up to 50 MeV”, *NUCL. INSTRUM. METHODS PHYS. RES.* **B288**, 94–101 (2012).
- [229] R. Adam Rebeles, P. Van den Winkel, A. Hermanne, “Activation cross section of deuteron induced reactions on natural thallium for the production of ^{203}Pb ”, *J. KOREAN PHYS. SOC.* **59**, 1975–1978 (2011).
- [230] P. Bém, L. Bittmann, V. Burjan, U. Fischer, M. Götz, M. Honusek, V. Kroha, J. Novák, S. Simakov, E. Šimečková, “The activation of Cu and Al by deuterons at energies up to 20 MeV”, *Proc. Int. Conf. Nuclear Data for Science and Technology*, 22–27 April 2007, Nice, France. eds: O. Bersillon, F. Gunsing, E. Bange *et al.*, Volume **2**, p 1003 (2008) EDP Sciences; EXFOR D0453.
- [231] C.B. Fulmer and I.R. Williams, “Excitation Functions for Radioactive Nuclides Produced by Deuteron Induced Reactions on Copper”, *NUCL. PHYS.* **A155**, 40–48 (1970); EXFOR B0121.
- [232] A. Hermanne, R. Adam Rebeles, P. Van den Winkel, F. Tárkányi, S. Takács, “Activation of ^{112}Cd by Deuteron Induced Reactions up to 50 MeV: An alternative for ^{111}In production?”, *NUCL. INSTRUM. METHODS PHYS. RES.* **B339**, 26–33 (2014).
- [233] A. Hermanne, R. Adam Rebeles, F. Tárkányi, S. Takács, M.P. Takács, A.V. Ignatyuk, “Cross sections of deuteron reactions on ^{nat}Cr up to 50 MeV: experiments and comparison with theoretical codes”, *NUCL. INSTRUM. METHODS PHYS. RES.* **B269**, 2563–2571 (2011).
- [234] E. Šimečková, P. Bém, M. Honusek, M. Štefánek, U. Fisher, S.P. Simakov, R.A. Forrest, A.J. Koning, J.C. Sublet, M. Avrigeanu, F.L. Roman, V. Avrigeanu, “Low and Medium Energy Deuteron-induced Reactions on $^{63,65}\text{Cu}$ Nuclei”, *PHYS. REV.* **C84**, 014605 (2011); EXFOR D0653; *J. KOREAN PHYS. SOC.* **59**, 1928–1931 (2011). Preliminary data, figures + tables given in *EUR. PHYS. J., CONF. SERIES* **8**, 07002 (2010).
- [235] S. Takács, F. Tárkányi, B. Király, A. Hermanne, M. Sonck, “Evaluated Activation Cross Sections of Longer-lived Radionuclides Produced by Deuteron-induced Reactions on Natural Copper”, *NUCL. INSTRUM. METHODS PHYS. RES.* **B251**, 56–65 (2006); EXFOR D4176.
- [236] J.L. Gilly, G.A. Henriet, M. Preciosa Alves, P.C. Capron, “Absolute cross sections and excitation functions for (d,p) and $(d,2n)$ reactions on ^{55}Mn , ^{63}Cu , ^{65}Cu , ^{66}Zn , and ^{68}Zn between 3 and 11.6 MeV”, *PHYS. REV.* **131**, 1727 (1963); EXFOR R0042.
- [237] H. Okamura and S. Tamagawa, “Excitation functions for the deuteron-induced reactions on ^{63}Cu and ^{65}Cu ”, *NUCL. PHYS.* **A169**, 401–406 (1971); EXFOR B0044.
- [238] Cheng Xiaowu, Wang Zhenxia, Wang Zhenjie, Yang Jinqing, “Some measurements of deuteron induced excitation function at 13 MeV”, *ACTA PHYSICA SINICA* **22**, 250 (1966); EXFOR S0060.
- [239] P.P. Dmitriev and N.N. Krasnov, “Excitation function of the $^{65}\text{Cu}(d,2n)^{65}\text{Zn}$ reaction and yield of ^{65}Zn isotope”, *ATOMIC ENERGY* **18**, 184 (1985); EXFOR F1221.
- [240] F.W. Pement and R.L. Wolke, “Compound-statistical features of deuteron-induced reactions. II”, *NUCL. PHYS.* **86**, 429–442 (1966); EXFOR P0115.
- [241] S. Takács, F. Tárkányi, M. Sonck, A. Hermanne, S. Sudar, “Study of deuteron induced reactions on natural iron and copper and their use for monitoring beam parameters and for thin layer activation technique”, *Proc. 14th Int. Conf. Application of Accelerators in Research and Industry*, 6–9 November 1996, Denton, Texas, USA, eds: J.L. Duggan, I.L. Morgan, *AIP. CONF. PROC.* **392**, 659 (1997) AIP Woodbury, NY; EXFOR D4044.
- [242] J.W. Clark, C.B. Fulmer, C. Williams, “Excitation functions for radioactive nuclides produced by deuteron-induced reactions in Iron”, *PHYS. REV.* **179**, 1104 (1969); EXFOR T0199.
- [243] J.W. Irwine, “The Science and Engineering of Nuclear Power”, ed. C. Goodman, Vol **II**, 223 (1949), Addison-Wesley Press Inc., Cambridge, Massachusetts, USA. Data were taken from [339].
- [244] M.U. Khandaker, H. Haba, J. Kanaya, N. Otuka, “Activation cross sections of deuteron induced nuclear reactions on natural iron up to 24 MeV”, *NUCL. INSTRUM.*

- METHODS PHYS. RES. **B315**, 33-41 (2013); EXFOR E2439
- [245] B. Király, S. Takács, F. Ditrói, F. Tárkányi, A. Hermanne, “Evaluated activation cross sections of longer lived radionuclides produced by deuteron induced reactions on natural iron up to 10 MeV”, *NUCL. INSTRUM. METHODS PHYS. RES.* **B267**, 15-22 (2009); EXFOR D4185.
- [246] S. Sudar, S.M. Qaim, “Excitation functions of proton and deuteron induced reactions on iron and alpha-particle induced reactions on manganese in the energy region up to 25 MeV”, *PHYS. REV.* **C50**, 2408 (1995), EXFOR D4018.
- [247] Tao Zhenlan, Zhu Fuying, Qui Huiyuan, Wang Gonging, “Excitation functions of deuteron induced reactions on natural iron”, *ATOMIC ENERGY SCI. TECHNOL.* **5**, 506 (1993); EXFOR S0015.
- [248] Landolt-Bornstein, New Series Group I, Volume **13**, Subvolume F, “Production of Radionuclides at Intermediate Energies: Interactions of Deuterons, Tritons and ^3He nuclei with Nuclei”, Editor: H. Shopper, Contributors: V.G. Semenov, M.P. Semenova, N.M. Sobolevsky (1995).
- [249] L. Závorka, E. Šimečková, M. Honusek, K. Katovský, “The Activation of Fe by Deuterons at Energies up to 20 MeV”, *J. KOREAN PHYS. SOC.* **59**, 1961–1964 (2011); final results published in M. Avrigeanu, V. Avrigeanu, P. Bém, U. Fisher, M. Honusek, K. Katovský, C. Manailescu, J. Mrázek, E. Šimečková, L. Závorká, “Low energy deuteron-induced reactions on Fe isotopes”, *PHYS. REV.* **C89**, 044613 (2014); EXFOR D0672.
- [250] Zhao Wen-Rong, Lu Han-Lin, Yu Wei-Xiang, Cheng Jian-Tao, “Excitation functions for reactions induced by deuteron in iron”, *CHIN. J. NUCL. PHYS.* **17**, 163–166 (1995); EXFOR S0044.
- [251] A. Budzanowski and K. Grotowski, “Elastic scattering angular distributions and total cross sections for the interactions of 12.8 MeV deuterons with Ni-58 and Ni-60 nuclei”, *PHYS. LETT.* **2**, 280 (1962); EXFOR D4053.
- [252] P.P. Coetzee and M. Peisach, “Activation cross sections for deuteron-induced reactions on some elements of the first transition series up to 5.5 MeV”, *RADIOCHIM. ACTA* **17**, 1–6 (1972); EXFOR D4054.
- [253] M. Cogneau, L.J. Gilly, J. Cara, “Absolute cross sections and excitation functions for deuteron-induced reactions on nickel isotopes between 2 and 12 MeV”, *NUCL. PHYS.* **A99**, 686–694 (1967); EXFOR D0076.
- [254] F. Haddad, “Ni foils in stacks with Sc and Ti monitors”, private communication, 2013; to be published.
- [255] A. Hermanne, F. Tárkányi, S. Takács, S.F. Kovalev, A. Ignatyuk, “Activation cross sections of the $^{64}\text{Ni}(d,2n)$ reaction for the production of the medical radionuclide ^{64}Cu ”, *NUCL. INSTRUM. METHODS PHYS. RES.* **B258**, 308–312 (2007); EXFOR D4182.
- [256] A. Hermanne, S. Takács, R. Adam Rebeles, F. Tárkányi, S. Takács, “New measurements and evaluation of database for deuteron induced reaction on Ni up to 50 MeV”, *NUCL. INSTRUM. METHODS PHYS. RES.* **B299**, 8–23 (2013); EXFOR D4282
- [257] S. Takács, M. Sonck, A. Azzam, A. Hermanne, F. Tárkányi, “Activation cross section measurements of deuteron induced reactions on ^{nat}Ni with special reference to beam monitoring and production of ^{61}Cu for medical purpose”, *RADIOCHIM. ACTA* **76**, 15–24 (1997); EXFOR D4045.
- [258] S. Takács, F. Tárkányi, B. Király, A. Hermanne, M. Sonck, “Evaluated activation cross sections of longer-lived radionuclides produced by deuteron-induced reactions on natural nickel”, *NUCL. INSTRUM. METHODS PHYS. RES.* **B260**, 495-507 (2007); EXFOR D4178.
- [259] J. Zweit, A.M. Smith, S. Downey, H.L. Sharma, “Excitation functions for deuteron induced reactions in natural nickel: production of no-carrier-added ^{64}Cu from enriched ^{64}Ni targets for positron emission tomography”, *APPL. RADIAT. ISOT.* **42**, 193-197 (1991); EXFOR D4056.
- [260] N. Amjed, F. Tárkányi, F. Ditrói, S. Takács, “Activation cross-sections of deuteron induced reaction of natural Ni up to 40 MeV”, *APPL. RADIAT. ISOT.* **82**, 87-99 (2013); EXFOR D4288.
- [261] M. Blann and G. Merkel, “Reactions Induced in ^{58}Ni with 0-24 MeV Deuterons: Statistical Model Analysis”, *PHYS. REV.* **131**, 734 (1963); EXFOR C0705.
- [262] C.K. Cline, “Reaction mechanisms and shell structure effects in $^{54}\text{Fe} + ^6\text{Li}$ and $^{58}\text{Ni} + d$ reactions”, *NUCL. PHYS.* **A174**, 73–96 (1973), EXFOR D4061.
- [263] Zhu Fuying, Tao Zhenlan, Wang Zhenxia, “Measurements of excitation functions for Ni-58(d, α), Ni-58(d, α +n) and Ni-58(d,t)”, *CHIN. J. NUCL. PHYS.* **5**, 166 (1983); EXFOR S0016.
- [264] O.D. Brill, “He-3 light nucleus interaction cross sections”, *YADERNAYA FISIKA* **1**, 55 (1965); EXFOR F0207, Numerical values taken from [248]
- [265] D.R.F. Cochran, J.D. Knight, “Excitation Functions of Some Reactions of 6- to 24-MeV ^3He -Ions with Carbon and Aluminum”, *PHYS. REV.* **128**, 1281–1286 (1962); EXFOR T0214.
- [266] S.N. Kondratév, I.Yu. Lobach, Yu.N. Lobach, V.D. Sklyarenko, “Production of residual nuclei by ^3He -induced reactions on ^{27}Al and ^{nat}Cu ”, *APPL. RADIAT. ISOT.* **48**, 601–605 (1997); EXFOR A0606
- [267] J.F. Lamb, UCRL report **UCRL-18981**, Lawrence Berkeley Laboratory, University of California, Berkeley, 1969. Numerical values taken from Ref. [268].
- [268] P. Albert, G. Blondiaux, J.L. Debrun, A. Giovagnoli, M. Valladon, “Activation Cross-sections for Elements from Lithium to Sulphur”, *Handbook of Nuclear Activation Data*, **IAEA Technical Reports Series No. 273**, p. 479 (IAEA Vienna, 1987).
- [269] O. Lebeda, “New measurements at Rez for ^3He -induced reactions on Al and Ti”, private communication, 2016.
- [270] W. Michel, G. Brinkmann, R. Galas, R. Stuck, “Production of ^{24}Na and ^{22}Na by ^2H Induced Reactions on Aluminium; Production of ^{24}Na and ^{22}Na by ^3He Induced Reactions on Aluminium”. Data provided by W. Michel to the EXFOR database (1982); EXFOR A0158
- [271] D.J. Frantsvog, A.R. Kunselman, R.L. Wilson, C. S. Zaidins, C. Detraz, “Reactions induced by ^3He and ^4He ions on natural Mg, Al and Si”, *PHYS. REV.* **C25**, 770 (1982); EXFOR A0171
- [272] F. Ditrói, M.A. Ali, F. Tárkányi, I. Mahunka, “I. Investigation of the ^3He induced reactions on natural Ti for the purpose of activation analysis and nuclear implantation”, *Proc. Int. Conf. Nuclear Data for Science and Technology*, Trieste, 19-24 May 1997, ed. G. Reffo, A. Ventura, C. Grandi, **59**, 1746 (1997), SIF Bologna.
- [273] F. Ditrói, F. Tárkányi, M.A. Ali, L. Andó, S.J. Hes-

- elius, Yu.N. Shubin, Zhuang Youxiang, M.G. Mustafa, "Investigation of ^3He induced reactions on natural Ti for Thin Layer Activation (TLA), monitoring, activation analysis and production purposes", *NUCL. INSTRUM. METHODS PHYS. RES.* **B168**, 337–346 (2000); EXFOR D4112.
- [274] F. Szelecsényi, Z. Kovács, K. Nagatsu, M.-R. Zhang, K. Suzuki, "Production Cross Sections of Radioisotopes from ^3He -particle Induced Nuclear Reactions on Natural Titanium", *APPL. RADIAT. ISOT.* **119**, 94-100 (2017); EXFOR D4360.
- [275] F. Tárkányi, F. Szelecsényi, P. Kopecky, "Cross Section Data for Proton, ^3He and α -particle Induced Reactions on ^{nat}Ni , ^{nat}Cu and ^{nat}Ti for Monitoring Beam Performance", *Proc. Conf. Nuclear Data for Science and Technology*, Jülich, Germany, 13-17 May 1991, ed. S.M. Qaim, 529–532 (1992) Springer-Verlag, Berlin; EXFOR: D4080
- [276] A.J. Koning, D. Rochman, J. Kopecky, J.-Ch. Sublet, E. Bauge, S. Hilaire, P. Romain, B. Morillon, H. Duarte, S. van der Marck, S. Pomp, H. Sjostrand, R.A. Forrest, H. Henriksson, O. Cabellos, S. Goriely, J. Leppanen, H. Leeb, A. Plompen and R.W. Mills, "TENDL-2015: TALYS-based evaluated nuclear data library". Available online at https://tendl.web.psi.ch/tendl_2015/tendl2015.html
- [277] H.H. Bissem, R. Georgi, W. Scobel, J. Ernst, M. Kaba, J. Rama Rao and H. Strohe, "Entrance and Excit Channel Phenomena in d- and ^3He -induced Preequilibrium Decay", *PHYS. REV.* **22**, 1468 (1980); EXFOR A0347.
- [278] E.A. Bryant, D.R.F. Cochran, J.D. Knight, "Excitation Functions of Reactions of 7 to 24 MeV ^3He Ions with ^{63}Cu and ^{65}Cu ", *PHYS. REV.* **130**, 1512 (1963); EXFOR B0079001.
- [279] N.W. Golchert, J. Sedlet, D.G. Gardner, "Excitation Functions for ^3He -induced Nuclear Reactions in Cu", *NUCL. PHYS.* **A152**, 419 (1970); EXFOR T0120001.
- [280] F. Tárkányi, F. Ditrói, S. Takács, M. Al-Abyad, M.G. Mustafa, Yu. Shubin, Y. Zhuang, "New data and evaluation of ^3He -induced nuclear reactions on Cu", *NUCL. INSTRUM. METHODS PHYS. RES.* **B196**, 215–227 (2002); EXFOR D4109001.
- [281] E. Lebowitz and M.W. Greene, "An Auxiliary Cyclotron Beam Monitor", *INT. J. APPL. RADIAT. ISOT.* **21**, 625–627 (1970); EXFOR B0154001.
- [282] G.H. Bouchard Jr. and A.W. Fairhall, "Production of ^7Be in 30-42 MeV α -Ion Bombardment of Oxygen, Aluminium and Copper", *PHYS. REV.* **116**, 160–163 (1959).
- [283] W.W. Bowman and M. Blann, "Reactions of ^{51}V and ^{27}Al with 7-120 MeV α -Particles (Equilibrium and Non-Equilibrium Statistical Analyses)", *NUCL. PHYS.* **A131**, 513–531 (1969); EXFOR B0009.
- [284] M. Ismail, "Measurement and Analysis of the Excitation Function for Alpha-Induced Reactions on Ga and Sb Isotopes", *PHYS. REV.* **C41**, 87 (1990); EXFOR A0523.
- [285] H.-J. Lange, T. Hahn, R. Michel, T. Schiekel, R. Roessel, U. Herpers, H.-J. Hofmann, B. Dittrich-Hannen, M. Suter, W. Woelfli, P.W. Kubik, "Production of Residual Nuclei by Alpha-Induced Reactions on C, N, Mg, Al, Si up to 170 MeV", *APPL. RADIAT. ISOT.* **46**, 93–112 (1995); EXFOR A0517.
- [286] S. Mukherjee, B.B. Kumar, N.L. Singh, "Excitation Functions of Alpha Particle Induced Reactions on Aluminium and Copper", *PRAMANA J. PHYS.* **49**, 253-261 (1997); EXFOR O1180.
- [287] R.H. Lindsay and R.J. Carr, "He-Ion Induced Reactions of Aluminum and Magnesium", *PHYS. REV.* **118**, 1293–1297 (1960); EXFOR P0123.
- [288] R. Michel, G. Brinkmann, W. Herr, "Alpha-Induced Production of ^{24}Na and ^{22}Na from Al", IAEA report **INDC(GER)-22**, ed. S.M. Qaim, 45-47 (1980); EXFOR A0153.
- [289] N.T. Porile, "Study of the $^{27}\text{Al}(\alpha, ^7\text{Be})^{24}\text{Na}$ Reaction from Threshold to 41 MeV", *PHYS. REV.* **127**, 224 (1962); EXFOR C0984.
- [290] H.J. Probst, S.M. Qaim, R. Weinreich, "Excitation Functions of High-Energy α -Particle Induced Nuclear Reactions on Aluminium and Magnesium: Production of ^{28}Mg ", *INT. J. APPL. RADIAT. ISOT.* **27**, 431-441 (1976); EXFOR B0174.
- [291] S.S. Rattan and R.J. Singh, "Alpha Particle Induced Fission of ^{209}Bi ", *RADIOCHIM. ACTA* **38**, 169–172 (1985).
- [292] S.S. Rattan and R.J. Singh, "Alpha Particle Induced Fission of ^{209}Bi and $^{63,65}\text{Cu}$ ", *RADIOCHIM. ACTA* **39**, 61– 63 (1986); EXFOR A0353.
- [293] S.S. Rattan, A. Ramaswami, R.J. Singh, Satya Prakash, "Alpha particle induced reaction on ^{27}Al at 55.2 and 58.2 MeV", *RADIOCHIM. ACTA* **51**, 55–57 (1990); EXFOR D6005.
- [294] O.N. Visotskiy, S.A. Gaydaenko, A.V. Gonchar, O.K. Gorpnic, E.P. Kadkin, S.N. Kondratev, V.S. Prokopenko, S.B. Rakitin, L.S. Saltykov, V.D. Sklyarenko, Yu.S. Strizh, V.V. Tokaryevskiy, "The Absolute Cross Sections of Long-Lived Radionuclides in Reactions of Alpha-Particles on Aluminium-Nuclei", *39th Annual Conf. Nucl. Spectrosc. Nucl. Structure*, Tashkent, USSR, 365 (1989); EXFOR A0424.
- [295] J.R. Benzakin and H. Gauvin, private communication, 1970. Data from Ref. [339].
- [296] E. Gadioli, E. Gadioli Erba, J. Asher, D.J. Parker, "Analysis of $^{59}\text{Co}(x\text{pyn}\alpha)$ Reactions up to 170 MeV Incident Alpha Energy", *Z. PHYS.* **A317**, 155–168 (1984); EXFOR D0394.
- [297] B. Gordon, "Nuclear and Radiochemical Research on Special Isotopes. Excitation Functions. Alpha particles on Aluminum-27", BNL report **BNL-50082(S-70)**, p. 82 (1967).
- [298] C.O. Hower Jr., "The $(\alpha, ^7\text{Be})$ Reaction in Light Elements at Energies below 42 MeV", thesis, University of Washington, Seattle, Washington State USA, 1962. Data from Ref. [339].
- [299] M. Ismail and A.S. Divatia, "Measurements and Analysis of Alpha-induced Reactions on Ta, Ag and Co", *PRAMANA J. PHYS.* **30**, 193–210 (1988); EXFOR A0442.
- [300] M. Lindner and R.N. Osborne, "The Cross Section for the Reaction $^{27}\text{Al}(\alpha, \alpha 2pn)^{24}\text{Na}$ from Threshold to 380 MeV. *PHYS. REV.* **91**, 342 (1953); EXFOR C0381.
- [301] C.M. Baglin, E.R. Norman, R.M. Larimer, G.A. Rech, "Measurement of $^{107}\text{Ag}(\alpha, \gamma)^{111}\text{In}$ Cross Sections", *Int. Conf. Nuclear Data for Science and Technology*, 27 September - 1 October 2004, Santa Fe, New Mexico, USA, eds: R.C. Height, M.B. Chadwick, T. Kawano and P. Talou, AIP CONF. PROC. **769**, Part 2, 1370 (2005) AIP, Melville, New York; EXFOR C1474.

- [302] C.N. Chang, J.J. Kent, J.F. Morgan, S.L. Blatt, “Total Cross Section Measurements by X-ray Detection of Electron-capture Residual Activity”, *NUCL. INSTRUM. METHODS* **109**, 327–331 (1973); EXFOR C0951.
- [303] A. Hermanne, M. Sonck, S. Takács, F. Szelecsényi, F. Tárkányi, “Excitation functions of nuclear reactions induced by alpha particles up to 42 MeV on ^{nat}Ti for monitoring purposes and TLA”, *NUCL. INSTRUM. METHODS PHYS. RES.* **B152**, 187–201 (1999); EXFOR D4089. Data of A. Hermanne *et al.* (1999) are grouped into seven sets of data in the original publication, whereas the compiler has reproduced them on the appropriate figure as two different datasets labelled (a) and (b).
- [304] A. Iguchi, H. Amano, S. Tanaka, “ (α, n) cross sections for ^{48}Ti and ^{51}V ”, *J. ATOMIC ENERGY SOC. JAPAN* **2**, 682 (1960); EXFOR E1930.
- [305] B. Király, F. Tárkányi, S. Takács, A. Hermanne, S.F. Kovalev, A.V. Ignatyuk, “Excitation functions of α -induced nuclear reactions on natural erbium”, *NUCL. INSTRUM. METHODS PHYS. RES.* **B266**, 549–554 (2008); EXFOR D4199
- [306] R. Michel, G. Brinkmann, R. Stück, “Integral Excitation Functions of α -Induced Reactions on Titanium, Iron and Nickel”, *RADIOCHIM. ACTA* **32**, 173–189 (1983); EXFOR A0148.
- [307] A.J. Morton, S.G. Tims, A.F. Scott, “The $^{48}\text{Ti}(\alpha, n)^{51}\text{Cr}$ and $^{48}\text{Ti}(\alpha, p)^{51}\text{V}$ cross sections”, *NUCL. PHYS.* **A537**, 167–182 (1992); EXFOR D0061.
- [308] S. Takács, private communication, 2005. Data discussed in S. Takács, A. Hermanne, F. Tárkányi, A. Ignatyuk, “Cross-sections for α -particle Produced Radionuclides on Natural Silver”, *NUCL. INSTRUM. METHODS PHYS. RES.* **B268**, 2–12 (2010).
- [309] S. Takács, F. Tárkányi, A. Hermanne, “Cross Section Measurements of Nuclear Reactions on Cu and Ti Targets by α -Bombardment for Monitoring Use”, unpublished work, 2007.
- [310] M.S. Uddin and B. Scholten, “Excitation Functions of Alpha Particle Induced Reactions on ^{nat}Ti up to 40 MeV”, *NUCL. INSTRUM. METHODS PHYS. RES.* **B380**, 15–19 (2016); EXFOR O2304.
- [311] H. Vonach, R.C. Haight, G. Winkler, “ (α, n) and Total α -reaction Cross Sections for ^{48}Ti and ^{51}V ”, *PHYS. REV.* **C28**, 2278–2285 (1983); EXFOR C0318.
- [312] Xiufeng Peng, Fuqing He and Xianguan Long, “Excitation Functions for the Reactions Induced by Alpha-particle Impact of Natural Titanium”, *NUCL. INSTRUM. METHODS PHYS. RES.* **B140**, 9–12 (1998); EXFOR O1074.
- [313] R. Adam Rebeles, A. Hermanne, P. Van den Winkel, F. Tárkányi, S. Takács, L. Daraban, “Alpha Induced Reactions on ^{114}Cd and ^{116}Cd : An Experimental Study of Excitation Functions”, *NUCL. INSTRUM. METHODS PHYS. RES.* **B266**, 4731–4737 (2008)
- [314] H.D. Bhardwaj, A.K. Gautam, R. Prasad, “Measurement and Analysis of Excitation Functions for Alpha-Induced Reactions in Copper”, *PRANAMA J. PHYS.* **31**, 109–123 (1988); EXFOR: A0465
- [315] O. Bonesso, M.J. Ozafran, H.O. Mosca, M.E. Vazquez, O.A. Capurro and S. J. Nassiff, “Study of Preequilibrium Effects on α -Induced Reactions on Copper”, *J. RADIOANAL. NUCL. CHEM.* **152**, 189–197 (1991); EXFOR D0092.
- [316] A. Hermanne, R. Adam Rebeles, F. Tárkányi, S. Takács, “Alpha Particle Induced Reactions on ^{nat}Cr up to 39 MeV: Experimental Cross-sections, Comparison with Theoretical Calculations and Thick Target Yields for Medically Relevant ^{529}Fe Production”, *NUCL. INSTRUM. METHODS PHYS. RES.* **B356–357**, 28–41 (2015).
- [317] M. Hille, P. Hille, M. Uhl, W. Weisz, “Excitation Functions of (p, n) and (α, n) Reactions on Ni, Cu and Zn”, *NUCL. PHYS.* **A198**, 625–640 (1972); EXFOR B0058.
- [318] A.V. Mohan Rao, S. Mukherjee, J. Rama Rao, “Alpha Particle Induced Reactions on Copper and Tantalum”, *PRANAMA J. PHYS.* **36**, 115–123 (1991); EXFOR D0136.
- [319] S.J. Nassiff and W. Nassiff, “Cross Sections and Thick Target Yields of Alpha-Particle Induced Reactions”, IAEA final report contract /R1/RB2499 (1983), unpublished; EXFOR D0046 (updated in 2017, O. Bonesso *et al.* “Cross Sections and Thick Target Yields of Alpha-Induced Reactions”, IAEA report INDC(ARG)-14 (IAEA, Vienna, 2017)) .
- [320] K.G. Porges, “Excitation Functions of Silver and Copper”, *PHYS. REV.* **101**, 225 (1956); EXFOR R0039.
- [321] N.T. Porile and D.L. Morrison, “Reactions of ^{63}Cu and ^{65}Cu with Alpha Particles”, *PHYS. REV.* **116**, 1193 (1959); EXFOR B0156.
- [322] I.A. Rizvi, M.A. Ansari, R.P. Gautam, R.K.Y. Singh, A.K. Chaubey, “Excitation Functions Studies of $(\alpha, xpyn)$ Reactions for $^{63,65}\text{Cu}$ and Pre-Equilibrium Effect”, *J. PHYS. SOC. JAPAN* **56**, 3135–3144 (1987); EXFOR D0090.
- [323] M. Shahid, K. Kim, G. Kim, M. Zaman, M. Nadeem, “Measurement of Excitation Functions in Alpha Induced Reactions on ^{nat}Cu ”, *NUCL. INSTRUM. METHODS PHYS. RES.* **B358**, 160–167 (2015); EXFOR D7016.
- [324] N.L. Singh, B.J. Patel, D.R.S. Somayalulu, S.N. Chintalapudi, “Analysis of the Excitation Functions of $(\alpha, xnyp)$ Reactions on Natural Copper”, *PRANAMA J. PHYS.* **42**, 349–363 (1994); EXFOR D0099.
- [325] P.H. Stelson and F.K. McGowan, “Cross Sections for (α, n) Reactions for Medium Weight Nuclei”, *PHYS. REV.* **133**, B911 (1964); EXFOR C0185.
- [326] M. Sonck, Y. Van Hoyweghen, A. Hermanne, “Determination of the External Beam Energy of a Variable Energy Multiparticle Cyclotron”, *APPL. RADIAT. ISOT.* **47**, 445–449 (1996).
- [327] F. Szelecsényi, K. Suzuki, Z. Kovács, M. Takei, K. Okada, “Alpha Beam Monitoring via $^{nat}\text{Cu} + \text{Alpha}$ Processes in the Energy Range from 40 to 60 MeV”, *NUCL. INSTRUM. METHODS PHYS. RES.* **B184**, 589–596 (2001); EXFOR E1996.
- [328] F. Szelecsényi, Z. Kovacs, K. Nagatsu, K. Fukumura, K. Suzuki, K. Mukai, “Investigation of Direct Production of ^{68}Ga with Low Energy Multiparticle Accelerator”, *RADIOCHIM. ACTA* **100**, 5–11 (2012); EXFOR D4276.
- [329] F. Tárkányi, F. Szelecsényi, S. Takács, A. Hermanne, M. Sonck, A. Thielemans, M.G. Mustafa, Yu. Shubin, Zhuang Youxiang, “New Experimental Data, Compilation and Evaluation for the $^{nat}\text{Cu}(\alpha, x)^{66}\text{Ga}$, $^{nat}\text{Cu}(\alpha, x)^{67}\text{Ga}$ and $^{nat}\text{Cu}(\alpha, x)^{65}\text{Zn}$ Monitor Reactions”, *NUCL. INSTRUM. METHODS PHYS. RES.* **B168**, 144–168 (2000); EXFOR D4085.
- [330] O.A. Zhukova, V.I. Kanasevich, S.V. Laptev, G.P. Chursin, “Excitation Functions of α -Particle Induced Re-

- actions on Copper Isotopes at Energies up to 38 MeV”, *IZV. AKADEMIYI NAUK. KAZ. SSR. SER. FIZ.-MATEM.* **4**, 1 (1970); EXFOR A0647.
- [331] J. Zweit, H. Sharma and S. Downey, “Production of ^{66}Ga , a Short-lived Positron Emitting Radionuclide”, *APPL. RADIAT. ISOT.* **38**, 499–501 (1987); EXFOR D0119.
- [332] F. Ditrói, private communication, 2002. Data published in F. Tárkányi, F. Ditrói, F. Szelecsényi, M. Sonck, A. Hermanne, “Measurement and Evaluation of the Excitation Functions for Alpha Particle Induced Nuclear Reactions on Niobium”, *NUCL. INSTRUM. METHODS PHYS. RES.* **B198**, 11–31 (2002).
- [333] H.P. Graf and H. Munzel, “Excitation Functions for Alpha Particle Reactions with Molybdenum Isotopes”, *J. INORG. NUCL. CHEM.* **36**, 3647–3657 (1974); EXFOR B0040.
- [334] A. Hermanne, F. Tárkányi, S. Takács, Z. Szücs, Yu.N. Shubin, A.I. Dityuk, “Experimental Study of the Cross-sections of Alpha-particle Induced Reactions on ^{209}Bi ”, *APPL. RADIAT. ISOT.* **63**, 1–9 (2005); EXFOR O1272.
- [335] F.S. Houck and J.M. Miller, “Reactions of Alpha Particles with Iron-54 and Nickel-58”, *PHYS. REV.* **123**, 231 (1961); EXFOR P0058.
- [336] S.Y. Lin and J.M. Alexander, “Reactions of ^{237}Np with ^4He Near the Interaction Barrier”, *PHYS. REV.* **C16**, 688 (1977); EXFOR B0088.
- [337] F.H. Ruddy, “The Formation of the Compound Nucleus ^{68}Ge ”, dissertation, Simon Fraser University, Canada, 1963.
- [338] F. Tárkányi, F. Ditrói, S. Takács, A. Hermanne, “Measurement and Evaluation of the Excitation Functions for Alpha Particle Induced Nuclear Reactions on Nb and Pt”, unpublished results, 2007.
- [339] J. Tobailem, C.-H. de Lassus St-Genies and L. Leveque, “Sections Efficaces des Reactions Nucleaires Induites par Protons, Deutons, Particules Alpha. I Reactions Nucleaires Moniteurs”, CEA note **CEA-N-1-1466(1)**, CEA, France, 1971; EXFOR D0128.